

COMPARATIVE REACTIVITIES OF PETROLEUM COKES

C F Gray and W. J. Metrailler

Esso Research Laboratories
Humble Oil & Refining Company · Baton Rouge Refinery
Baton Rouge, Louisiana

INTRODUCTION

Petroleum coke is produced by coking of high boiling petroleum fractions (residua) to obtain more valuable lighter hydrocarbon products and coke. The two more prominent commercial processes for carrying out the coking operation are Fluid Coking and Delayed Coking.

Fluid Coking is a continuous process. It is carried out in equipment similar to that used extensively for Fluid Catalytic Cracking (1,2). A two vessel system is used in which the small product coke particles are heated by partial combustion in a burner vessel and these particles are circulated to the coking vessel to supply the heat needed. Finely dispersed residuum feed is injected into the coking vessel which operates at 900-975°F. The coke formed by cracking is deposited on the surface of the small coke particles which are then returned to the burner. The burner is, of course, operated at a higher temperature than the reactor. This results in some devolatilization of the coke. These volatiles along with part of the product coke (if necessary) are burned to supply heat.

In the Delayed Coking process, residuum is preheated in a furnace and is then introduced into a soaking drum. This large drum provides sufficient holding time to crack the residuum with the light hydrocarbons passing overhead. The drum eventually fills with coke which is then mechanically removed. Delayed Coking is thus a cyclic process. Coking temperatures in the drum may vary between 800 and 850°F.

In both processes the coke product represents a bottoms fraction and its chemical quality is dependent on the quality of the residuum feed. Non-volatile metals and ash constituents in the feed are deposited essentially 100% in the coke. Sulfur compounds, which are usually concentrated in the heavier petroleum fractions, are further concentrated in the coke to the extent that petroleum coke product normally contains 1.2 to 2.0 times the sulfur concentration of the residuum feed.

The volatiles content and physical properties of petroleum coke produced by Fluid Coking are quite different from the coke produced in Delayed Coking. Fluid coke is exposed to a higher temperature than is delayed coke, about 1100-1150°F. vs. 800-850°F. As a result green (i.e., uncalcined) fluid coke contains about 7 wt.% volatiles (measured at 1742°F.) vs. 10-15 wt.% volatiles in green delayed coke. Also, in Fluid Coking a layer of coke is deposited during each pass and the product has a characteristic onion ring structure, whereas delayed coke product is amorphous in nature. The differences between the two cokes are illustrated by photomicrographs in Figure 1, which

shows cross sections of particles of the two cokes.

Petroleum cokes vary in their resistance to oxidation. This is an important property of coke in many end uses. Good quality cokes, i.e., those having low metals and sulfur contents, generally are calcined and then find their way into carbon electrodes where resistance to oxidation is desirable. Low quality cokes generally are used green as a fuel and rapid oxidation is desirable.

In the work described in this paper, the reactivity of the various cokes was measured by placing the coke in a flowing stream of CO_2 at 1742°F . and recording the weight loss continuously. This technique permits close control of test conditions and does not require removal of large quantities of heat. Other investigators have studied the reaction of CO_2 with carbon. In a recent paper (3), Givry and Scalliet reported on an investigation relating anode reactivity with CO_2 to performance in an electrolytic reduction cell.

EXPERIMENTAL

MATERIALS

Samples of green fluid coke from several commercial fluid coking units were calcined in a muffle furnace to a temperature of 2400°F . The delayed cokes and the coal tar coke were from commercial production. These cokes had been calcined for use in carbon electrodes prior to receipt. Normally, a calcining temperature of about 2400°F . is used in this commercial operation.

A commercially available coal tar binder was used in the preparation of all of the molded carbon specimens. This material was obtained from the Barrett Division of Allied Chemical Company.

PHYSICAL AND CHEMICAL INSPECTIONS OF MATERIALS

Pertinent inspections of the calcined cokes used in this study are given in Table I. All tests and inspections were obtained by using techniques which are common in the carbon industry. The coal tar binder had a 215°F . softening point, a coking value of 67.5 and C/H ratio of 1.6.

REACTIVITY TEST

The reactivity of the cokes with carbon dioxide ($\text{CO}_2 + \text{C} \rightarrow 2\text{CO}$) was measured in the reactivity apparatus shown in Figure 2. The sample of carbon was dried overnight at 275°F . and then was placed in the quartz tube. After heating to 1742°F . in an atmosphere of purified nitrogen, a flow of purified CO_2 was started over the sample. The CO_2 rate was about 12 liters per hour. This gave a velocity of 2.2 cm./sec. in the annulus between the sample and the quartz tube. A continuous weight recording device measured the loss of weight of the sample due to reaction with CO_2 . The inlet and exit gas rates and exit gas composition were obtained. The CO concentration in the off-gases ranged from about 3 to 30 percent varying with the reactivity of the sample.

Test data were obtained on granular coke samples and on samples of coke which had been molded into cylindrical test specimens, bound together with coal tar binder. When the reactivity of a granular coke sample was to be measured, a 16 gram sample of 14-35 mesh coke was supported in a platinum mesh basket. Reactivities of the molded carbon specimens were determined by suspending the sample on a platinum wire which passed through a small hole in the specimen. Upon completion of the test on molded specimens, the carbon body was cooled and weighed and then brushed with a stiff bristle brush. Loosely held carbon particles which could be brushed from the sample were reported as "dust." The amount of "dust" measured in this manner is related to the amount of carbon which will be lost from the carbon body as it is consumed.

PREPARATION OF THE CARBON SPECIMENS

The molded carbon specimens used in this study were prepared by mixing the coke and pitch binder in a steam jacketed sigma blade mixer. Mixing was continued for 30 minutes at 300°F. The mixture was molded to form a 3 inch diameter by 5 inch long carbon body which was then baked slowly to about 1900°F. in a muffle furnace. Reactivity test specimens about 3/4 inch in diameter by 2 inches long were cored from the baked carbon body. Three levels of binder content were used in the work reported herein and both fine grained and coarse grained carbon aggregates were employed. The fine grained aggregate consisted of about 75 wt.% 35-200 mesh coke and 25 wt.% coke ground to pass a 100 mesh screen. The coarse grained aggregate was made up of 50 wt.% 4-48 mesh coke and 50 wt.% coke ground to pass a 100 mesh screen.

RESULTS AND DISCUSSION

Comparison of Granular Coke Reactivity

Results of the study of cokes in granular form (14-35 mesh) show that fluid cokes react with CO₂ at a much lower rate than do delayed cokes. (Table I) The coal tar coke which was prepared in a manner similar to delayed coke had the highest reactivity. These data confirm results obtained by Walker et al (4) in a more detailed study of cokes. It is well known that oxidation of carbon occurs more rapidly along crystal edges than along the basal planes. Deposition of carbon in relatively thin layers on the spherical fluid coke particles results in the onion skin structure of fluid coke (5) which is shown in Figure 1. The carbon in this thin onion skin layer is probably oriented such that basal planes of the carbon structure are exposed to a greater extent than are the crystal edges. Thus, one would expect that the reactivity of fluid coke would be low. It is also possible that the higher temperature at which carbon is deposited in fluid coking results in the lower reactivity of this material compared to delayed coke.

The reactivity of petroleum coke increases with its total ash content (Figure 3). The coke was also analyzed for V, Ni, Fe, Na, Ti, Cu, Al, Cr, and Si. Among these metallic contaminants, the concentration of iron appears to correlate best with coke reactivity. It is evident that, for a given ash content, the reactivity of fluid coke is lower than that of delayed coke.

Reactivities of Baked Carbon Specimens

The reactivities of baked carbon specimens prepared from the various granular cokes are given in Table II. It is seen in Figure 4 that the rate of consumption of the carbon specimen is directly related to the reactivity of the granular cokes. This means that the bodies prepared with fluid cokes have lower consumption rates than those prepared from delayed cokes. The carbon bodies prepared with 28 wt.% binder show a higher reactivity than those prepared with 16-18 wt.% binder. This is not surprising in that the binder coke from coal tar has a higher reactivity than any of the petroleum cokes. Also, the binder coke is not baked (calcined) to as high a temperature as were the petroleum cokes and this would be expected to result in its having a higher reactivity.

The particle size distribution of the carbon aggregate does not appear to have a major influence on consumption rate of the carbon bodies. Only two comparisons of this factor were made in this study, one with delayed coke and one with fluid coke. Neither coke showed much difference in consumption rate between fine and coarse grained carbon bodies.

Most carbon bodies are consumed in commercial use either as part of the process operation or as a result of exposure to oxidizing atmospheres. When the carbon is consumed there is a tendency to form loose particles of carbon or "dust." The generally accepted explanation for "dusting" is that the binder carbon is consumed faster than the carbon aggregate. The unconsumed portion of the carbon aggregate then becomes loose and can be brushed from the main body of carbon. The amount of loose carbon formed during our experiments is shown in Table II. It is immediately obvious that the quantity of "dust" formed was much lower for the carbon bodies prepared with fluid cokes than for those prepared from delayed cokes. This is true for both fine grained and coarse grained carbon aggregates. However, the fluid coke specimens were not as reactive and less total carbon was consumed in the standard four hour test. Additional data will have to be obtained at equivalent total consumption to establish how the amount of "dusting" obtained with fluid coke aggregate compares with delayed coke at a given consumption level.

Data have been obtained which show (Figure 5) that the use of low reactivity fluid coke to supply the carbon fines reduces the formation of "dust." High reactivity delayed coke was used to supply the coarse carbon aggregate in these samples, which were made up of 50 wt.% coarse coke and 50 wt.% fine coke as described previously. For comparison, samples were prepared using delayed coke having the same particle size distribution. Both reactivity and dust formation (at the same carbon consumption) were lower for the carbon specimens containing the low reactivity fine fluid coke. One possible explanation is that the low reactivity coke fines act as a diffusion barrier and reduce the rate of consumption of the bonding carbon. Thus the overall reactivity of the carbon surface is more in balance and less dust is formed.

CONCLUSIONS

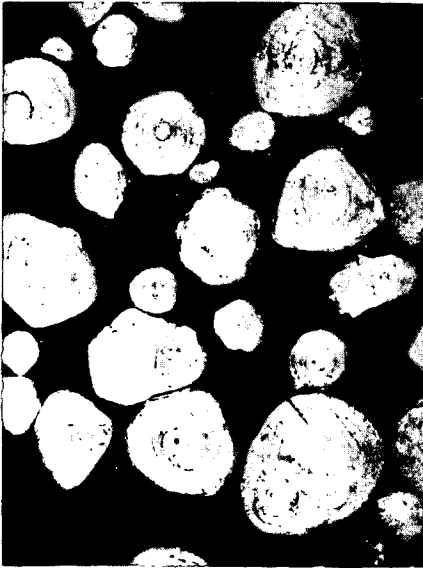
Data on nine commercially available cokes show that the process used to prepare the coke is a major factor influencing its reactivity. Ash content,

particularly iron content, is of secondary importance. Fluid coke has a lower reactivity than delayed coke at the same impurity level. The lower reactivity measured on granular cokes is carried over into carbon bodies prepared from these cokes. Binder content also influences reactivity of the carbon body. There is also an indication that less carbon dust (loose carbon) is formed when low reactivity coke is used to supply the fine coke aggregate.

LITERATURE REFERENCES

1. Voorhies, A., Jr. "Fluid Coking of Residua", Proceedings of the Fourth World Petroleum Congress, Section III F, Reprint 1. Rome: Carlo Colombo Publishers, 1955.
2. Voorhies, A., Jr. and Martin, H. Z. Oil Gas J. 52, No. 28, 204-7 (1953).
3. Givry, J. P. and Scalliet, R., Paper presented at the AIME Annual Meeting, February 18-22, 1962, New York, New York.
4. Walker, P. L., Jr., Rusinko, F., Jr., Rakazawski, J. F., and Liggett, L. M. "Proceedings of 1957 Conference on Carbon", 643-58. New York: Pergamon Press, 1957.
5. Dunlop, D. D., Griffin, L. I., Jr. and Moser, J. F., Jr. Chemical Engineering Progress 54, No. 8, 39-43 (1958).

FIGURE 1
COMPARISON OF UNCALCINED COKES



FLUID

ABOUT 63X



DELAYED

ABOUT 425X

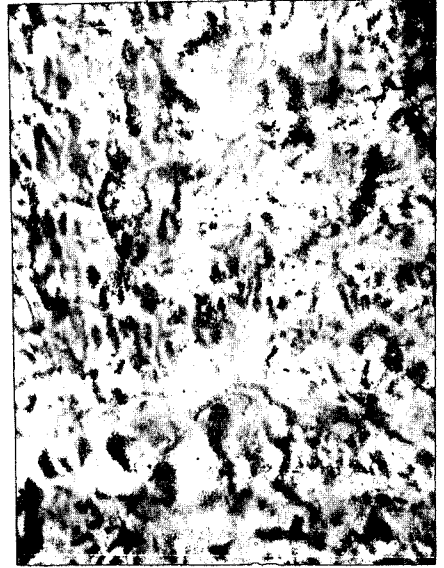


FIGURE 2
REACTIVITY MEASURING APPARATUS

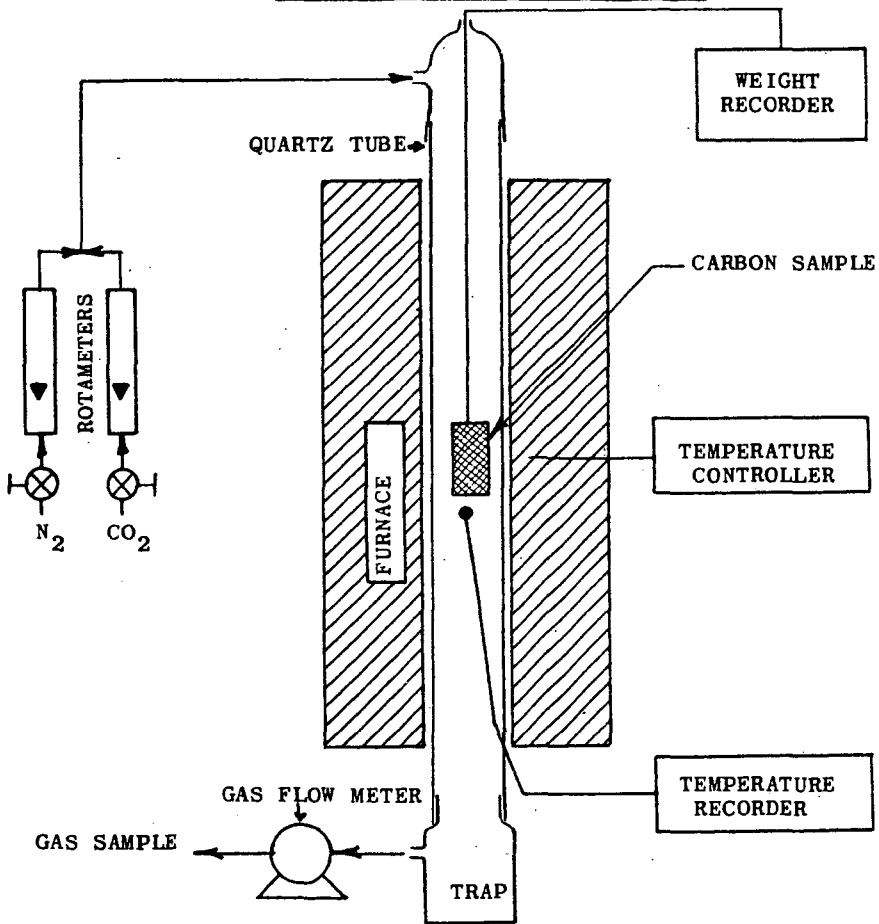


FIGURE 3
CARBON REACTIVITY IS AFFECTED BY ASH CONTENT

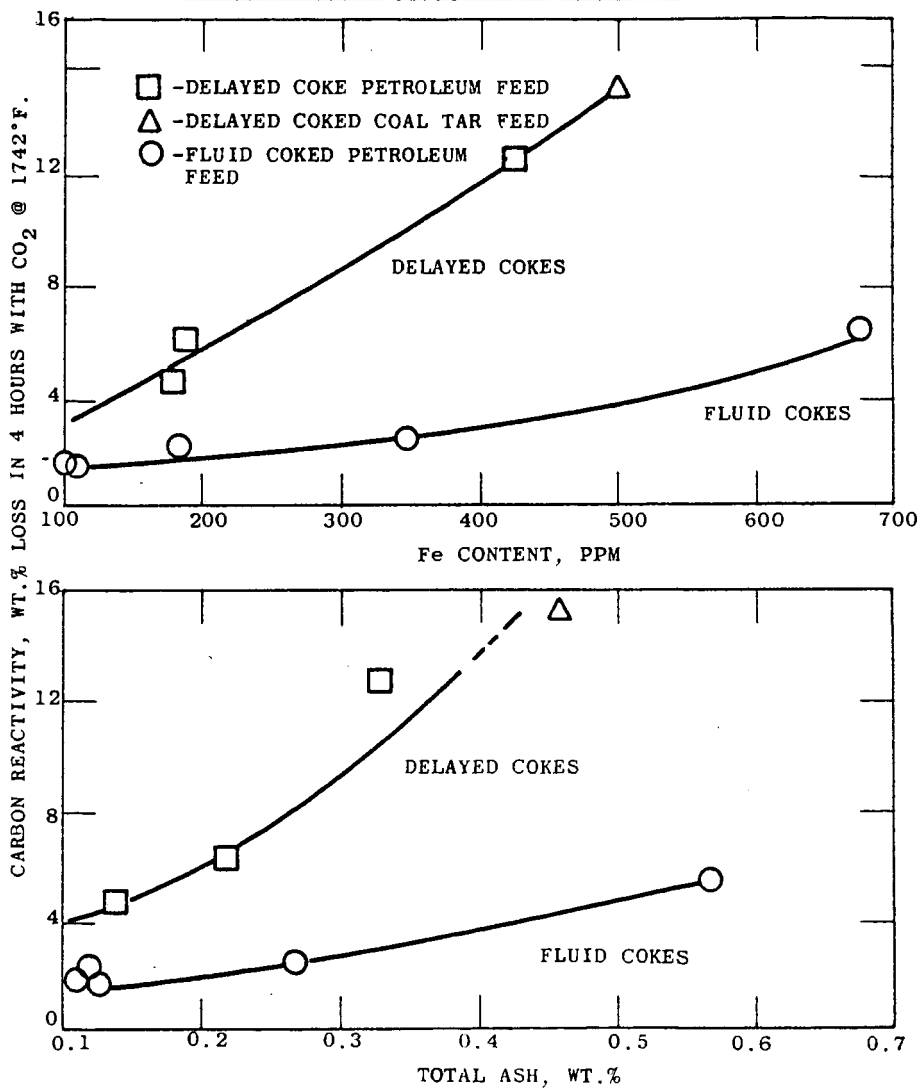


FIGURE 4
COMPARISON OF REACTIVITIES OF CARBON BODIES AND GRANULAR COKES

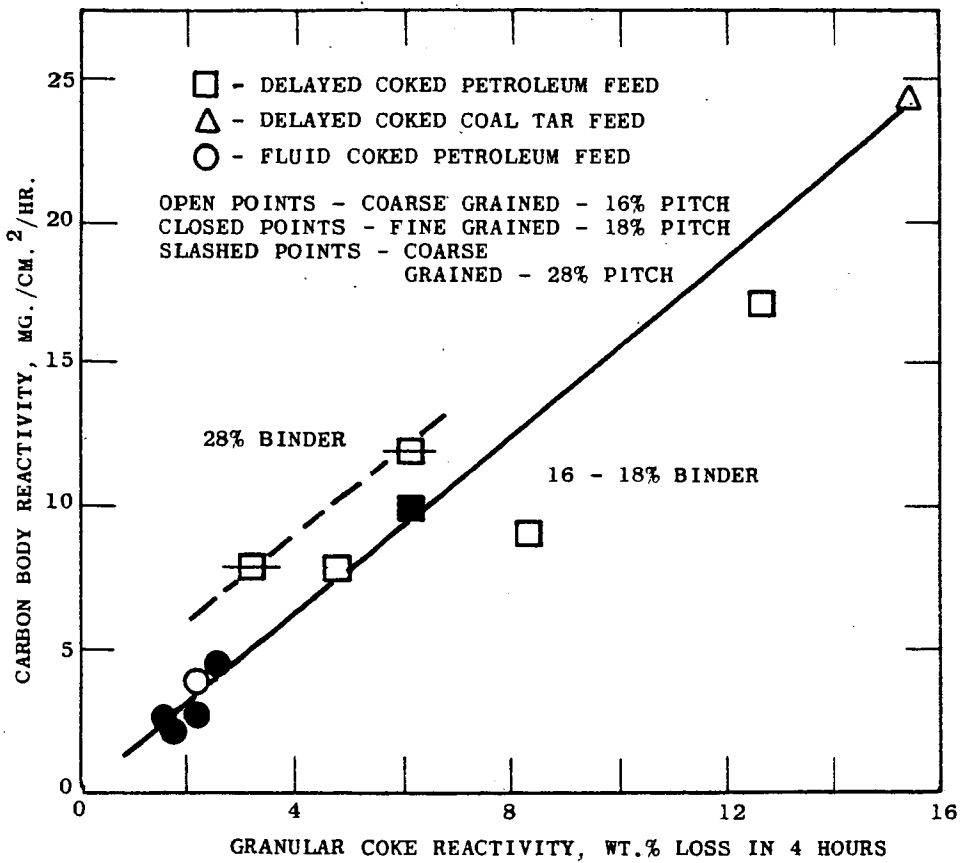


FIGURE 5

CARBON DUST FORMATION VS. CARBON CONSUMPTION IN COARSE GRAINED SPECIMENS

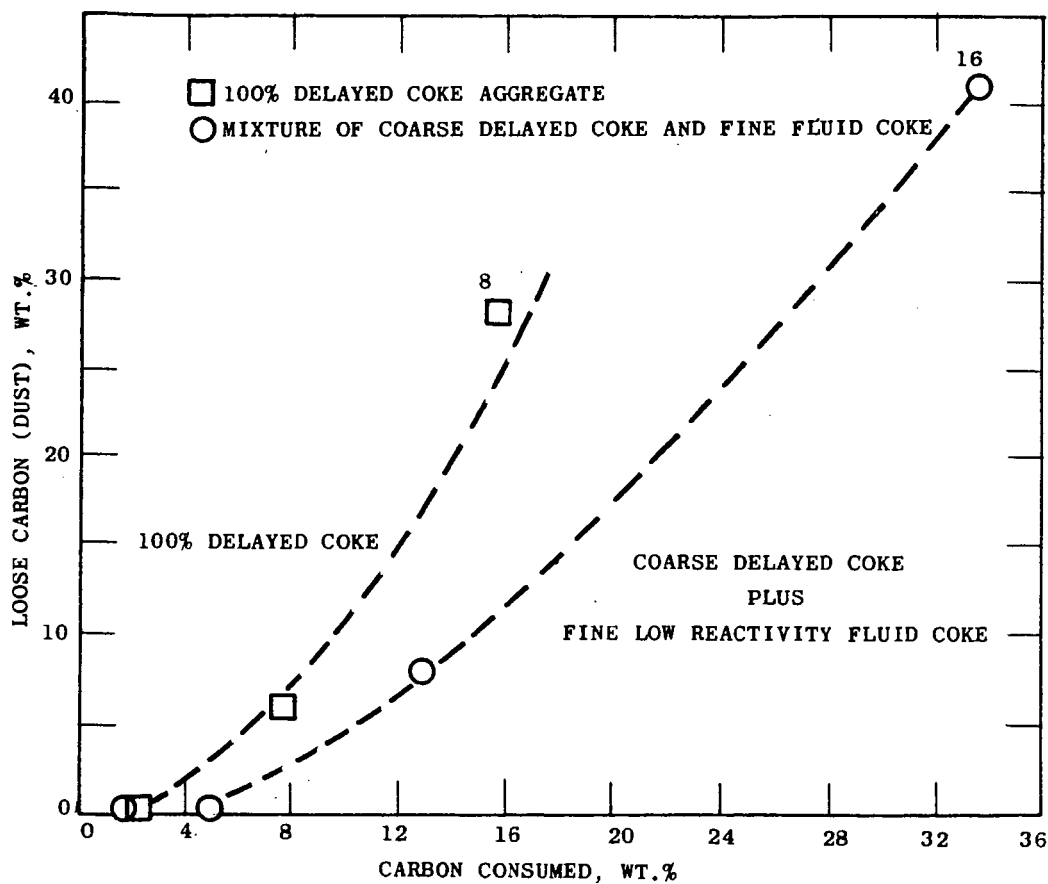


TABLE I

DATA ON GRANULAR COKES

ALL COKES WERE CALCINED AT ABOUT 2400° F.

Sample No.	Coking Process Used	Feed Source	Impurities in Coke		Granular Coke Reactivity* Loss, Wt. % in 4 Hrs.
			Total Ash, Wt. %	Fe, Wt. %	
DP-1	Delayed	Petroleum	0.14	180	4.7
DP-2	Delayed	Petroleum	0.22	190	6.2
DP-3	Delayed	Petroleum	0.31	430	12.7
FP-1	Fluid	Petroleum	0.12	185	2.2
FP-2	Fluid	Petroleum	0.11	100	1.7
FP-3	Fluid	Petroleum	0.13	110	1.6
FP-4	Fluid	Petroleum	0.27	350	2.5
FP-5	Fluid	Petroleum	0.57	670	6.5
DCT	Delayed	Coal Tar	0.46	500	15.4

* Measured by exposing 14-35 mesh coke to CO₂ @ 1742° F. - 750C

/hc
3/22/62

TABLE II
 REACTIVITY OF MOLDED CARBON SPECIMENS

Coke Aggregate	% Binder	Reactivity Test Time, Hrs.	Carbon Loss		Loose Carbon, Wt. %
			mg./cm. ² /hr.	Wt. %	
<u>Coarse Grained</u>					
DP-1	16	4.0	7.9	5.5	3.2
DP-2	16	4.0	9.7	6.7	9.2
DP-3	16	4.0	17.0	11.5	7.8
DCT	16	4.0	24.5	15.4	11.4
FP-1	16	4.0	4.3	3.0	0.3
<u>Fine Grain</u>					
DP-1	18	4.0	7.9	5.3	3.4
FP-1	18	4.0	2.9	1.9	0.2
FP-2	18	4.0	2.2	1.5	0.3
FP-3	18	4.0	2.5	1.6	0.2
FP-4	18	4.0	4.7	3.0	0.3
<u>Coarse Grained</u>					
DP-1	28	1.5	9.9	2.4	0.3
DP-1	28	4.0	→11.9	7.5	5.9
DP-1	28	8.0	12.3	15.5	27.7
DP-1	28	16.0	12.1	31.9	**
DP-1 + FP-1*	28	1.5	7.0	1.8	0.1
DP-1 + FP-1*	28	4.0	→7.8	5.2	0.5
DP-1 + FP-1*	28	8.0	9.5	12.7	7.1
DP-1 + FP-1*	28	16.0	12.4	33.8	40.9

* Sample FP-1 used to supply the fine coke portion.

** Unconsumed carbon disintegrated.

/hc

3/22/62

Reactivities of Low Rank Coals

Neal Rice and Edward Prostel

Natural Resources Research Institute
University of Wyoming
Laramie, Wyoming

During the past years, various investigations were undertaken at the University of Wyoming on the utilization of low rank coal. In several of these, the reactivity of the coal products was important and therefore was given consideration. In connection with the development work on reducing carbon, the reaction of the carbon to CO_2 was tested and in connection with the use of processed coal for barbecue briquets, the reactivity to air was investigated. Results of this work are reported here as they appear of general significance.

Carbon Dioxide Reactivity

In order to show results from as wide a rank of coals as possible, three Wyoming coals were chosen, ranking from high volatile C Bituminous to subbituminous C. These coals were carbonized in a closed retort to 950°C . The heating rate was 5°C per minute. Table I shows the proximate and ultimate analyses, also the heating values of the chars. Listed are also the coals from which the chars are derived and two commercial cokes, one Western coke furnished by the Colorado Fuel and Iron Corporation and one Eastern coke furnished by Pittsburgh Coke and Chemical Company.

TABLE I
ANALYSES OF COKES, CHARS AND COALS
(Moisture Free, in Percent)

NAME AND RANK			VM	FC	Ash	H_2	C	O_2	N_2	S	Btu/lb.
Cokes	Pitt. Foundry	Hvab	0.4	93.9	5.7	0.2	91.2	1.4	1.0	0.4	13140
	C F and I	Hvab	3.5	83.6	13.1	1.1	83.5	0.8	1.0	0.5	12250
950° Chars											
	DOClark	Hvab	1.1	93.4	5.5	0.7	91.0	1.4	0.9	0.5	13580
	Elkol	Subb	2.5	93.2	4.3	1.0	90.7	2.2	1.4	0.4	13510
	Wyodak	Subc	2.1	82.2	14.7	1.1	80.6	1.3	0.9	0.4	12400
Coals	DOClark	Hvcb	39.3	57.0	3.7	5.8	72.2	15.4	1.6	1.3	13220
	Elkol	Subb	43.0	54.5	2.5	5.0	72.4	17.8	1.5	0.8	12580
	Wyodak	Subc	42.3	47.7	10.0	4.5	65.6	17.8	1.1	1.0	11340

The reactivity of the char to carbon dioxide was measured by conducting CO_2 over the char and measuring the proportion of CO to CO_2 in the effluent. As it is known that the surface area often is closely related to the reactivity, the densities, in methanol as well as in mercury, were also measured. From the densities, the porosities were calculated. Results are shown in Table II.

The chars from a lower rank coal have a higher reactivity than the chars from a higher rank coal and all are higher than the reactivities of the cokes. In Figure I, this relationship is shown graphically. The lower the rank of the coal, the higher the reactivity of the carbon residue.

TABLE II
 Reactivity, Density and Porosity
 of
 Chars and Cokes
 Moisture Free

Rank	Rank	Reactivity		Density	Porosity
		CO ₂	McOH	Hg	
Hvab	Foundry Coke	13.3	2.031	1.736	0.145
Hvab	C F & I Coke	71.8	1.869	1.617	0.135
Hvcb	DOClark Char	119.1	1.820	1.415	0.223
Subb	Elkol Char	137.5	1.840	1.382	0.249
Subc	Wyodak Char	146.0	1.810	1.100	0.392

It appears that this tendency is related to the porosity of the material. The higher porosity of the low rank chars facilitates the access of the oxidizing gas to the carbon surfaces. It is widely believed that diffusion is a limiting factor in reaction rates when gas reacts with a porous solid. It would perhaps be more to the point to say that the reactivity is governed by the concentrations of CO₂ and CO at the surfaces regardless how these concentrations were achieved. It would appear logical to assume that the rough low rank surfaces are more open to attack by the CO₂ than the glossy surfaces of the coke. The surface area of the lowest rank char under study, Wyodak, is about 27 m² per g whereas those of the two cokes are 2 and 3 m² per g respectively.^{1.)} Diffusion deeply into the piece of coke or char may take place but reaction is retarded by mounting concentrations of the product gas, CO, within the particle. The concentrations of the two gases are affected by the rate at which the one is supplied and the other is removed, and by the relative concentrations which prevail.

Milliken^{3.)} has suggested that the micelles of the lower rank coals may be composed at least partially of di-phenyl linkages and that these linkages are oriented about sixty degrees from planar. This results in steric hindrance which prevents formation of large blocks of oriented and planar molecules, thus leaving a greater random porosity. It also should be considered that the lower rank coals yield much water and carbon dioxide while being carbonized in the lower temperature ranges. There are thus many carbon-to-OH and carbon-to-oxygen linkages broken and probably left in a condition which encourages reaction of the peripheral carbon molecules with the oxidizing gas. The higher rank coke, never having been freed of such an amount of water and oxygen, has fewer sites open for attack and thus a lower reactivity.

In order to examine the possibility that the analysis of the coal substance would throw some light on these differences in reactivity, the ultimate analyses of the moisture and ash free chars and cokes are shown in Table III. As will be seen carbon and hydrogen content is similar down the columns. Oxygen, determined by difference, is not significant. As has been pointed out by Peters^{2.)}, it would appear that the chemical analysis gives no explanation for the differences in reactivity.

The two commercial cokes shown in Figure I were made under conventional coking conditions which involve comparatively slow temperature rise and longer periods at maximum temperature. The longer period at coking temperature, this so-called soaking period, also affects the CO₂-reactivity of the coke. Extended periods at high temperature reduce the CO₂-reactivity. Thus the two points, 1 and 2, would have been higher, closer to the level of the chars, if the cokes had been made at the same conditions as the chars.

TABLE III
 Ultimate Analyses of Chars and Cokes
 (Moisture and Ash Free)

Rank	Name	H ₂	C	O ₂	N ₂	S
Hvab	Foundry Coke	0.6	96.8	1.2	1.0	0.4
Hvab	C F & I Coke	1.0	96.3	1.3	0.9	0.5
Hvcb	DOClark Char	0.7	96.4	1.5	0.8	0.6
Subb	Elkol Char	1.0	95.0	2.2	1.4	0.6
Subc	Wyodak Char	1.2	95.8	1.1	1.0	0.5

To examine the effect of heat soak on reactivity, a char from DOClark coal was heat soaked for various periods, and then subjected to the reactivity test. The results are shown in Figure II. Heat soaking for 3 hours reduced the reactivity by about 15% and soaking for 48 hours by 35%. It is known that any char and any coke shrinks with continued heat soaking. This, of course, results in higher densities and lower porosities, and it must be expected that such changes result in closure or partial closure of openings and a reduction of the reaction surface. Thus, reactivity to CO₂ and doubtless to other gases is decreased with extended heating cycles. However, the nature of the surface of the char made from subbituminous coal is so open that no amount of heat soaking will lower its reactivity to that of a metallurgical coke.^{4.)}

The higher reactivity of the chars made from lower rank coals must be ascribed to their surface structure, and such chars must find applications where high reactivity is an advantage.

Reactivity Measured by Ignitability of Smokeless Briquets

Several investigations were made on the suitability of processed coal for barbecue briquets. Such briquets should be easy to ignite and should develop a reasonable amount of heat. Further, they should burn with a minimum of odor or smoke. The amount of heat, intensity of smoke and odor are outside the scope of this discussion. Remains the ignitability. This is determined to a large extent by the shape and size of the briquet, and especially by the degree of compaction which affects the apparent specific gravity. If, however, these and other factors of processing are kept uniform, the ignitability can serve as measure of the reactivity of the carbon substance.

In the ignition test, 5 briquets of uniform pillow shape are placed on a brick, four in a square, one-fourth inch apart, and one on top. The brick is placed off the floor. Room temperature is kept uniform and noticeable draft is avoided. 30 ml of lighter fluid is poured over the briquets uniformly and the briquets are ignited. The percentage of surface burning is estimated at close intervals for each briquet, and the average recorded. The time elapsed when 80% of the surface is burning is termed "Ignition time". It is not too difficult to train an operator within a few days so that the estimating can be done with reasonably close reproducibility.

Figure III shows the ignitability relative to the volatile content. The coal used was air-dry North Dakota lignite with 9.6% of moisture, 36.0% of volatile matter and 10.2% of ash. The coal was carbonized to various volatile contents, and the char briquetted with cereal binder. As will be seen from the curve, the optimum ignition time was achieved with 15 to 18% of volatile matter. At this stage, the volatile matter of the coal has been reduced by about 80%. All carbon dioxide has been evolved, and there is apparently an optimum compounded of the amount of volatile matter retained by the char and the quality of this volatile matter.^{1.)} It had been known for a long time that in the stated volatile range, the coal is best suited for

effective combustion at ordinary furnace temperatures. It may be surprising, however, that under the stated extreme conditions where the low ambient temperature slows the combustion, the same volatile content indicated the highest reactivity.

A great number of various lignites were carbonized, the char briquetted, and the briquets subjected to the ignition test. Processing conditions were uniform. There were again considerable variations in ignition time. Some were traced to variations in ash content, some to aggregate size. Yet there remained distinct differences. These were traced finally to the structure of the coal. In every instance, the lower ignition time was achieved with char from a coal with laminated structure, at least in part of the coal. Figure IV shows samples of the laminated and of the more compact structure. The former is black and has a shiny, velvety appearance, the latter is dull and often brownish. The one apparently originates from either leafy or bark matter, and the other from solid wood.

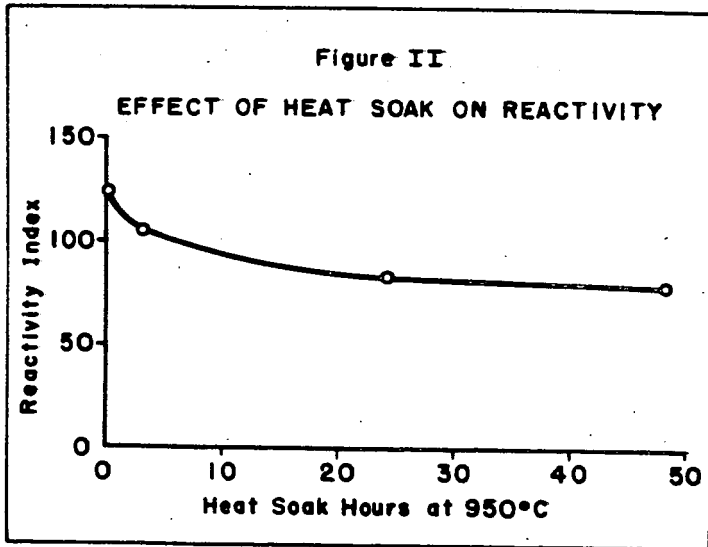
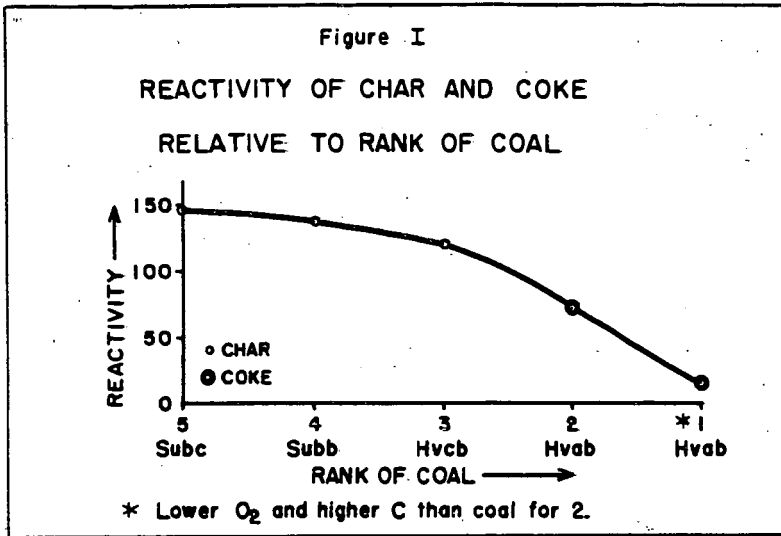
In another investigation, briquets were tested which were produced from char derived from subbituminous C coal. The volatile matter was kept uniform, also the ash content. To vary the amount of reaction surface, the size of the aggregate was varied. Changes in ignitability obtained with changes in aggregate size are shown in Figure V. The aggregate sizes shown are nominal. All aggregates were graded, and uniform grading was used in each case. It will be seen that the tests were confined between U.S. No. 20 and 70 screen sizes. Sizes beyond these limits had to be ruled out for reasons of operating procedures. Within the stated limits, the ignitability increased with decreasing aggregate size.

All the reported results point to the importance of sufficient reaction surface. However, there are, apparently, other factors involved. Many briquets of commercial production were tested which showed an ignition time of 40 minutes. Good smokeless briquets usually showed an ignition time of less than 30 minutes. Very good briquets showed 20, 19, or even 18 minutes ignition time. But this seemed to be the minimum. Any possible introduction of promoters or oxidizing agents is ruled out here and only the reactivity of the coal substance and the oxygen of the air is considered. It appeared that further reduction in aggregate size or further reduction in ash content did not lower the ignition time further.

The oxidation of the char is of course a heterogeneous process^{5.)}, and rather complicated. To accomplish it, however, there must be not only sufficient reaction surface but also sufficient open space for the air to enter and for the products of combustion to leave. For this reason the amount of specific surface beyond a certain optimum cannot be utilized.

References

- 1.) Inouye, K., Rice, Neal and Prostel, Edward, "Properties of Chars Produced from Low Rank Coals of the Rocky Mountain Region", FUEL, London, Volume XLI, pp. 81, January 1962.
- 2.) Werner Peters Dr. rer. nat.; "Comparison of Reactivity Tests on Coke", GLUECKAUF, Volume 96, 16, pp. 997-1006, July 30, 1960.
- 3.) Milliken, Spencer R. - Doctor's Thesis, College of Mineral Industries, Pennsylvania State University, June, 1954.
- 4.) Mueller, W. J., and Jandl, E. A., "Rapid Method for Determining the Reactivity of Coke With CO₂", BRENNSTOFF CHEMIE, Volume 19, No. 2, pp. 45-48, 1938.
- 5.) H. Sommers and W. Peters, "The Kinetics of the Oxidation of Coal at Moderate Temperatures", CHEMIE-INGENIEUR - TECHNIK, pp. 441-453, 1954.



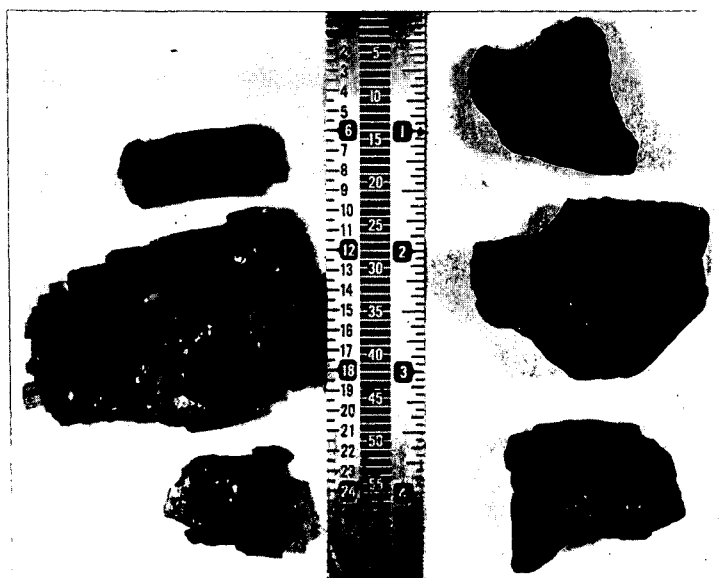
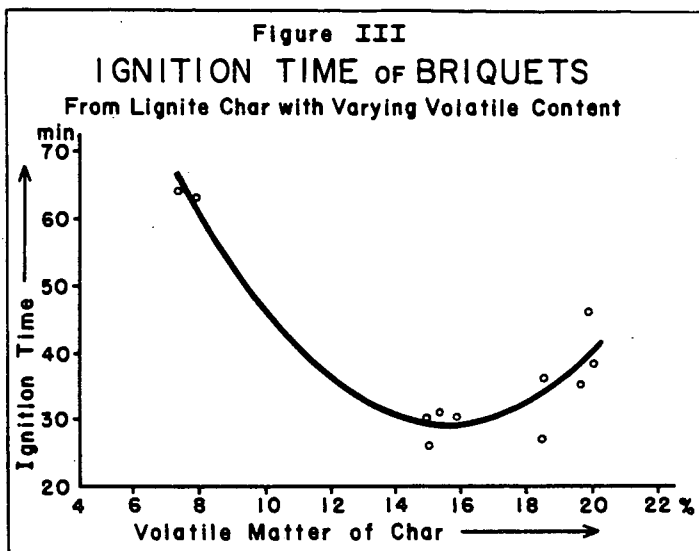
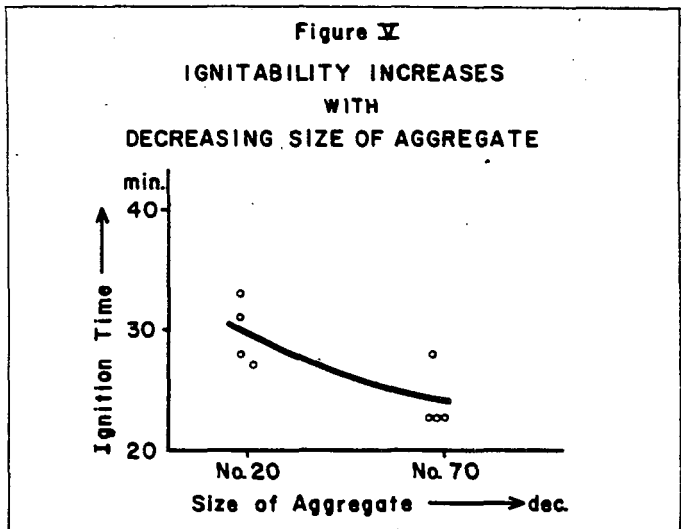


FIGURE IV



ROLE OF FUEL REACTIVITY IN SINTERING

U. N. Bhrany
E. A. Pelczarski

United States Steel Corporation
Applied Research Laboratory
Monroeville, Pennsylvania

Introduction

The sintering process is used to agglomerate the smaller sizes of iron ores that are too small to be fed directly into the blast furnace. In this process, a heterogeneous mixture of iron ore, fuel, and usually flux is deposited as a bed about 8 to 15 inches deep on an endless, moving sinter strand. The strand moves over a series of windboxes that by means of suction draw a downdraft of air through the bed. As the bed moves into position over the first windbox, the fuel in the top of the bed is ignited by gas burners. After ignition, the air flow through the bed sustains the oxidation reaction and at the same time causes the combustion zone to propagate downward to the bottom of the bed. In this manner, only a comparatively small region (combustion zone) of the bed is being heated to sintering temperatures at any one time. Much of the heat released in the combustion zone is then transferred by forced convection, radiation, and conduction to preheat the portion of the bed lying beneath the advancing combustion zone. Thus, because of good heat recovery, the process requires only a small amount of fuel (about 3 to 5% carbon).

The fuel is randomly distributed throughout the bed and may be considered as discrete particles embedded within a massive matrix of inert material. Furthermore, because of the low concentration of fuel in the bed, the fuel particles are well dispersed and can be visualized as distinct entities oxidizing essentially independently of each other when enough air is available for their combustion.

The combustion process can be considered¹⁾ to occur in two regions, as follows: (1) the region where true chemical reaction controls the oxidation rate, and (2) the region in which the mass transfer of oxygen from the bulk gas stream to the carbon surface is controlling. At temperatures below about 1500 F, the reaction rate is independent of air velocity, whereas above this temperature the rate of combustion is directly influenced by velocity and is limited by the mass transfer rate of oxygen. Kuchta, Kant, and Damon²⁾ have shown that in the second region the reaction rate is proportional to the 0.47 power of the air velocity. Furthermore, at very high air velocities the rate approaches that given by the Arrhenius equation for an activation energy of about 30 k cal/g mole. Meyer³⁾ reported similar activation energies and he as well as Mei Chio Chen, et.al.,⁴⁾ showed that the oxidation of carbon is first order with respect to the partial pressure of oxygen.

Wicke⁵⁾ suggests that for the combustion of carbon the activation energy is about 58 k cal/g mole and that lower values than this are probably due to diffusional effects in the porous interior of the carbon. He further states that differences in reactivity are due solely to variations in internal surface area and that depending upon the type of carbon being oxidized, the specific surface may increase by as much as 1400 percent as carbon is gasified. Smith and Polley⁶⁾ report similar results for the oxidation of fine thermal carbon at 600 C. They concluded that because the increase in surface area is not accompanied by a decrease in particle diameter, the particle must develop internal porosity. These results are in accord with Wicke's and tend to confirm his observation that a reaction also occurs on the internal carbon structure. The bulk of the work reported in the literature for oxidation rates of carbon has dealt with low-ash-content materials. However, Grendon and Wright⁷⁾ have studied the combustion of cokes and coals as well as low-ash carbons

through ash barriers. They advance the possibility that the permeability of the residual ash layer surrounding partially burnt commercial fuels influences the burning rate.

Schluter and Bitsianes⁸⁾ have used the combustion model proposed by Tu et al.¹⁾ in an attempt to predict the width of the fuel combustion zone present in sintering processes. In general, the measured widths were two to three times larger than those predicted. In a prepared discussion of their paper, they have stated that since the rate of combustion of fuel in the sintering process is diffusion controlled, the reactivity of the fuel should have little effect on the processes inherent in sintering. However, no experimental data are presented in substantiation. Furthermore, their model is limited to a case where the fuel is assumed to be a dense sphere of shrinking radius that burns only on its surface and hence cannot allow for the effect of porosity and ash that would affect the diffusional resistances.

Dixon and Voice⁹⁾ state that the sintering process demands a relatively unreactive fuel. Too high a reactivity lowers the thermal efficiency of the process and necessitates a higher fuel content in the sinter bed. For example, with fuel reactivities varying from critical air blast (C.A.B.) values of 0.092 to 0.035 ft³/min, no appreciable effect on the thermal efficiency of the sintering process was noted. However, with a highly reactive wood charcoal (C.A.B. = 0.003 ft³/min), there was a considerable drop in thermal efficiency.

The present paper gives the results of a study completed with eight different fuels for characterizing the fuels with respect to their performance in the sintering process, in which a unique combustion situation exists. The oxidation kinetics of cokes containing different amounts of ash are also included. From these studies, a reactivity index is developed for classifying fuels with regard to their behavior in the sintering operation.

Materials and Experimental Work

The materials used in this work were commercially available cokes, coals, and charcoal. The chemical composition and the physical properties are given in Table I.

A Stanton Thermobalance,^(a) two rotameters, and associated hardware for transporting a synthetic air mixture to the reaction chamber were used in this work. Figure 1 is a schematic drawing of the experimental assembly.

The Thermobalance is an integral unit housing a continuously recording temperature controller, a height-adjustable muffle furnace, and an automatic continuously weighing and recording analytical balance. Mounted on one pan of the balance is a silica rod for supporting a fuel sample in the muffle furnace. The furnace may be raised or lowered by means of pulleys to provide access to the sample holder. Furnace temperatures are indicated and controlled by means of a thermocouple located near the furnace wall (see Figure 1). Two other thermocouples situated directly above and below the carbon sample measure the incoming and exit gas temperatures. For all runs, except for the temperature study, the muffle furnace was set at a control point of 1250 plus or minus 4 F.

A typical run was made as follows: the furnace was set at the desired temperature and allowed to come to equilibrium with a synthetic air mixture flowing through the furnace at a flow rate of 11 liters per minute. The coke sample (0.5000 gram each) obtained by riffing a large batch of coke (-20 +28 Tyler mesh) was dried at 130 C for two hours prior to weighing. The sample was then placed in an inconel wire basket having inside dimensions of 0.6 by 0.6 by 0.5 inch. The bed depth of the coke sample in the basket was 0.12 inch. After the basket containing the coke was placed on the silica support rod of the Thermobalance, the muffle furnace was lowered in place; the loss of weight with time was recorded continuously.

(a) Made in England and distributed by Burrell Scientific Company.

Theory

In the manner proposed by Tu et.al.,¹⁾ it can be shown that the combustion rate of carbon is given by

$$N_c = \frac{P_g}{R_d + R_c} \quad (1)$$

where P_g is the partial pressure of oxygen in the bulk gas stream (atm)
 R_d is the diffusional resistance to mass transfer (hr)(atm)/lb mole
 R_c is the chemical resistance (hr)(atm)/(lb mole)
 N_c equals the rate of carbon consumption (lb moles/hr)

Now if reaction conditions are chosen such that chemical reaction controls the rate of carbon consumption, that is, $R_c \gg R_d$, equation (1) reduces to

$$N_c = \frac{P_g}{R_c} = ak p_g \quad (2)$$

where a = area available for reaction
 k = the specific reaction rate constant as given by the Arrhenius equation

In the case of a packed bed of particles having appreciable depth, p_g varies with the depth of the bed. Hence, under isothermal conditions, it becomes necessary to integrate equation (2) between the limits of the inlet and outlet gas compositions to obtain the average value of the rates existing in every part of the bed. Generally it is difficult to maintain isothermal conditions, because the oxidation of carbon is highly exothermic and the reaction temperature tends to rise. However, by use of a differential reactor, rising temperatures are easily treated because rate data may be obtained at each incremental temperature change. Under these circumstances, equation (2) becomes

$$N_c = \alpha a \quad (3)$$

where α is a constant

Equation (3) describes the oxidation of carbon in a chemical-reaction-controlled regime. However, the sintering process occurs at high temperatures of about 2700 F. In this region, the oxidation rate of carbon is controlled by the mass transport of oxygen from the bulk gas phase to the carbon surface; that is, diffusional resistance is much larger than the resistance due to chemical reaction. Hence the carbon combustion can be approximated by modifying equation (1) to

$$N_c = \frac{P_g}{R_d} = k_g a p_g = \frac{DPa}{RTz P_{bm}} p_g \quad (4)$$

where D = diffusion coefficient (ft²/hr)
 R = gas constant (ft³)(atm)/(lb mole)(°R)
 P = total pressure (atm)
 k_g = mass transfer coefficient (lb moles)/(hr)(ft²)(atm)
 z = effective film thickness (ft)
 T = temperature (°R)
 P_{bm} = log mean pressure of inert gas in the film

Equation (4) implies that in a diffusion-controlled regime, the oxidation rate is independent of the carbon being burned and depends only on the transport of oxygen. Within limits, this is true; but with cokes or carbons of widely different porosities and varying ash contents, the effective film thickness (z) and the area available for reaction (a) may be vastly different at identical air flow rates. Second, with fuels having a high ash content, it is known that an ash structure can surround the unburnt carbon⁷⁾ and may impede combustion through its effect on the diffusion

coefficient. Thus the properties of the fuel can influence the combustion rate of carbon in the sintering-temperature (diffusion-controlled) region.

Results and Discussion

The Effect of Temperature on the Oxidation Rate of Coke

Most of the kinetics work was performed with coke C because it had been found to be an excellent fuel for sintering. In the study of the effect of temperature on the oxidation rate, the correlating temperatures were the exit gas temperatures leaving the bottom of the differential reactor. In general, these temperatures are about 150 F higher than the furnace temperature. But optical-pyrometer measurements of the top of the packed bed of particles at temperatures above 1400 F gave temperatures about 25 to 50 degrees higher than the exit gas temperatures. Visual observation of the bed showed a considerable nonuniformity in burning; discrete particles of coke could be seen burning more brilliantly than others in various parts of the bed. Consequently, exit gas temperatures were assumed to be representative of the bed temperature.

The results of the oxidation tests at various temperatures are presented in Figure 2. In these tests, the exit gas temperature increases and reaches a maximum and thereafter decreases with time to a constant level. For proper evaluation of the reaction rate, the weight-loss data must be corrected for volatile matter. This was done by heating the coke to various temperatures in N_2 and obtaining devolatilization rate curves. The volatile matter loss is then subtracted from the gross weight loss to obtain the weight loss due to oxidation.

With these data, an Arrhenius plot was made of the reaction rate expressed in pound moles of carbon consumed per hour per square foot of total surface area. The results are presented in Figure 3. Also included in this plot are the data given by Wicke²⁾ for electrode carbon. Only at temperatures below about 1400 F do the experimental data lie along the curve given by Wicke. This corresponds to an activation energy of 58 k cal/g mole, which indicates that the oxidation of carbon is controlled by chemical reaction. As the temperature is increased above 1400 F, the effect of diffusion becomes increasingly significant and the data deviate considerably from the straight-line Arrhenius relationship.

From the kinetic data of curve 2, Figure 2, the total surface area of coke C was calculated with the use of a known specific reaction rate constant for electrode carbon. The calculated surface area based on points taken over the entire curve was $3.0 \text{ m}^2/\text{gram}$ (standard deviation 0.39). Experimental nitrogen adsorption (BET) surface-area measurements showed that the surface area of coke C was essentially constant at $3.4 \text{ m}^2/\text{gram}$ at various degrees of oxidation. A similar calculation for charcoal H (Figure 4) at 30 percent weight loss gave a total surface area of $4.8 \text{ m}^2/\text{gram}$, whereas the BET method gave a value of $5.2 \text{ m}^2/\text{gram}$ for a fresh sample. These values indicate that the combustion of different fuels is primarily dependent on the surface area of the material. It should be mentioned that these calculations are based only on the fixed carbon available in the coke sample, whereas the BET method makes no distinction between ash and carbon contributions to the total area. Consequently, for high-ash materials it is expected that the adsorption technique will yield surface areas considerably different from those calculated from the oxidation curves.

These two fuel samples cover the extreme oxidation rates encountered in this report; that is, coke C burns at the slowest rate and charcoal H at the most rapid. As the oxidation rates for both fuels correlate rather well with their BET surface areas, it appears that the gross oxidation phenomenon in a chemical-reaction-controlled regime where excess oxygen is always available is directly related to the total surface area of the solids. However, a more fundamental study would probably reveal that

additional carbon properties such as anisotropy and lattice defects influence the true kinetics of oxidation. In addition, the impurities also have an effect on the oxidation rate.

The Air Oxidation of Various Sinter Fuels

To determine their relative ease of oxidation, eight different fuels were oxidized in air at a furnace temperature of 1250 F. (The compositions of the fuels are given in Table I.) The results of this study are presented in Figure 4.

Each fuel was tested in duplicate runs to check on data reproducibility. Figure 4 indicates that the fuels can be ranked in order of increasing reactivity, that is, ease of oxidation, as follows: C, E, G, F, D, A, and H. Coke B behaves somewhat anomalously in that it has the fastest initial burning rate, but quickly slows down. We believe that because of its high ash content (Table I), the ash can decrease the carbon surface available for reaction and also increase the diffusional path across which the mass transfer of O_2 occurs. Consequently, as more and more carbon is consumed, the ash becomes increasingly significant in preventing the exposure of carbon surface to the oxidizing gas, and the rate of oxidation diminishes.

Several tests were also completed to obtain oxidation data at a furnace temperature of 1600 F. The results of this work are presented in Figure 5. A comparison of Figures 4 and 5 shows that in general the oxidation curves for both low- and high-temperature tests are ranked in the same manner; that is, coke C is still represented as the slowest burning coke regardless of the temperature of oxidation, and similarly for the other cokes. A slight anomaly does exist: the low-temperature work indicates that charcoal D and coke A should behave similarly, whereas the high-temperature data suggest a higher reactivity for the activated charcoal. It is believed, however, that this difference is due to the experimental technique and may be explained as follows. The size of the sample and the cross-sectional area of the reactor basket used in both cases were the same. Consequently, the height of the sample in the basket for coke A as compared with the height for charcoal D varies with the ratio of the apparent specific gravities. Thus the sample height for coke A is 1.48 times that for charcoal D. This has two adverse effects on the oxidation rate: (1) the pressure drop across the basket increases causing more air to flow around the basket rather than through it, and (2) the partial pressure of CO_2 increases in the bed. These two factors tend to depress the reaction rate. At low temperatures, this result is not evidenced because the reaction rate is slow and the air flow is large enough to offset any effects due to changes in partial pressure of oxygen.

A short study was made to determine the variation of the coke particle size with increasing degree of oxidation. These data, for coke C initially minus 20 plus 28 mesh, are presented in Table II. The particle size is relatively independent of the percent oxidation. Even after 87 percent weight loss, the oxidized sample still contained 71.5 percent of the original screen size. This is in agreement with the results reported by others.^{5,6} A sample oxidized at a furnace temperature of 1600 F exhibited considerable fusion of the particles as reflected by the creation of 21.2 percent of a plus 20-mesh fraction. As the initial particle size was all minus 20 plus 28 mesh, the data suggest that at higher temperatures, the oxidation rate of high-ash fuels may be affected by partial fusion or sintering of the ash. In particular, if the ash becomes sufficiently fluid to occlude the surface of the carbon, a corresponding decrease in rate should occur.

The Reactivity Index as a Measure of Fuel Performance in Sintering

In the sintering process, only the fixed carbon is considered to be useful for generating the required heat flux. Voice and Dixon⁹) in summarizing the available literature on the subject report that any heat generated by the combustion of volatiles lowers the thermal efficiency of the sintering process.

As no one property of the fuel, such as ignition temperature, fixed carbon content, or ash content, can adequately describe its behavior during the combustion process, a reactivity index based on 50 percent weight loss of fuel has been defined. For this purpose, we choose to set the air oxidation test conditions just outside of the region in which chemical reaction alone controls the oxidation rate, where the differences in the reactivities of fuels could be easily distinguished. For our equipment, this corresponds to an air flow rate of 11 liters per minute and a furnace temperature setting of 1250 F.

A measure of the reactivity of fuels under these conditions is the area under the percent weight loss versus time curve (Figure 4). In this manner, fuels having a fixed carbon content of as low as 50 percent may be included in this index. The area under the curve is then normalized to place all measurements on a per gram of fixed carbon basis. Thus the reactivity index ϕ is defined as

$$\phi = \frac{\int_0^{t_{50}} \frac{m(t) dt}{m_0/f}}{10^{-4} F} = 10^{-4} F \int_0^{t_{50}} w(t) dt \quad (5)$$

where t_{50} = time for 50 percent weight loss
 $m(t)$ = weight loss in grams as a function of time
 m_0 = initial sample weight (grams)
 f = weight fraction of fixed carbon in sample
 $w(t)$ = percent weight loss of sample as a function of time
 F = percent weight fraction of fixed carbon in sample

The reactivity index ϕ is correlated with sinter production rate as shown in Table III. Sufficient samples were not available for sinter pot tests to be run on all the fuels studied. However, the data establish the general trend. Fuels having a reactivity index greater than 1.65 appear to yield a sinter production rate of about 4.2 tons per day per square foot. These fuels are acceptable for the sintering process. Below an index of 1.65, the production rate decreases. The performance of those fuels having a reactivity index between about 1.35 and 1.65 can be improved by blending with a better-quality fuel. Fuels having an index of less than 1.35 are unsatisfactory for use as sinter fuel.

Fuel Reactivity and the Mechanism of Sintering

We have observed that the oxidation of the more reactive fuels results in a higher carbon monoxide concentration in the waste gas. This is due to incomplete combustion of the fuel and/or the gasification of carbon. In either case, the thermal efficiency of the sintering process is lowered and a higher fuel content in the sinter bed is often required to accomplish the desired result. Highly reactive fuels also tend to minimize thermal efficiency because of their susceptibility to rapid weight loss at relatively low temperatures. The decrease in thermal efficiency may be visualized by considering the temperature profile that exists in a sinter bed.

In general, there are three regions of major interest: the sinter-mix preheat zone, the combustion zone, and the sinter cooling zone.¹⁰⁾ In a downdraft sintering process, these zones leave the bottom of the packed bed in the given order. Consider now only the preheat and combustion zones. As sinter feed mixture passes under the ignition burner, the fuel in the top part of the bed is ignited to initiate the formation of the combustion zone. At the same time, the downdraft of air drawn through the bed is rapidly transferring heat from the combustion zone to the immediately preceding preheat zone. At this particular time, the unreacted fuel in the preheat zone is exposed to temperatures varying between the ambient bed temperatures and those of the approaching flame front. If the fuel is highly reactive, then a significant portion of the carbon may be lost through oxidation with air in the preheat zone. This results in smaller amounts of carbon being available for combustion in the combustion zone, and thus reduces the heat flux for sintering. Furthermore, the

reactive fuel burns quickly and generates an intense heat in a narrow combustion zone. Consequently, the normal heat-transfer process from gas to solid cannot keep up with the rapidly moving combustion zone, and the result is the formation of a weak sinter.

If a less reactive fuel is used, premature oxidation of the carbon in the preheat zone is minimized, and more complete burning occurs. This causes a relative increase in the width of the combustion zone that (1) permits the heat-transfer processes occurring in the bed to operate in phase with the combustion process, and (2) prevents localized melting because more uniform temperatures are obtained in the combustion zone. It is known that excessive fusion tends to cause the sinter bed to slag over and thus to depress production rates, whereas too little fusion results in weak sinter. Consequently, a good sinter fuel will permit operation between these two extremes.

On the basis of the reactivity index, as well as the oxidation data of Figure 4, the results tend to indicate that the slower burning fuels are most desirable for sintering purposes. This is consistent with our present understanding of the sintering process. In general, the reactivity index appears to yield useful information on the expected production rate that may be obtained with a given fuel. It ranks sinter fuels on a relative scale with respect to their performance in the sintering process. The test is particularly useful for the evaluation of small samples.

Conclusions

Evidence is presented that tends to show that in a chemical-reaction-controlled regime, the oxidation kinetics of carbonaceous fuels depend upon the total (BET) surface area of the fuel particles. This is in agreement with the observations of Wicke.⁵⁾

A reactivity test based on the oxidation characteristics of various sinter fuels has been developed. This index correlates with the production rates of iron-ore sinters. In general, the best sinter production rates are obtained when the sinter fuels are slow burning; that is, when they are relatively unreactive.

References

1. Tu, C. M., Davies, H., and Hottel, H. C., IEC, 26, 749, 1934.
2. Kuchta, J. M., Kant, A., and Damon, G. H. IEC, 44, 1559, 1952.
3. Meyer, Z., Physik. Chem., BL7, 385, 1932.
4. Mei Chio Chen, Christensen, C. J., and Eyring, H., J. Phys. Chem., 59, 1146, 1955.
5. Wicke, E., 5th Symposium on Combustion, Pittsburgh, 245, 52, 1954 (Published 1955).
6. Smith, W. R., and Polley, M. H., J. Phys. Chem., 60, 689, 1956.
7. Grendon, H. T., and Wright, C. C., "Transactions of the Eleventh Annual Anthracite Conference of Lehigh University," May 7-8, 1953, Bethlehem, Pa.
8. Schluter, R., and Bitsianes, G., in "Agglomeration," edited by Knepper, W. A., Interscience Publishers, New York, 1962, p. 585.
9. Dixon, K. G., and Voice, E. W., Journal of the Institute of Fuels, 251, p.529, 1961.
10. Ban, T. E., et.al. in "Agglomeration" edited by Knepper, W. A., Interscience Publishers, New York, 1962, p. 511.

TABLE I
The Chemical Composition of Various Sinter Fuels

Fuel	A (coke)	B (coke)	C (coke)	D (charcoal)	E (coal)	F (coke)	G (coke)	H (charcoal)
Sulfur*	0.65	0.78	1.22	0.10	0.57	0.93	3.61	0.11
Fixed Carbon	86.08	60.61	85.40	86.69	74.16	87.75	86.80	86.83
Volatile Matter	6.29	12.87	4.30	5.83	7.80	4.21	12.65	8.16
Ash	4.94	25.51	10.01	4.08	16.26	7.28	0.51	4.55
Total Carbon	86.92	66.32	87.90	88.67	76.47	88.43	90.70	87.80
Moisture	2.69	1.01	0.29	3.40	1.78	0.76	0.04	0.46
True Specific Gravity	1.65	1.69	1.89	1.77	1.70	1.81	-----	-----
Apparent Specific Gravity	1.05	1.60	1.70	1.55	1.64	1.46	1.33	1.291

*Compositions in weight percent.

TABLE II

The Effect of Air Oxidation on the Particle Size
of Coke C

Percent Oxidized*	0	10	21	40***	67.5	87****
Screen Analysis of**						
Oxidized Fuels (Cumulative %)						
Tyler Mesh						
+20	0	5.1	2.4	-	5.7	21.2
-20 +28	100	96.0	93.1	85.4	77.5	71.5
+35	-	98.6	96.5	91.5	96.0	89.1
+48	-	98.8	96.9	93.2	97.9	92.5
+65	-	98.9	97.3	96.1	99.1	95.4
+100	-	99.0	98.0	97.7	99.6	96.8

* Samples oxidized at a furnace temperature of 1250 F at an air flow rate of 11 liters per minute.

** Screen analysis obtained by hand screening of samples for two minutes.

*** Ro-tapped for 15 minutes.

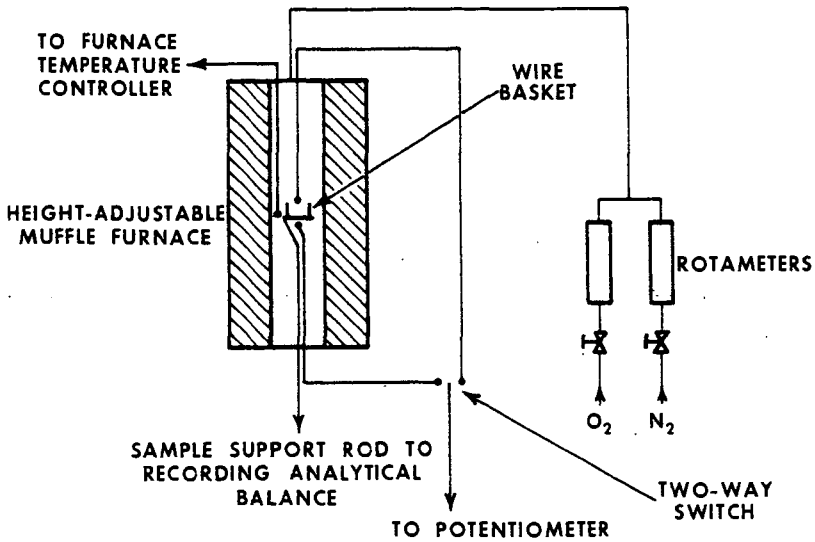
**** Furnace temperature 1600 F.

TABLE III

The Correlation of Sinter Production Rate With the
Reactivity Index of Sinter Fuels

Fuel	Reactivity Index (\emptyset)	Sinter Production Rate Tons/day/ft ²
C (coke)	2.50	4.2
E (coal)	1.84	4.2
F (coke)	1.70	---*
G (coke)	1.68	4.2
D (charcoal)	1.43	---*
A (coke)	1.40	3.8
H (charcoal)	1.25	---*
B (coke)	1.24	3.4

*Insufficient sample to run sinter pot test.



SCHMATIC DRAWING OF EXPERIMENTAL EQUIPMENT

FIGURE 1

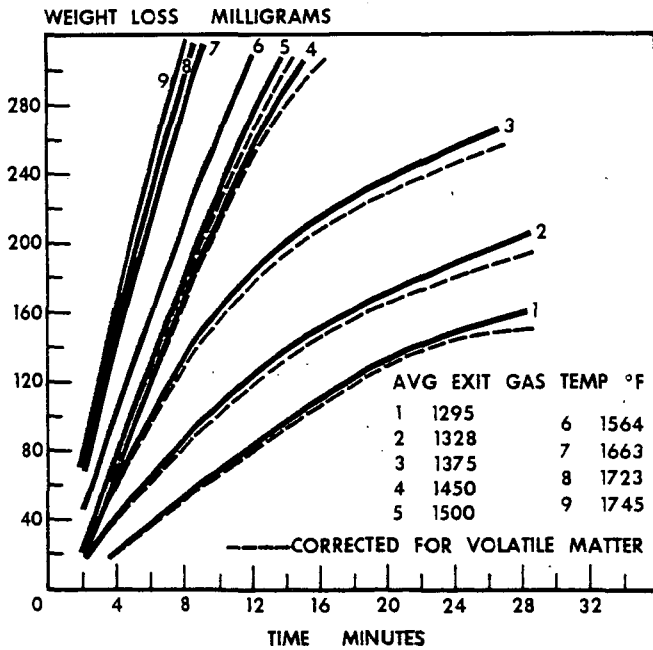


FIGURE 2

AIR OXIDATION OF COKE C AT VARIOUS TEMPERATURES

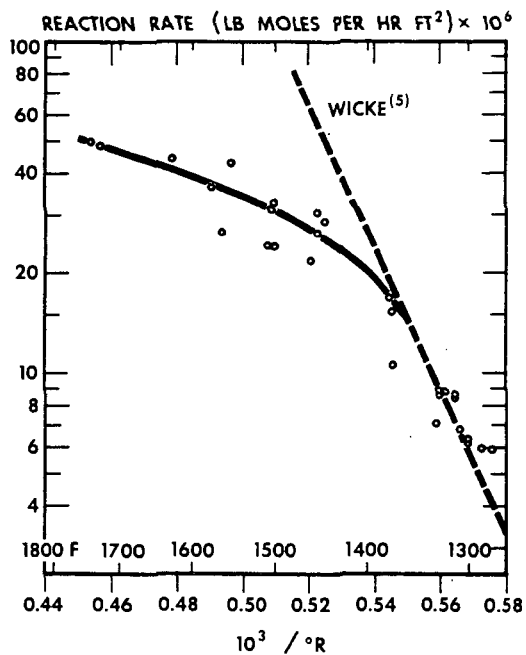


FIGURE 3

EFFECT OF TEMPERATURE ON THE SPECIFIC REACTION RATE OF COKE C

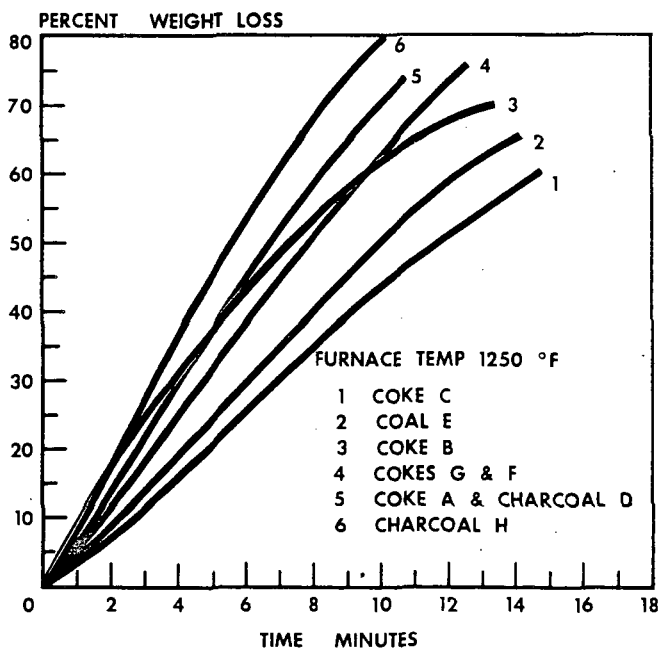


FIGURE 4

AIR OXIDATION OF VARIOUS FUELS

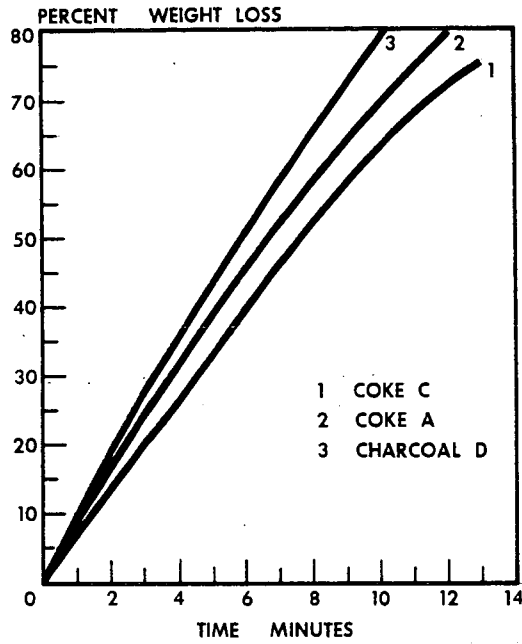


FIGURE 5

AIR OXIDATION OF VARIOUS FUELS AT 1600 F

BLAST FURNACE TESTS WITH COKES OF DIFFERING REACTIVITY

By A. A. Triska

Great Lakes Carbon Corporation, Chicago 1, Illinois

Pig iron is produced in blast furnaces by heating and reducing iron ore with furnace coke and products of combustion. Combustion and gasification of the coke near the bottom of the furnace provide the required temperatures and reducing atmosphere. This paper deals with coke savings observed on commercial blast furnaces when petroleum coke was added to the coal blend before carbonizing in by-product ovens. An analysis of the furnace operating results indicate that changes in coke structure which affect reactivity were responsible for reduction in coke rate.

HISTORY

Blakley and Cobb (1) in England, and Broche and Nadelman (2) in Germany, are typical of many investigators who have speculated for many years on desirable coke characteristics for blast furnace use. They concluded that a coke arriving at the tuyeres in larger proportions was desirable. To attain this, the gasification of coke carbon further up the shaft must be reduced. This gasification is called "solution loss" which involves the reaction of coke carbon with carbon dioxide originating from indirect reduction of iron oxides and calcination of carbonates.

Our experience with special foundry coke indicates that a furnace coke less reactive to gasification in the upper and cooler portion of the furnace can be produced. A coke of this type contains less internal pore surface and thicker cell walls. When used in cupolas, a coke reduction is experienced, in addition to use of more air per pound of coke charged, higher combustion temperatures, and higher concentration of carbon dioxide in the off-gas. The increased carbon dioxide concentration indicates that the reaction of coke carbon with carbon dioxide can be depressed in cupolas. Thus, if the same can be accomplished in a blast furnace, the "solution loss" would be reduced.

The practical advantage experienced by the use of special foundry coke in cupolas led to the idea that blast furnace coke could similarly be improved. Hence, plant scale blast furnace tests were planned.

PRELIMINARY PLANT TESTS AT OBERSCHELD, GERMANY

A one month test, with a low internal surface dense foundry coke, was made in a small blast furnace producing foundry pig iron at Hessische Berg-Und Huttenwerke, Oberscheld, Germany. In this test various proportions of normal furnace coke were replaced with dense H-C Coke, a special foundry coke. This coke was produced by Verkaufs Vereinigung Fur Teererzeugnisse who operate under a license agreement with Great Lakes Carbon Corporation.

Table I summarizes the results of a 166-hour test on the Oberscheld blast furnace in which 33.4 percent H-C Coke was substituted for normal coke. The data show the average practice for normal coke and for a mixture of 2/3 normal coke and 1/3 of H-C Coke.

The replacement of 33.4 percent normal coke by H-C Coke was accompanied by an increase in silicon and a reduction of sulphur in the hot metal, reflecting increased hearth temperatures. As a result, the operator chose the following changes in practice while producing iron of comparable sulfur content :

- 1) Coke rate reduction of 44 pounds per ton of hot metal
- 2) Blast temperature reduction of 144°F
- 3) Increase in hard to reduce ore of 174 pounds per ton of hot metal
- 4) Reduction of scrap iron of 192 pounds per ton of hot metal
- 5) Reduction in stone rate of 138 pounds per ton of hot metal with equal slag volume at a basicity reduction from 1.40 to 0.95.

TABLE NO. I

H-C COKE PERFORMANCE VS NORMAL COKE
OBERSCHELD BLAST FURNACE TEST II
 (Working Volume - 7230 Cu. Ft.)

<u>TEST CONDITIONS</u>	<u>NORMAL COKE</u> (28 Days)	<u>H-C COKE MIX</u> (166 Hours)
<u>FURNACE COKE</u>		
Normal Coke, %	100 Days	66.6
H-C Coke, %	-	33.4
<u>COKE ANALYSIS</u>		
Ash, %	8.7	7.2
Sulfur, %	0.92	0.97
<u>FURNACE CHARGE</u>		
Pounds Coke/THM (As charged)	1860	1816
Pounds Stone/THM	384	246
Ore, % Fe	40.2	41.7
Pounds Scrap Iron/THM	426	234
Pounds Hard To Reduce Ore/THM	224	398
Pounds Oxygen in Ore/THM	618	732
<u>PRODUCTION</u>		
Tons Hot Metal Per Day	167.0	173.6
Hot Metal, % Silicon	3.22	2.93
% Sulfur	0.016	0.021
Slag Volume, Pounds/THM	1338	1342
Slag Basicity, Base/Silica and Alumina	1.40	0.95
Off Gas, % Carbon Dioxide	8.2	9.1
% Carbon Monoxide	32.3	31.5
% Hydrogen	2.4	2.0
% Nitrogen	57.1	57.4
<u>OPERATING CONDITIONS</u>		
Blast Temperature, °F	1526	1382
Blast Pressure, PSIG	9.38	9.41
Wind Delivered, CFM	10430	10400

It was difficult to evaluate the results given in Table I in respect to coke savings by the use of H-C Coke as the burden used during the test period differed considerably from the one normally used. During the test period on H-C Coke 398 pounds of so called hard to reduce ore were used per ton of hot metal compared with 224 pounds during the base period. With normal practice it was reported an excess of 250 pounds or hard to reduce ore results in cold iron at Oberscheld. The significance of an increase of 174 pounds of ore per ton of hot metal cannot be fully appreciated unless it is pointed out that extremely dense Kiruna D, Swedish Magnetite, was charged in 4-6 inch lumps. Such ores would tend to contribute to carbon dioxide at low levels in the blast furnace and result in more solution loss. A reduction in the scrap per ton of hot metal from 426 pounds in the base period to 234 pounds in the test period is also significant because an additional amount of iron had to be reduced from ore.

In order to obtain a better understanding of coke saving, the practice values obtained were evaluated with the use of the Flint Coke Rate Formula (3) (4) which corrects for burden and iron analysis variations. The results thus calculated are shown on Graph No. I. The significance of this Graph was that a calculated coke saving occurred and increased linearly with H-C Coke replacement of normal furnace coke. Of special importance was the excellent correlation of the results with variation of percentages of H-C Coke used from which it was concluded that the data obtained are reliable. This conclusion ultimately led to the development of a special furnace coke.

TABLE NO. II

RESULTS OF H-C COKE REACTIVITY
OBERSCHELD TEST II

<u>OPERATING VARIABLES</u>	<u>CHANGE IN PRACTICE VALUE</u>
Coke Reduction, pounds/THM	87 (a)
Blast Temp. Reduction °F	144
Stone Reduction, Pounds/THM	138
Slag Basicity Reduction, Base/Silica and Alumina	0.45
CO ₂ , Increase in Off-Gas, %	0.9

(a) Corrected for burden variation with Flint Coke Rate Formula.

Table No. II. shows that the preliminary Oberscheld blast furnace tests with special foundry coke resulted in reduced coke rate, reduced stone usage and increased carbon dioxide content in the off-gas. Of special interest is the fact that normal desulfurization was obtained despite the reduction of 0.45 slag basicity from 1.40 to 0.95 at equivalent slag volume and slag sulfur content. (1.3). These findings were anticipated from our cupola experience with dense foundry coke.

DEVELOPMENT OF P-C COKE

Before making further blast furnace tests a special low cost furnace coke was developed simulating the useful reactivity characteristics displayed by 33.4 percent H-C Coke mixtures with normal furnace coke. This coke, called P-C Coke, was manufactured in normal by-product ovens and was produced from coal blends containing appropriately sized petroleum coke. A three (3) month and a one (1) month plant scale blast furnace test were made with this coke at two (2) large steel plants in the States.

COOPERATIVE COLORADO FUEL AND IRON CORPORATION TESTS

The initial use of P-C Coke in a blast furnace was made at the Pueblo Plant of The Colorado Fuel and Iron Corporation. This coke was produced from their normal high volatile coals and the replacement of low volatile coals with minus 1/8 inch petroleum coke furnished by Great Lakes Carbon Corporation. Petroleum coke is the residue obtained from coking residual petroleum oil.

TABLE NO. III

P-C COKE PERFORMANCE VS REGULAR COKE
CF&I THREE MONTH PLANT TEST

(Hearth Dia., 20 Ft., 3 In., Working Vol., 26015 Cu. Ft.)

<u>TEST CONDITIONS</u>	<u>REGULAR COKE</u>	<u>P-C COKE</u>	
	<u>BASE PERIOD</u> (158 Days)	<u>AVERAGE</u> (85 Days)	<u>AVERAGE</u> ^(a) (23 Days)
<u>COKE ANALYSIS</u>			
Ash, %	11.6	11.8(b)	11.8(b)
Sulfur, %	0.57	0.63	0.61
<u>FURNACE CHARGE</u>			
Pounds Coke/THM (As charged)	1514	1414	1350
Pounds Stone/THM	605	547	509
Theoretical Pig Yield, %	53.3	52.8	53.6
<u>PRODUCTION</u>			
Tons Hot Metal Per Day	651	655	709
Hot Metal, % Silicon	1.13	1.10	1.08
Hot Metal, % Sulfur	0.044	0.045	0.047
<u>OPERATING CONDITIONS</u>			
Blast Temperatures, °F	1075	981	1000
Blast Pressure, PSIG	19.9	21.5	21.4
Wind Delivered, CFM	35560	34410	35320

Note (a) Snowfall 0.1" water compared to normal of 0.03".

Note (b) Problems in Washery caused coal ash increase. Petroleum coke contains 0.3 percent Ash.

Table III summarizes the results of a three (3) month blast furnace P-C Coke test in comparison with normal practice. The data shown in Table III represent the average values obtained. It is to be noted that the information was gathered from operating records. The values appearing in the last column under the heading "Average" (23-day) represent a 23 day, consecutive period included in the 85 day test run. A review of Table III indicated the following :

1. Hearth Temperature Increase - Visual inspection of the tuyeres, at the time, when P-C Coke first reached the hearth, showed an increase in temperature. An increase in the percent of silicon and a reduction in sulfur in the hot metal produced also reflected an increase in hearth temperature. This increase in hearth temperature permitted, and in fact required, changes in practice to produce hot metal of the usual analysis.

Average changes in practice for the 85 day period on P-C Coke follows :

1. Coke rate reduced 100 pounds.
2. Stone rate reduced by 58 pounds.
3. Blast temperature reduced by 94° F.

Inasmuch as the carbon content of the coke remained essentially constant a reduction of this order of magnitude in the coke rate indicates that more heat was obtained from each pound of P-C Coke charged. This follows because the heat required per ton of iron did not change significantly as the chemical and physical character of the burden remained fairly constant.

2. Solution Loss - A reduction in solution loss is indicated by the use of more air (1.8 cubic feet) per pound of P-C Coke charged, despite a reduction of 2620 cubic feet of wind per ton hot metal. This shows that a larger percentage of the coke reaches the tuyeres and less of it was gasified above the tuyeres. The reduction in gasification above the tuyeres is attributed to the lower reactivity of the P-C Coke towards carbon dioxide. The twofold effect of decreasing solution loss and bringing more carbon to the tuyeres is larger than one might at first anticipate.

For simplicity it will be assumed that solution loss of carbon is decreased by 48 pounds or 4 pound mols per ton hot metal.

HEAT EFFECTS OF REDUCING SOLUTION LOSS

Heat Loss due to Solution Loss	$4C + 4 CO_2$	$= 8 CO$	296,780 BTU
Heat Gain due to Combustion	$4C + 2O_2$	$= 4 CO$	190,200 BTU
Additional Heat Available			486,980 BTU

Thus from the above tabulation it can be seen that a reduction in solution loss of 50 pounds increases the available heat by about 500,000 BTU per ton of hot metal.

3. Blast Temperature - Because the furnace was a little tighter the operators chose to operate with a 94°F lower blast temperature on P-C Coke. By improving the physical character of the burden (such as pellets, etc. ,) so as to reduce blast pressure, a still further improvement in coke rate would have been possible by keeping the blast temperature closer to normal levels. As an alternate some 3 to 4 grains of moisture could have been added to the blast to obtain a faster rate of driving and more tonnage. The effect of blast humidity is manifest in the 23 day period when the average rainfall (snow) was above normal. Hot metal tonnage and coke rates were more favorable during this period as shown in Table III.
4. Blast Pressure - The slight tightening of the furnace with P-C Coke resulting in a blast pressure increase of 1.6 pounds was, in the main, ascribed to a reduction of the volume of the raceway. The reasoning for this was that the conditions appeared similar to those experienced by others with increased blast temperature (5) or oxygen enrichment (6). Credence to this hypothesis was further given by the practice in the 23 day period resulting in normal wind rates and 9 percent capacity increase with a 164 pound coke reduction. The increased coke rate reduction shows the potentials that exist with improved practice such as increased humidity in blast and better gas solid contact.

Further, foundry experience with dense coke leads to the theory that the maximum carbon dioxide concentration in the combustion zone with P-C Coke is higher and located closer to the tuyeres than with normal coke. A condition of this type would explain the tightening of the furnace and loosening with steam.

OPERATING VARIABLES CHANGED BY USE OF P-C COKE

Table IV summarizes the change in practice values attributed, in the main, to improved useful coke reactivity. To some extent the reduction in coke rate was also contributed to by the increase of 11.0 to 14.2 percent in the iron concentration in the charge caused by a reduced coke and lime volume in the 85 and 23 day periods respectively. The increase in air requirement per pound of coke charged and reduction in air required per ton of hot metal is in agreement with our dense foundry coke experience in cupolas and is significant.

Manes and Mackay (7) with thermal and equilibrium data, constructed a simplified model of a blast furnace to derive a quantitative estimate of coke rate. They show a coke saving results from an increase in air per pound of coke charged with concomitant reduction in air per ton hot metal. This is the same finding as found in the CF&I test.

TABLE IV.RESULT OF P-C COKE REACTIVITY
CF&I THREE MONTH PLANT TEST

<u>OPERATING VARIABLES</u>	<u>CHANGE IN</u>	
	<u>PRACTICE VALUE</u>	
	<u>AVERAGE</u>	<u>AVERAGE</u>
	<u>(85 Days)</u>	<u>(23 Days)</u>
More-Air/Pound Coke Chg., Cu. Ft.	1.8	1.5
Less Air/THM, Cu. Ft.	2620	6450
Less Coke/THM, Pounds	100	164
Less Blast Temp. °F	94	75
Less Stone/THM, Pounds	58	96
Increase in Daily Metal Production, %	0.6	8.9

P-C COKE STRUCTURE

Before reviewing the reducing and temperature conditions in a blast furnace as related to fundamentals of coke gasifications, the significant structural characteristics of P-C Coke are discussed. Of special importance are those P-C Coke characteristics which affect its rate of gasification at various temperatures experienced in a blast furnace.

The physical coke characteristics relating to gasification are significantly affected by inclusion of petroleum coke in the coal blend when producing P-C furnace coke. These become readily apparent when viewed under a microscope.

The effect of replacement of low volatile coal with petroleum coke in a given blast furnace coal blend is shown in Figures 1 and 2 at 10X magnification. In Figure 1 the normal blast furnace coke produced with low volatile coals is shown. The black portions are the pores filled with a black resin while the light portions are the cell walls. The specimen before photographing requires a high degree of polish. In this operation, great care was exercised so that some of the fragile extremely thin cell walls are not in part destroyed. Normal furnace coke in Figure 1 at 10X magnification gives the appearance of discontinuity of some of the fine white cell walls. When this is viewed under a microscope at 40X magnification the continuity of the cell walls can be observed. It is, however, to be noted that in Figure 4 at 40X magnification the discontinuity of the fine cell walls is again noted. The reason for this is the lack of photographic sensitivity with the bright lighting required. This type of lighting is required for accentuating the petroleum coke highlights and was used for all photographs. When keeping this in mind it is noted that the normal furnace coke shows a larger number of relatively small pores with considerable thin cell walls as compared to P-C Coke shown in Figure 2. Further comparing the 10X magnification of normal and P-C Coke it is noted that P-C Coke has larger pores.

In Figure 2, attention is called to the amorphous-appearing white highlights in the cell walls. These highlights are petroleum coke particles which are firmly bonded into carbonized coal matrix. Close inspection as shown by 40X magnification of P-C Coke in Figure 3 also reveals that larger particles of petroleum coke are tightly bonded into the matrix and that fine petroleum coke particles are included in the cell walls thus contributing to their thickness. For comparison purposes Figure 4 shows a 40X magnification of normal furnace coke. This again shows in comparison to Figure 3 that the cell walls in P-C Coke are massive and thick. In order to observe the effect of low volatile coal in the normal furnace blend, a coke was produced in a commercial oven without the use of low volatile coal in the high volatile coal blend. The coke thus produced is shown in Figure 5 at 40X magnification. An inspection shows that even thinner cell walls resulted with the removal of low volatile coal from the normal furnace coke blend. Therefore, the thicker cell walls in P-C Coke are not attributed to the removal of low volatile coal from the blend, but rather to its replacement with petroleum coke. To accomplish this the petroleum coke must have altered the coalescence of the plastic coal in such a manner as to produce thicker cell walls in the P-C Coke.

That petroleum coke contributes to the coalescence of cell walls at first may seem surprising as it does not become plastic in the same manner as bituminous coking coals on heating. In order to assist in clarification of this property, petroleum coke was macroscopically inspected before and after carbonization. Figure 6 shows a 10X magnification of petroleum coke before carbonization. The black portions are the pores filled with a black resin and the light portion represents the cell walls. Of interest are the black lines traversing the cell walls. These lines are thermal shrinkage cracks and on carbonization result in structural weakness in the P-C Coke produced. In order to eliminate this weakness, petroleum coke must be precrushed to about 90 percent or more minus 1/8 inch in size, before inclusion in the coal blend. An impact type mill has been found quite satisfactory for this purpose.

On carbonization of petroleum coke the thermal shrinkage cracks are accentuated as illustrated in Figure 7. These fissures, of course, can be substantially eliminated by precrushing. The amorphous appearing cell walls are bordered by a darker appearing homogeneous mass. This is the carbonization product of the heavier volatile content of the petroleum coke as it was expelled thermally from the internal portion of the petroleum coke. At one point of the thermal treatment during carbonization this material was plastic. This plastic portion of petroleum coke is not visible in P-C Coke. It was therefore concluded that it is diffused with the plastic material from the coal contributing to both bonding and coalescence of the cell walls.

However, as the plastic mass is limited, petroleum coke does not exhibit the bonding characteristics on heating typical of bituminous coking coals. This may explain why a more thorough blending with petroleum coke is desirable for higher tumbler values. From the macroscopic analysis it was concluded that the major structural differences between P-C Coke and normal furnace coke are :

1. Carbon Concentration - There is a higher concentration of carbon or a more continuous outside carbon surface of P-C Coke due to thicker cell walls caused by coalescence and inclusion of fine petroleum particles in the cell walls. (This is also confirmed by a 12.5 percent increase in apparent specific gravity of P-C Coke as compared to normal furnace coke.)
2. Internal Surface - There is a substantial reduction of internal surface area due to reduction of the number of fine pores.
3. Larger Pores - There are larger pores in P-C Coke due to coalescence of the plastic material from coals.

These enumerated P-C Coke characteristics enhanced the coke performance in the blast furnace test runs.

Before discussing the gasification characteristics of P-C Coke in relation to blast furnace conditions it may be well to enter into a brief review of the fundamental coke gasification concepts.

FUNDAMENTALS OF COKE GASIFICATION

Coke gasification has been studied extensively by a larger number of investigators over the years and reported in the literature. The accepted theory states gasification is a surface phenomenon which is greatly accelerated by temperature and retarded by surface films. The surface film which is the boundary between coke and oxidizing gases varies in thickness depending on the rate of coke gasification and disengagement of these gases. This is a dynamic balance and increased gas velocities passing over the coke reduce the film thickness. Diffusion through the surface film to the coke at high temperatures follows the mass law in that increase in available reactants results in increased rate of coke gasification in a given volume and thus higher temperatures result. This has been amply demonstrated in blast furnaces with oxygen enrichment of the blast. This same phenomenon occurs with a variation of apparent specific gravity of coke. Increased specific gravity results in more available carbon per unit surface under the film, as the carbon is more densely packed. In the past it has been demonstrated in the blast furnaces that higher temperatures and better driving rates were obtained when relatively light charcoal was replaced by heavier beehive coke and then again, when beehive coke was replaced by heavier high temperature by-product coke.

The work reported by Tu, et al., (13) sheds further light on the film diffusion theory of carbon combustion. Graph No. III summarizes some of the pertinent results showing variation of combustion rate with temperature, gas velocity oxygen concentration. He also shows that the rate of combustion varies linearly with percent oxygen up to 25 percent. At high temperatures where diffusion through the surface film is controlling, the rate of reaction varies as the 0.4 to 0.7 power of the mass velocity. In addition in this range, the rate of combustion varies approximately as the 0.6 to 1.1 power of the arithmetic mean temperature in degrees Kelvin. The work of Dubinsky (14) shows carbon gasification with carbon dioxide increases enormously in the temperature range of 1200 to 1400°C. In this range, temperature has relatively little effect on the rate of combustion for a given carbon in air.

Investigators have shown that coke gasification can be considered to occur in three steps, depending on temperature (8), (9), (15), (16). Graph No. IV, according to Wicke, illustrates this concept.

STEP I - At low temperatures, Step I occurs. In this range the rate of conversion of carbon dioxide to carbon monoxide is determined by total available surface carbon and the activation energy of coke. The total available (carbon) surface, includes both the external surface and internal pore surface which, for furnace coke, is in the range of two (2) square meters per gram.

From Graph IV it is noted that the rate of reaction increases rapidly with temperature in Step I.

STEP II - With increasing temperatures, the rate of increase of the reaction slows and a transition stage "a" is entered. Subsequently, Step II is reached in which the rate of reaction is so rapid that carbon dioxide, as it approaches the coke and its pores through the gas film, is in part converted and therefore the amount of carbon dioxide concentration reaching the internal pore surfaces of the coke is reduced.

This area, for convenience, can be referred to as pore diffusion zone. As a result less total effective surface becomes available for reaction and the rate of increase of the reaction is reduced to one half of that in Step I. The temperature range in which it occurs, by definition, is Step II.

STEP III - At further increasing temperatures, the rate of increase of the reaction slows and a transition stage "b" is entered. Subsequently, Step III is reached in which the rate of reaction is so high that no carbon dioxide is available for internal pore diffusion. In this area gas diffusion through the film is controlling. The diffusion coefficient is only slightly affected by temperature increases and therefore the rate of reaction increase is slowed down.

BLAST FURNACE CONDITIONS AFFECTING COKE GASIFICATION

An analysis was made of the fundamentals concerning blast furnace conditions and coke gasification to permit an explanation of the significant coke savings obtained with P-C Coke. A literature search revealed a considerable fund of information which must be carefully sifted to permit rationalization applicable to conditions existing in a blast furnace.

Of considerable interest on coke gasification is the work reported by B. Heynert and J. Williams (8), N. Peters and H. Echterhoff (9) and others (10), (11), (12). One of the main difficulties is to assess the relation of temperature in the blast furnace with gas composition. An approximation of this is possible with the sampling procedure used by Schurmann et al (10).

Graph II -A, based on work by Schurmann, shows the relation of temperature, with percent carbon monoxide, carbon dioxide, and total percent of carbon gases in a commercial blast furnace. The concentrations of carbon monoxide and dioxide, are strongly affected by temperature and the Boudouard reaction. From this Graph, it readily can be seen, that a desirable coke is one that will depress the reduction of carbon dioxide, to carbon monoxide. It is to be noted, that in the temperature

region where reactions of this type predominate, carbon dioxide is available from carbonate and iron oxide reduction in addition to that from carbon monoxide oxidation accompanied by carbon deposition. Therefore, a coke saving results with a coke which promotes increased concentration of carbon dioxide in the off gas, as it is more effectively used in oxygen removal.

The relation of temperature at various blast furnace elevations above the tuyeres, with percent carbon monoxide, carbon dioxide and the total percent of carbon gases, as reported by Heynert and co-workers, is shown in Graph II. Analyzing this curve from the point of view of carbon gases, four distinct zones are apparent.

ZONE I - The combustion zone in front of the tuyeres is considered as Zone I. In this zone for practical purposes no iron oxides are present and temperatures are at 3000°F and somewhat higher. Under these conditions the overall reaction of coke carbon with hot blast is :

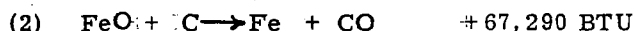


This reaction provides heat and reducing gases for iron ore reduction. High temperatures are developed which play an important role in hearth reactions. High temperatures result in hot metal with high silicon and low sulfur content due to the slag reactions. High temperatures, other conditions being equal, are the result of more carbon reaching the tuyeres and therefore the coke rate can be reduced to obtain comparable quality iron. If, however, the higher temperatures are also contributed to by the combustion characteristics of the coke then additional coke savings are possible by a stone saving to obtain comparable iron.

ZONE II - The area immediately above the combustion zone is characterized by the absence of carbon dioxide. This is due to the existing high temperatures at which carbon dioxide is unstable and, in the presence of carbon, decomposes to carbon monoxide. This area is the pure "direct reduction zone" in which the overall reaction of iron oxide is :



This reaction is pictured as going through the following mechanism :



Since reaction (2) consumes a considerable amount of heat the temperature drops rapidly in this area and as carbon monoxide is formed its concentration increases rapidly.

ZONE III - This area above the "direct reduction zone" is characterized by the appearance of stable carbon dioxide as temperatures have dropped sufficiently and a reduction of carbon monoxide occurs. The termination of this zone is the temperature range in which the Boudouard reaction reverses. To assist in showing

this the total carbon oxides are plotted on Graph II. Zone III can be referred to as "indirect reduction" zone. It is, of course, recognized that even though the direct reduction has been depressed some of it still proceeds. Besides this reaction a number of others occur with the end products consisting principally of Wustite, sponge iron, carbon monoxide and carbon dioxide.

The bulk of these reactions requires less heat than "direct reduction" and therefore the temperature drop in this zone is less until a point is reached where a strong endothermic reaction occurs. This area is where the main portion of the carbonates decompose and possibly other endothermic reactions occur. As there is an excess of carbon monoxide from Zone II for conversion of iron oxides to carbon dioxide, it is obvious that an unreactive coke, minimizing the reduction of carbon dioxide in Zone III, results in a coke rate reduction.

ZONE IV- Zone IV is characterized by the falling off of the total carbon oxide concentration and a rapid drop in ambient temperature. The total carbon oxide volume is reduced due to carbon deposition from the reaction of two volumes of carbon monoxide to one volume of carbon dioxide. The iron ore reduction reactions, similarly as in Zone III, proceed in this area with the modification that the end products favor carbon dioxide formation over carbon monoxide formation. The higher concentrations of carbon dioxide favor the oxidation of free metallics. Again in this zone it is obvious that a coke favoring the stabilization of carbon dioxide will result in a coke saving.

Inspecting the temperature profile on Graph II, it is noted that the carbon dioxide concentration is higher than predicted by the Boudouard equilibrium. This phenomenon is due to the fact that the temperature profile measures the ambient temperature while the Boudouard reaction is controlled by the reacting carbon surface temperature. This surface temperature is lower than the ambient temperature as strong endothermic reactions occur on its surface.

From the foregoing thermal and chemical considerations it was shown that a reduction in coke rate will occur in a blast furnace with a coke resulting in:

1. Increased temperature when gasified at the tuyeres.
2. Increased percent of coke gasifying at the tuyeres.
3. Reduced reaction rate with carbon dioxide to form carbon monoxide.

That an increase in the percent of coke gasified at the tuyeres results in coke saving was also demonstrated by M. Manes and J. S. Mackay (7). By means of a simplified mathematical model of a blast furnace, they showed that a coke rate reduction occurs with an increase in air per pound of coke charged with a concomitant reduction of air per unit of ore. They further deduced that "secondary reduction" (ore reduction below 1000°C) increased under these conditions.

DESIRABLE COKE CHARACTERISTICS

Considering the conditions affecting coke gasification in a blast furnace and the coke gasification fundamentals presented, it is apparent that a coke having the following characteristics will result in a coke rate reduction in a blast furnace:

1. Reduced Internal Surface

A coke with reduced internal surface will produce less carbon monoxide in the cooler upper portions of the stack and therefore a coke saving results. Further, a larger proportion will remain for gasification at the tuyeres and thus more heat is released in the hearth.

2. Increased Pore Diameter

A coke with increased pore diameters results in increased gasification with iron oxide in the pore diffusion range. This zone is significantly extended in a blast furnace from about 1000°C to as high as 1700°C due to the existing high gas velocities reducing surface film thickness. Therefore, a coke with large pores presents more available surface and gasifies more rapidly at temperatures existing in the direct reduction zone. The furnace level to which the direct reduction zone extends depends on temperature. As direct reduction consumes large amounts of heat, the acceleration of this reaction has a cooling effect and therefore the direct reduction zone stops at a lower level in the furnace.

3. Increased Carbon Concentration

A coke with higher concentration of carbon on its surface furnishes more reactants per unit area. Hence, at the tuyeres, the combustion temperature is increased as the reaction takes place in a smaller volume due to the mass action law. Consequently in the combustion zone, at equal total heat release, higher temperatures occur. Further it would appear that the carbon dioxide concentration becomes higher and also occurs at a point, closer to the tuyere nose. It may also be speculated that the higher temperatures occurring at the higher carbon dioxide concentration at localized areas in the combustion zone of the blast furnace contributes to the reduction of limestone usage (more acid slag) for proper metal quality control.

SUMMARY AND CONCLUSIONS

P-C Coke and H-C Coke, when used in blast furnaces, resulted in significant changes in operating results. These are summarized in Table V.

TABLE V.
EFFECT OF SPECIAL COKES VS NORMAL COKE IN BLAST FURNACES.

<u>OPERATING VARIABLES</u>	<u>P-C COKE</u>	<u>H-C COKE</u>
	<u>(85 Days)</u>	<u>(166 Hrs.)</u>
Burden Compared to Regular Practice	Normal	Variable
Coke Saving/THM, Pounds	100	87(a)
More Air/Pound Coke Charged, Cu. Ft.	1.8	-
Less Air/THM, Cu. Ft.	2820	6120
Less Blast Temp. Required °F	94	144
Stone Saving/THM, Pounds	58	138

(a) Corrected for burden variation.

Inspection of the changes in operating results obtained with P-C Coke and H-C Coke clearly indicates that use of these special cokes effect a substantial coke saving as a result of reactivity characteristics differing from normal by-product furnace coke. In the case of P-C Coke, and by the indications obtained with H-C Coke, it was noted :

1. More air was required at the tuyeres per pound of coke charged, showing that a smaller proportion of coke is gasified in the stack and a larger proportion at the tuyeres.
2. Less air was required per ton of hot metal produced showing that the coke carbon was more effectively used with the oxygen from the ore.
3. Higher temperatures were experienced in the combustion zone as verified by a reduction in stone usage while producing comparable quality iron despite a reduction of both coke rate and blast temperature.

In view of the results obtained and the fundamental concepts presented, it was concluded that the reduced coke rate obtained with P-C Coke was caused by improved useful coke reactivity. This improvement was attributed to the following coke characteristics :

1. Less internal surface,
2. Larger pores,
3. Thicker cell walls.

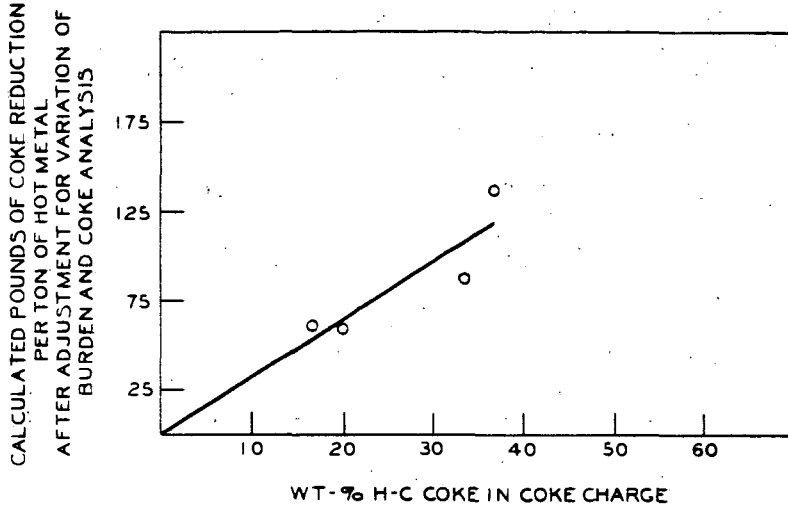
ACKNOWLEDGEMENT

This work could not have been accomplished without the active interest and efforts of J. D. Price, retired Coke Plant Superintendent, J. W. Carlson, Blast Furnace Superintendent, J. R. Purdy, Coke Plant Superintendent, and their staffs, all of The Colorado Fuel and Iron Corporation, and H. Loos, Works Manager, Hessische Berg U Huttenwerke AG, Oberscheld plant and his staff. Grateful thanks are extended to both these companies for permission to use data developed at their plants and to Professor T. L. Joseph for his many timely suggestions.

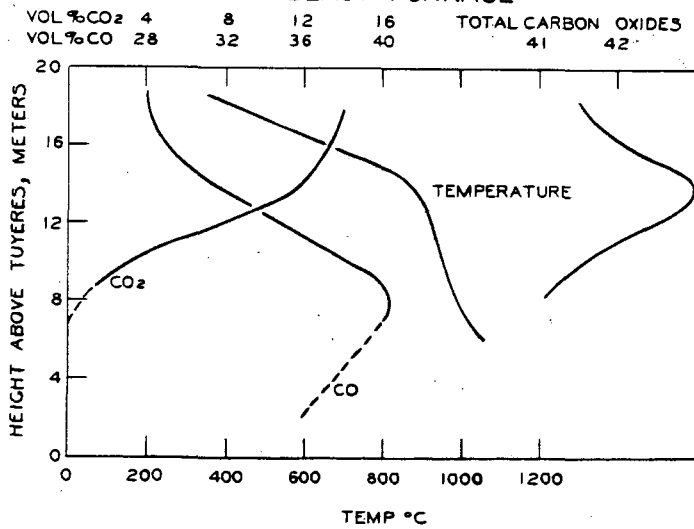
LITERATURE CITED

- (1) T. H. Blakley, J. W. Cobb, Inst. Gas Res. Fellowship Rept. 1931-1934 Com. No. 104
- (2) Broche and Nadelman Stahl U. Eisen, 53 (1953)
- (3) R. V. Flint, Blast Furnace & Coke Oven Proc. AIME (1952)
- (4) R. V. Flint, Blast Furnace & Steel Plt., 47-76, Jan. 1962
- (5) T. L. Joseph, Blast Furnace & Steel Plt., March & April 1961
- (6) M. A. Shapirovalov, Stahl, H-5, 535-538, May 1958
- (7) M. Manes and J. S. Mackay, Jr. of Metals, April 1962, 308-314
- (8) G. Heynert and J. Williams, Stahl U. Eisen, 79, 1545-1554, (1958)
- (9) W. Peters, H. Echterhoff, Blast Furnace & Coke Oven Proc. AIME (1961)
- (10) E. Schurman, W. Zischkale, P. Ischebeck and G. Heynert, Stahl U Eisen 80, 845-861, (1960)
- (11) G. Heynert, W. Zischkale and E. Schurman, Stahl U Eisen, 80, 931-990, (1960)
- (12) G. Hedden, Lecture "Second European Simp. on Chem. Engr." Amsterdam (1960)
- (13) C. M. Tu, H. Davis, and H. C. Hottell; Ind. Engr. Chem., 26, 749-759 (1934)
- (14) M. S. Dubinsky, Thesis, Mass. Inst. Tech. (1932)
- (15) E. Wicke, K. Hedden, and M. Rossberg, Brenst. Warme Kraft 8, (1956)
- (16) G. Hedden, Chem. Ind-Techn., 30, 125-132, (1958)
- (17) B. Osann, Stahl U Eisen, 36 (1916) 477-434 and 530-536.

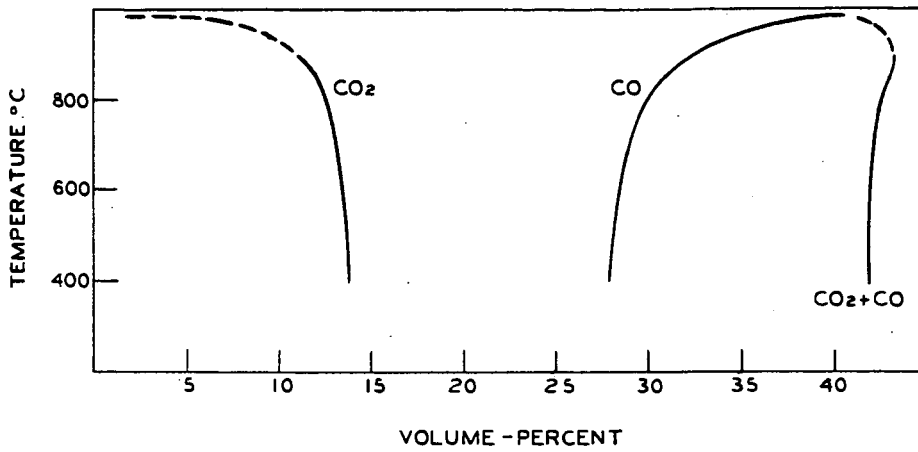
GRAPH I
 COKE SAVING VS WT-% OF H-C COKE IN CHARGE



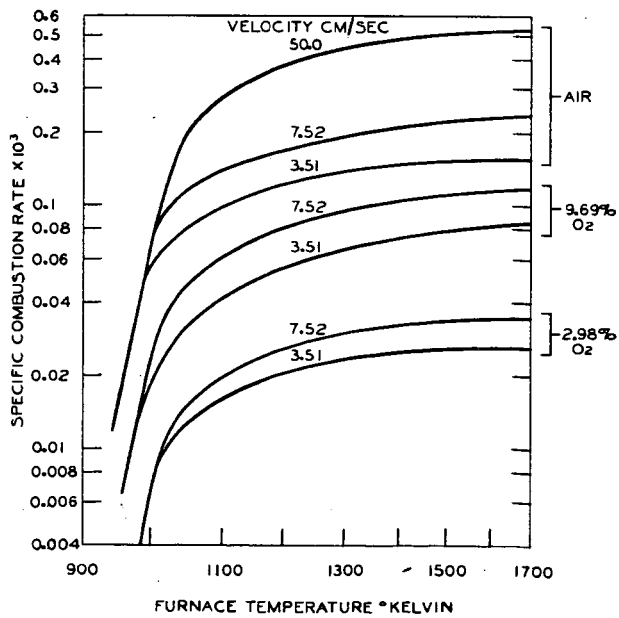
GRAPH II
 PROFILE OF TEMPERATURE AND OXIDES OF CARBON IN BLAST FURNACE



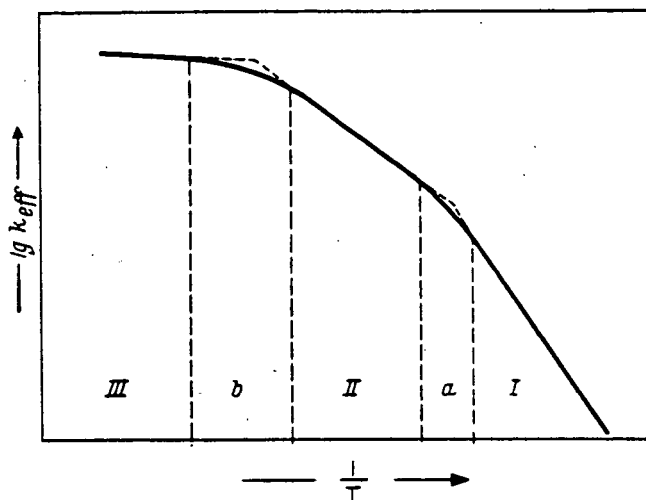
GRAPH II
OXIDES OF CARBON AT VARIOUS TEMPERATURES



GRAPH III
RATE OF COKE COMBUSTION WITH GAS VELOCITY
AND OXYGEN CONCENTRATION



GRAPH IV
RATE OF GASIFICATION



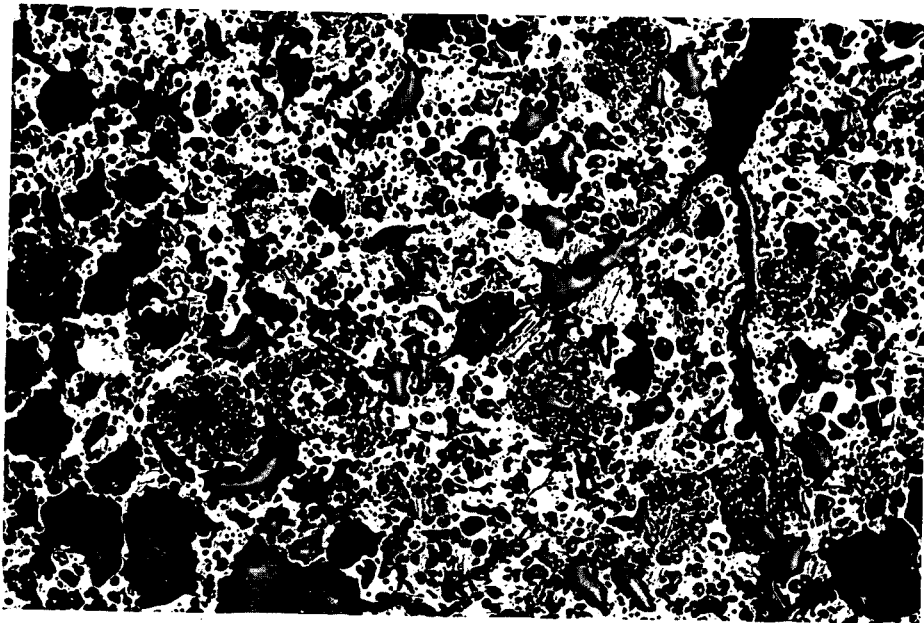


Fig. 1 CF&I NORMAL COKE, 10X

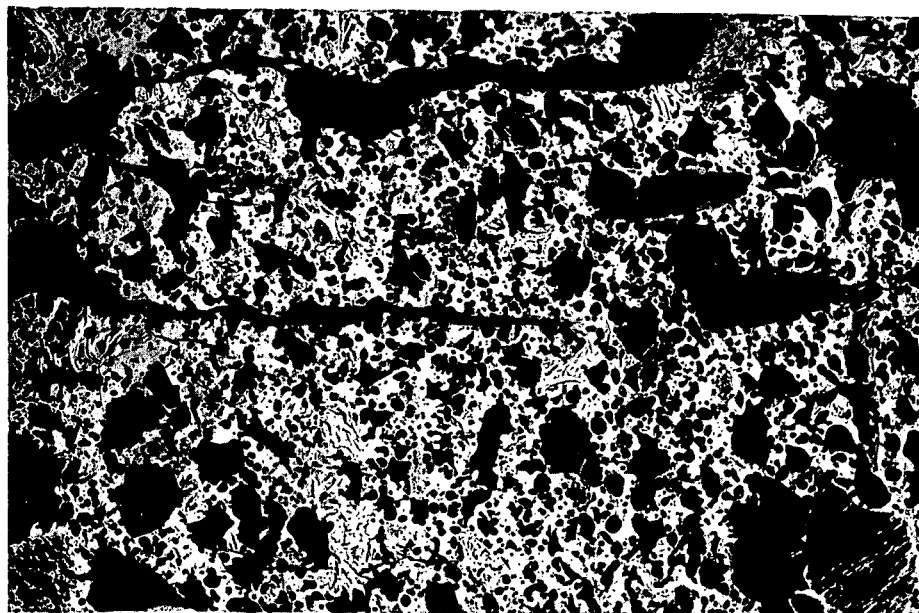


Fig. 2 CF&I P-C FURNACE COKE, 10X

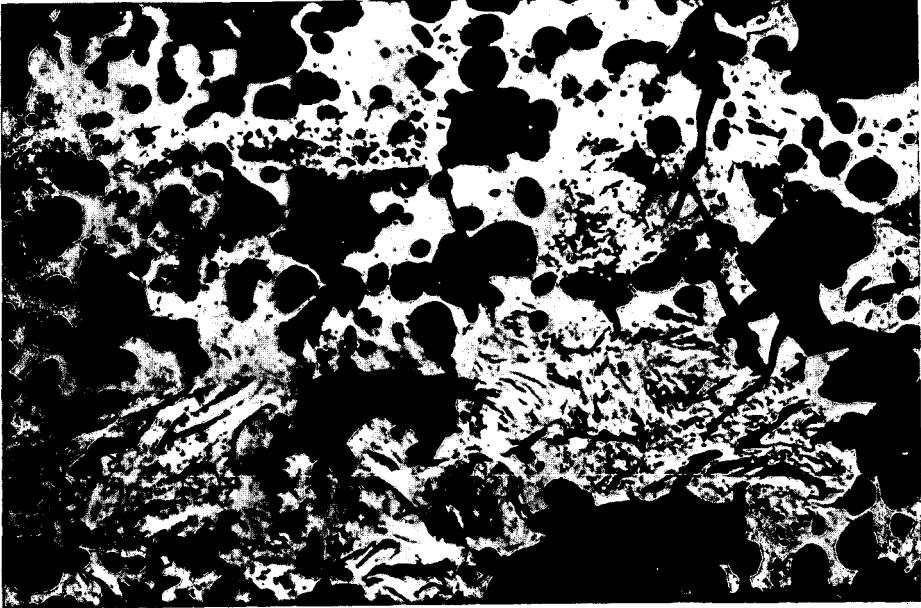


Fig. 3. CF&I P-C FURNACE COKE, 40X

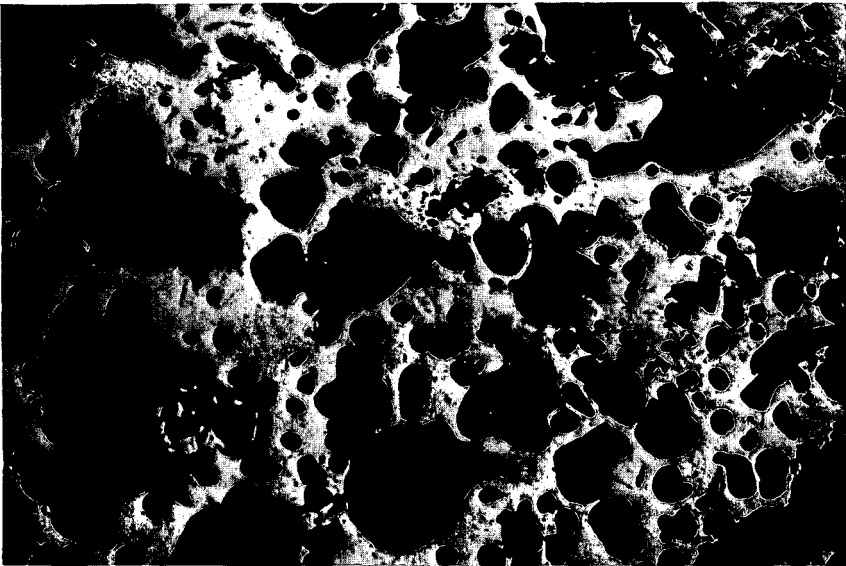


Fig. 4. CF&I NORMAL COKE, 40X

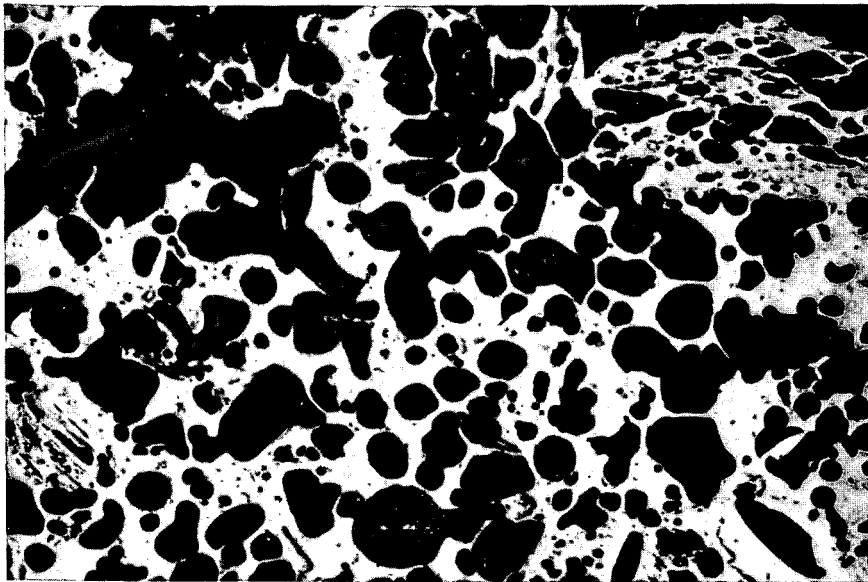


Fig. 5 COKE FROM 100% H. V. COAL, 40X

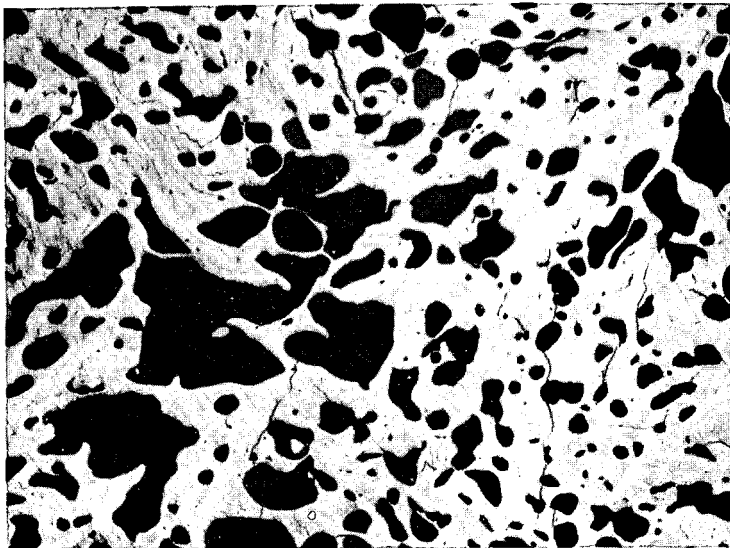


Fig. 6 RAW PETROLEUM COKE, 10X

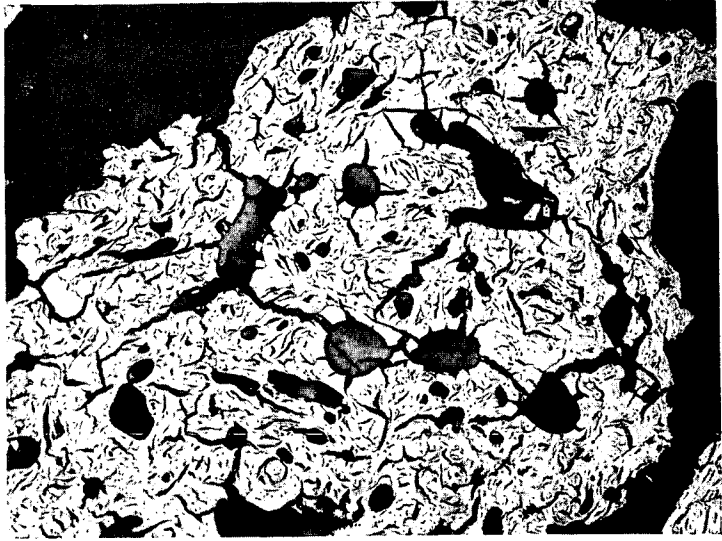


Fig. 7. CARBONIZED PETROLEUM COKE, 10X

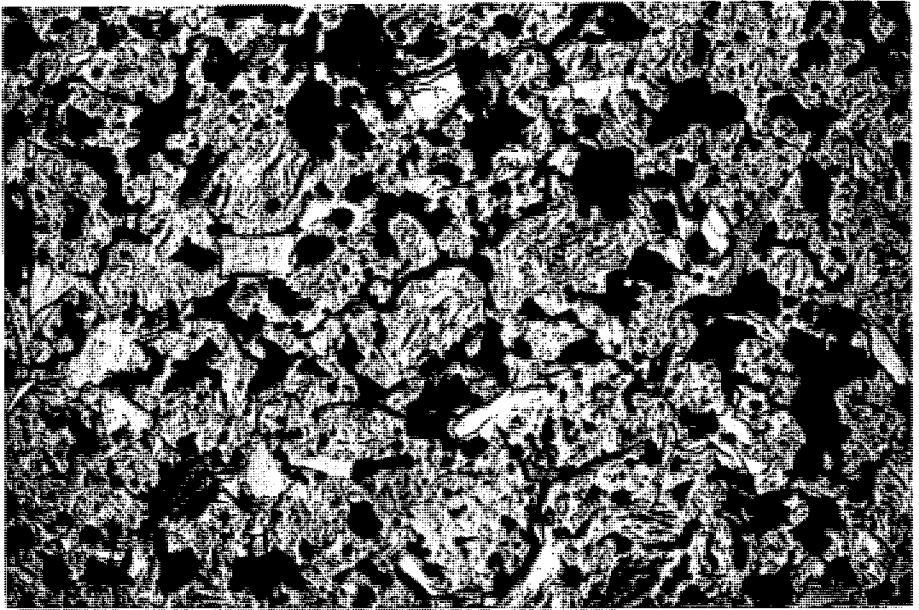


Fig. 8 DENSE FOUNDRY COKE, 10X

REACTIVITY OF COALS IN HIGH-PRESSURE GASIFICATION WITH HYDROGEN AND STEAM

Harlan L. Feldkirchner and Henry R. Linden

Institute of Gas Technology
Chicago 16, Illinois

One of the major obstacles to the design of a reactor for direct conversion of coal to high heating value gas by destructive hydrogenation at high pressure (hydrogasification) has been the lack of information on the rate and course of the reactions during the initial period of rapid conversion of the more reactive coal constituents. Kinetic studies have generally been made with highly devolatilized chars and carbons to avoid the problem of changes in feed composition during heatup. Where the rates of formation of low molecular weight hydrocarbons from reactive coals and low-temperature chars have been measured, experimental conditions did not permit both rapid heatup and short product gas residence times to minimize side and secondary reactions.

The primary variables affecting the rate of hydrogasification are coal reactivity, temperature, pressure and feed gas composition. The coal reactivity, in turn, varies with the initial coal properties, the extent of conversion, the length of time at reaction conditions and the severity of the reaction conditions. In previous studies, significant diffusional resistances have not been encountered (15,16), although they might become important at higher temperatures, or with more reactive feedstocks.

PREVIOUS WORK

In work at the Institute, the major objective has been the determination of the conditions for the direct production of a high heating value gas in a practical continuous reactor system. The feasibility of this approach had been indicated in batch reactor tests (4), and has recently been confirmed in a countercurrent moving-bed continuous reactor. Earlier results obtained with low-temperature bituminous coal char in a fluid-bed reactor at 1400° to 1500°F. and 500 to 2000 p.s.i.g. (10) did not fully attain the desired objective of 30 to 50% char conversion to a gas of 900 B.t.u. per SCF, (standard cubic foot at 60°F., 30 inches of mercury and saturated with water vapor). To obtain high conversions of hydrogen and coal to a high-methane content gas, long coal and hydrogen residence times and low hydrogen to coal feed ratios were used. These conditions make it difficult to interpret the rate data, since the effects of equilibrium hindrance cannot be accurately defined because of lack of thermodynamic activity data for coal and char at levels of conversion.

The U. S. Bureau of Mines (7-9) employed a reactor tube, 5/16 inch in inside diameter, which was heated by passing an electric current through it. Pressures up to 6000 p.s.i.g. and a nominal operating temperature of 800°C. (1472°F.) were investigated. During the 2-minute heatup period, and afterward, hydrogen was passed through the tube at a sufficiently high rate that gas residence times were only a few seconds. Substantial yields of liquids were obtained during the relatively long heatup period, so that the rates of gasification observed at 800°C. were for the less reactive, residual material. The liquids yields decreased with decreases in hydrogen rate as a result of the increase in residence time. For example, an increase in gas residence time from 6 to 30 seconds resulted in a decrease in liquid hydrocarbons from 26 to 4.5 weight % (moisture-, ash-free basis), of a high-volatile bituminous coal.

In contrast, negligible quantities of liquid hydrocarbons were formed in the fluid-bed tests at the Institute (10). In these tests, low-temperature bituminous coal char or lignite (-60, +325 sieve size, U. S. Standard) were fed cocurrently with hydrogen to the hot fluidized bed, resulting in rapid heatup. However, product gas residence times were on the order of one minute, so the absence of liquid products could have been the result of secondary vapor-phase reactions.

In the work described herein, tests were conducted in which both coal heatup and product gas residence time were of the order of a few seconds. No measurable amounts of liquid products were formed and methane was the major gaseous hydrocarbon produced, with only trace quantities of higher paraffins, olefins and aromatics being formed. Some carbon oxides and nitrogen were also evolved during the initial phases of the reaction.

APPARATUS

A flow diagram of the reaction system is shown in Fig. 1. The -16, +20 sieve size (U. S. Standard) coal charges were fed in single batches (usually 5 or 10 grams) from a hopper mounted on top of the reactor. At zero time, a full-opening, air-operated ball valve, connecting the reactor and feed hopper, was opened and the coal charge was dropped into the reactor. A synton vibrator was mounted on the hopper to aid in solids feeding. A pressure-equalization line connecting the top of the hopper and the reactor inlet kept both vessels at the same pressure.

Feed gases were preheated to the desired operating temperature within the reactor. Exit gases passed through a water-cooled coil, a liquids knockout pot, a high-pressure filter and a pressure-reducing back-pressure regulator, before sampling, metering and monitoring.

Gas inlet flow rates were controlled manually and were measured by an orifice meter. Steam was generated at the desired operating pressure in an electrically-heated stainless steel coil by feeding water from a weigh tank with a metering pump.

The reactor barrel was constructed of N-155 super alloy and was designed for operation at a maximum pressure of 1500 p.s.i.g. at a maximum temperature of 1700°F. A complete description of the reactor has been given elsewhere (11), along with design details concerning the use of externally-heated reactors at high temperatures and pressures. The reactor was 2 inches in inside diameter, 4 inches in outside diameter and 60 inches in inside length. An Inconel X thermowell, 3/8 inch in outside diameter, was mounted in the center of the bottom closure and extended 58 inches into the reactor. A removable, stainless steel insert, 1-5/8 inches in inside diameter and containing a 1/2-inch outside diameter thermowell sleeve, was installed in the reactor to contain the coal charge and provide for complete recovery of the coal charge after each test. The bottom of the insert was filled with sufficient alundum pellets to position the coal charge in the center of the third heating zone from the top.

Reactor temperatures were maintained by four individually-controlled electrical resistance heating elements, each 12 inches long. Reactor pressures were controlled at the desired values by means of a back-pressure regulator and were continuously recorded along with orifice pressures.

The double-ended reactor contained an Autoclave Engineers self-sealing (modified Bridgman) closure at each end. The closures were rated for 1400°F. operation at 1500 p.s.i.g. This high-temperature service was facilitated by use of either 16-25-6 or Inconel alloy seal rings. A boundary lubricant of molybdenum disulfide, applied in aerosol form to produce a thin boundary layer coating, was used on all closure threads and on the seal rings.

PROCEDURE

Feed gas mixtures, which were prepared by mixing during compression, were stored at pressures up to 3000 p.s.i.g. Commercially available grades of electrolytic hydrogen (99.8% pure), nitrogen (99.6% pure), helium (99.99% pure) and technical grade methane (95.0% pure) were used. All feed gases, except steam, contained approximately 2 mole % helium tracer for exit gas flow rate measurement.

The feed gas orifice was calibrated before each run with a wet test meter and the exit gases were also metered with this meter as a check on the helium tracer method for exit gas flow rate measurement. In tests with pure steam feed, helium sweep gas was used to purge, from the exit gas system, the small volumes of permanent gases formed. The exit gas specific gravity was monitored continuously with a recording gravitometer as an aid in selecting times for exit gas sampling. A sampling manifold was installed in the exit gas line, upstream of the metering and monitoring system to allow rapid sampling at small time intervals. Gas analyses were performed by mass spectrometer. The combined nitrogen and carbon monoxide

content of the exit gas, determined by mass spectrometer, less nitrogen introduced in the feed gas, was assumed to be carbon monoxide, except in selected tests where carbon monoxide was determined by infrared spectrophotometer.

The four coals investigated were a medium volatility anthracite, a North Dakota lignite, a Pittsburgh Seam bituminous coal and a low-temperature bituminous coal char. The char was prepared from bituminous coal from the Montour No. 10 Mine by a fluidized-bed pretreatment process of the Consolidation Coal Co. Analyses of these feeds are shown in Table 1.

Most runs were conducted for a total time of 15 minutes or less. The reactor was first heated up to the desired operating temperature. Then gas flow, at the desired rate, was started through the reactor. The heat input to the reactor was then adjusted so that all temperatures within the reactor remained constant. When the system was stabilized completely, the run was initiated by opening the valve between the feed hopper and reactor.

At typical conditions of 1500 p.s.i.g., 1700°F. and a hydrogen flow rate of 100 SCF per hour, the first hydrogasification products appeared in the exit gas at the sampling manifold in approximately 10 seconds. During the initial period of high conversion rate, samples were taken at time intervals as short as 5 seconds to delineate the exact course of the reaction. Temperatures at the center of the coal charge, at a point 6 inches above the charge and at the bottom of the insert were recorded continuously by means of a high-speed temperature recorder which recorded each temperature at approximately 3-second intervals.

When the reaction rate had reached a value too small to be measured accurately at the high gas rates employed (usually after about 600 seconds), the run was stopped. The electric heaters were turned off and the reactant gases were purged from the reactor with nitrogen. The reactor was kept filled with nitrogen until the temperature had reached a low enough value to allow retrieval of the coal residue.

RESULTS

Exploratory Tests

Before the test program was initiated, several exploratory tests were conducted at the base conditions of 1000 or 1500 p.s.i.g. and 1700°F., with a hydrogen flow rate of 100 SCF per hour. It was necessary to select sample weights which gave small temperature changes and low concentrations of methane in the exit gas, without impairing analytical accuracy.

Table 1.-COAL ANALYSES

Coal Type Source	Bituminous Coal Char Low Temperature Consolidation Coal Co. (Montour No. 10 Mine)	Anthracite Medium Volatility Anthracite Experiment Station, U. S. Bureau of Mines
Particle Size, U.S. Standard Sieve	-16, +20 -40, +50	-16, +20
Ultimate Analysis, wt % (dry basis)		
Carbon	78.3	83.3
Hydrogen	3.46	2.47
Nitrogen and Oxygen (by difference)	10.03	2.90
Sulfur	1.01	0.88
Ash	7.20	10.45
Total	<u>100.00</u>	<u>100.00</u>
Proximate Analysis, wt %		
Moisture	1.7	0.7
Volatile Matter	17.3	5.7
Fixed Carbon	73.9	83.2
Ash	7.1	10.4
Total	<u>100.0</u>	<u>100.0</u>
Coal Type Source	Bituminous Coal Pittsburgh Seam Consolidation Coal Co. (Montour No. 4 Mine)	Lignite North Dakota Truax-Traer Co. (Velva Mine)
Particle Size, U.S. Standard Sieve	-16, +20	-16, +20
Ultimate Analysis, wt % (dry basis)		
Carbon	75.9	65.4
Hydrogen	5.01	4.49
Nitrogen and Oxygen (by difference)	8.99	23.21
Sulfur	1.54	0.45
Ash	8.56	6.45
Total	<u>100.00</u>	<u>100.00</u>
Proximate Analysis, wt %		
Moisture	1.1	6.8
Volatile Matter	33.5	41.2
Fixed Carbon	56.9	46.0
Ash	8.5	6.0
Total	<u>100.0</u>	<u>100.0</u>

With 50- and 20-gram samples of low-temperature bituminous coal char (-8, +16 sieve size) the maximum exit gas methane content was too high and the temperature changes during the run were too great to allow the assumption of differential reaction conditions. In tests with 10- and 5-gram samples of -16, +20 sieve size low-temperature bituminous coal char, the exit gas methane contents approached the desired levels, and reaction rates (expressed as pounds carbon converted to gaseous hydrocarbons per pound of carbon remaining in bed per hour) were similar.

With low-temperature bituminous coal char at nominal run temperatures of 1700°F., two periods of high rate were observed (Fig. 2). The second period of high rate, occurring after approximately 30% carbon gasification, was a result of increases in the temperature of the char sample due to the inability to dissipate the high heat of reaction to the surroundings. This was substantiated by conducting a further test with a 3-gram sample weight. Here only a slight increase in rate was obtained at carbon conversions above 30%. In tests with unpretreated coals, and with bituminous coal char at 1300°F. and 1500°F., no second period of high rate was observed.

It was also necessary to select a coal particle size for the remainder of the test program. An effect of particle size on the rate of reaction could indicate the presence of significant diffusional resistances. Tests were conducted with 10-gram samples of -16, +20 and -40, +50 sieve size material (Fig. 3). These test results indicate negligible effects of particle size on the reaction rate. The displacement of the rate curve for the -40, +50 sieve size material was probably due to the slower feeding rate of the more finely divided material, or to an initial holdup in the coal feed hopper. Based on duplicate tests to check reproducibility, it was believed that these small differences were within the limits of experimental and analytical accuracy.

From the results of these exploratory tests, the following base conditions were selected for the remainder of the tests, unless otherwise noted:

Temperature:	1700°F.
Pressure:	1500 p.s.i.g.
Sample weight:	5 and 10 grams
Coal particle size:	-16, +20 sieve size
Feed gas flow rate:	100 SCF per hour

Typical results for the four feeds used in this study are given in Table 2.

Effects of Variables

The effect of temperature and extent of conversion on the rate of reaction of low-temperature bituminous coal char and hydrogen was measured in a series of tests conducted at 1500 p.s.i.g. and at 1300°F., 1500°F. and 1700°F. (Fig. 4). During the initial phases, the reaction rate was not significantly affected by temperature in the range studied. Only after approximately 20% carbon gasification did the effects of temperature become apparent. The rate constants for the residual char would be expected to follow the pseudo-first-order relationship:

$$r = kp$$

where r = rate of reaction in pounds of carbon as methane equivalent per hour per pound of carbon in bed.
Methane equivalent includes carbon in all gaseous hydrocarbons produced.

k = rate constant.

p = hydrogen partial pressure in atmospheres.

This expression has been shown by Blackwood (2) to be applicable in the temperature range of 650° to 870°C. (1202° to 1598°F.) for the reaction of coconut char with excess hydrogen at pressures up to 40 atmospheres. Birch (1) has also applied it successfully to correlate data on the hydrogenation of the residual (aromatic) carbon portion of Australian brown coal with excess hydrogen in a fluid-bed reactor for the temperature range from 750° to 950°C. (1382° to 1742°F.). Zielke and Gorin (15) showed that, in the temperature range of 1500° to 1700°F. and at 1 to 30 atmospheres, with devolatilized Disco bituminous coal char the apparent reaction order is 2 at low pressures and approaches 1 at high pressures.

In Table 3, pseudo-first-order hydrogasification rate constants for these chars are compared with the values for low-temperature bituminous coal char after 25 to 30% carbon conversion (Fig. 4). Agreement is quite good, except for the acid-extracted, high-temperature coconut char. The rates for this specially-prepared low-reactivity material are up to one order of magnitude lower, as would be expected.

All of the above results were obtained in differential-bed reactors of various types, except for the data for Australian brown coal, which were obtained in an integral fluid-bed reactor. However, methane concentrations in the product gases were low enough to minimize equilibrium hindrance effects. The data for coconut char are based on the carbon initially present in the bed, but this is not significant in view of the low conversions.

Table 3.-COMPARISON OF RATE CONSTANTS OF VARIOUS INVESTIGATORS

<u>Investigator</u>	Blackwood (1,2)	Birch (1)	Zielke and Gorin (15)	This Study
<u>Coal</u>	High-Temperature Coconut Char	Brown Coal	Disco Bit. Coal Char	Low-Temp. Bit. Coal Char
<u>Conversion</u>	Less than 10% Char Conversion	More than 40% Carbon Conversion	0-30% Carbon Gasification	25-30% Carbon Gasification
<u>Temperature, °F.</u>	k, rate constant*			
1300	1×10^{-4}	6×10^{-4}	--	2×10^{-3}
1500	9×10^{-4}	4×10^{-3}	$6-2 \times 10^{-3}$	4×10^{-3}
1700	6×10^{-3}	2×10^{-2}	1×10^{-2}	3×10^{-2}

* For Birch, Zielke and Gorin and this study, k has units of lb. of C as CH₄ equiv./lb. C in bed-hr.-atm. H₂ part. press. For Blackwood, units are lb. of C as CH₄ equiv./lb. C fed-hr.-atm. H₂ part. press.

Fig. 5 further demonstrates the similarity in hydrogasification rate constants of the residual portion of coals and chars with greatly different initial properties. The rate constants during the high-rate period are roughly proportional to the volatile matter content of the feed, but at high conversion levels they approach one another. It can be seen that the results obtained with 5-gram samples of lignite and anthracite could not be closely duplicated with 10-gram samples, whereas with bituminous coal good agreement was obtained. The apparent rate constants with the larger samples were much higher for lignite and considerably lower for anthracite. This is not believed to be primarily due to lack of reproducibility.

The combined effect of changes in total and in hydrogen partial pressure at 1500° and 1700°F. is shown in Figs. 6 and 7. The separate effect, at 1700°F., of a decrease in hydrogen partial pressure from 1500 to 1000 p.s.i. by the addition of nitrogen, is shown in Fig. 8. These results apparently reflect that, during the initial high-rate period, both pyrolysis and hydrogenolysis occur. Increases in hydrogen partial pressure would increase the rate of hydrogenolysis compared to pyrolysis. Thus, an increase in total pressure tended to broaden the range of the initial high-rate period. An increase in hydrogen partial pressure at constant total pressure both broadened the rate curve, and increased its peak, during the initial high-rate period.

The true effect of hydrogen partial pressure during the highly exothermic residual char hydrogenolysis period was obscured at 1700°F. by the large temperature increases, depending on sample weight. However, it can still be observed qualitatively that increases in total pressure as well as in hydrogen partial pressure gave the expected increases in rate.

With devolatilized Disco bituminous coal char, Zielke and Gorin showed that the effect of methane partial pressure on hydrogasification rate is simple equilibrium hindrance (15). However, the results obtained with a partial pressure of 500 p.s.i. of nitrogen and with a partial pressure of 500 p.s.i. of methane were not significantly different during the initial high-rate period (Fig. 8). This indicates no substantial equilibrium hindrance effect during this period, in spite of the large reduction in driving force for the reaction $C + 2H_2 \rightarrow CH_4$, if a carbon activity of 1 is assumed. On that basis, the equilibrium methane partial pressure at 1700°F. and 1500 p.s.i. is only about 700 p.s.i. The absence of a hindrance effect at low conversions is further evidence of the much higher initial carbon activity. The effect of 500 p.s.i. methane partial pressure in the feed gas during the low-rate period could not be determined because the product gas methane concentration measurement was not accurate enough to obtain meaningful data.

Course of Coal-Hydrogen Reactions

The description by Birch and others (1) of the sequence of coal-hydrogen reactions, at sufficiently high temperatures, pressures and residence times to give methane as the major product, is in agreement with observed experimental results of this study. In somewhat modified form, this sequence is:

1. A high-rate period comprising pyrolysis of the more reactive structural units such as aliphatic hydrocarbon side chains and oxygenated functional groups, and hydrogenation and hydrogenolysis of the intermediate pyrolysis products.
2. A low-rate period of direct attack of hydrogen on the residual aromatic carbon structure.

Evidence for the two steps during the high-rate period can be found in the increase in organic liquid products formation with decreases in product gas residence time observed by Hiteshue and others (7) at relatively low reaction temperatures encountered during heatup. Absence of substantial organic liquid product yields would correspond to the completion of the vapor-phase hydrogenolysis reactions, which would then be the chemical rate-controlling step in methane formation during the initial high-rate period. Since, in this study, there was no major effect on the high-rate period from temperature changes in the 1300° to 1700°F. range at a pressure of 1500 p.s.i.g., a physical process may have been controlling under these conditions of extremely rapid hydrogenolysis.

Although no measurable liquid hydrocarbon formation occurred, even at 1300°F., as a result of rapid heatup of the coal charge, the presence of small amounts of C₂- to C₄-aliphatic hydrocarbons during the high-rate period indicates the initial formation of higher molecular weight intermediates which have been converted to methane by hydrogenolysis (12-14). In this case, ethane would have to be present in quantities exceeding the methane-ethane-hydrogen equilibrium values. In tests with bituminous coal char, ethane concentrations actually did exceed equilibrium values at the peak of the high-rate period (Fig. 9). The formation of small amounts of benzene during the high-rate period is further evidence of the similarity with hydrocarbon hydrogenolysis.

A better picture of the sequence of coal-hydrogen reactions under coal hydrogasification conditions can be obtained from the changes in hydrogen distribution with conversion of various feeds. The upper set of plots in Fig. 10 shows the ratio of total hydrogen in the exit gas to the total hydrogen in the feed gas for a series of tests conducted at 1700°F. and 1500 p.s.i.g.. The lower set of curves in Fig. 10 shows the changes in gaseous feed hydrogen consumption with conversion, for the same series of tests.

It can be seen that the initial high rate period is characterized by donation of hydrogen from the coals and char, as well as by large consumption of feed hydrogen, indicating the occurrence of both pyrolysis and hydrogenolysis reactions. The maximum feed hydrogen consumption tends to occur at higher carbon gasifications than the maximum hydrogen evolution, in accordance with the sequential nature of the pyrolysis and hydrogenolysis reactions. The rate of feed hydrogen consumption is an excellent indication of feed reactivity, except that with the low-temperature bituminous coal char, a second period of high consumption occurs as a result of uncontrollable temperature increases.

Lignite, because of its high oxygen content, donated relatively little hydrogen and consumed a disproportionately large amount of gaseous feed hydrogen. This is due to the large amount of water formation which can be readily measured in flow reactors, but could not be determined experimentally in the present work. It should be noted that, at the high hydrogen partial pressures used in this study, the only other major path for oxygen rejection is as carbon monoxide, since carbon dioxide formation is practically suppressed.

Steam-Hydrogen Coal Gasification

Much kinetic information on the reaction of steam-hydrogen mixtures and char exists for temperatures of 1500° to 1700°F. at hydrogen partial pressures below 30 atmospheres (3,5,6,16). The addition of steam was found to substantially increase the rate of methane formation at these low hydrogen partial pressures. Extrapolation to hydrogen partial pressures sufficiently high to give rates of methane formation which are of practical interest, indicates that the effect of steam becomes less significant. In the present study, the rates of the steam-char and hydrogen-char reactions with an equimolar steam-hydrogen mixture were measured at 1700°F. and 1500 p.s.i.g. The rates of these two reactions (measured by the rates of evolution of gaseous carbon oxides and gaseous hydrocarbons) are shown in Fig. 11 as functions of total carbon gasification. The results of the two tests conducted with 5- and 10-gram sample weights are in good agreement, and the second high-rate period, characteristic of the char-hydrogen tests at 1700°F., is absent. This is probably due to smaller temperature changes, with both exothermic hydrogenation reactions and endothermic steam-carbon reactions occurring simultaneously.

Unlike much of the earlier work at relatively low hydrogen partial pressure, the char-hydrogen reaction proceeded much more rapidly than the char-steam reaction, especially at the higher conversions. However, from comparison with Figs. 7 and 8, the rate of char conversion to gaseous hydrocarbons was below the level expected for a feed gas hydrogen partial pressure of 750 p.s.i. Thus, the relatively high rates of

carbon oxide formation at low conversion levels may have been largely due to steam reforming, catalyzed by the reactor walls, of a portion of the gaseous hydrocarbons produced. However, even if the total gasification rate is considered in a comparison with char-hydrogen results, there is no indication of the acceleration of methane formation by steam addition which has been observed at lower hydrogen partial pressures.

The rate of the steam-char reaction with an equimolar steam-helium mixture at 1700°F. and 1500 p.s.i.g., shown in Fig. 12, was much higher than in the previous test with a steam-hydrogen feed at equal steam partial pressure. This is the result of the well-established inhibition of the steam-carbon reactions by hydrogen (6). Substantial quantities of gaseous hydrocarbons were also formed initially, probably largely by pyrolysis rather than by reaction of char with hydrogen formed in steam decomposition, or direct reaction of steam and char. This is supported by the fact that more hydrogen was produced than could be accounted for by carbon oxide-forming reactions.

CONCLUSIONS

Gasification of various coals with hydrogen and added steam at high temperatures and pressures, under conditions of very rapid coal heatup and product gas residence time of only a few seconds, has confirmed the generally accepted model derived from data without as detailed a definition of the critical initial stages of conversion. During this initial period, gasification rates are very rapid and the course of the methane-forming reactions is similar to that in hydrogenolysis of hydrocarbons. However, the reactivity of the pyrolysis intermediates formed during the high-rate period appears to be much greater than that of typical petroleum hydrocarbons since no measureable liquid products were obtained at temperatures as low as 1300°F., and methane was the predominant product. Materials as different as lignite, bituminous coal, anthracite and low-temperature bituminous coal behaved similarly, except that initial conversion rates increased roughly in proportion to their volatile matter content, and hydrogen consumption and carbon oxide formation was affected by oxygen content. However, the conversion rates of the relatively unreactive residues were approximately the same. At the high hydrogen partial pressures employed in this study, steam addition did not accelerate methane formation as observed in previous studies at relatively low hydrogen partial pressures. The inhibiting effect of hydrogen, on reactions with steam which form carbon oxides, was observed for the initial high-rate period, as well as during the conversion of the residual char.

ACKNOWLEDGMENT

This work was conducted under the sponsorship of the Research Department of the Consolidated Natural Gas System (now Con-Gas Service Corporation) under the guidance of F. E. Vandaveer and H. E. Benson. Thanks are due to E. B. Shultz, Jr., who designed most of the apparatus and helped develop the experimental procedure. A. E. Richter and R. F. Johnson assisted in data collection and D. M. Mason and J. E. Neuzil supervised the analytical work.

REFERENCES CITED

1. Birch, T. J., Hall, K. R., Urie, R. W., J. Inst. Fuel 33, 422-35 (1960).
2. Blackwood, J. D., Australian J. Chem. 12, 14-28 (1959).
3. Blackwood, J. D., McGrory, F., Australian J. Chem. 11, 16-33 (1958).
4. Channabasappa, K. C., Linden, H. R., Ind. Eng. Chem. 48, 900-5 (1956).
5. Goring, G. E., Curran, G. P., Tarbox, R. P., Gorin, E., Ind. Eng. Chem. 44, 1051-65 (1952).
6. Goring, G. E., Curran, G. P., Zielke, C. W., Gorin, E., Ind. Eng. Chem. 45, 2586-91 (1953).
7. Hiteshue, R. W., Anderson, R. B., Friedman, S., Ind. Eng. Chem. 52, 577-9 (1960).
8. Hiteshue, R. W., Anderson, R. B., Schlesinger, M. D., Ind. Eng. Chem. 49, 2008-10 (1957).
9. Hiteshue, R. W., Lewis, P. S., Friedman, S., Paper CEP-60-9, Operating Section, American Gas Association, 1960.
10. Pyrcioch, E. J., Linden, H. R., Ind. Eng. Chem. 52, 590-4 (1960).
11. Shultz, E. B., Jr., Feldkirchner, H. L., Pyrcioch, E. J., Chem. Eng. Progr. Symposium Ser. 57, No. 34, 73-80 (1961).
12. Shultz, E. B., Jr., Linden, H. R., Ind. Eng. Chem. 49, 2011-16 (1957).
13. Shultz, E. B., Jr., Linden, H. R., I and EC Process Design and Development 1, 111-6 (1962).
14. Shultz, E. B., Jr., Mechaes, N., Linden, H. R., Ind. Eng. Chem. 52, 580-3 (1960).
15. Zielke, C. W., Gorin, E., Ind. Eng. Chem. 47, 820-5 (1955).
16. Zielke, C. W., Gorin, E., Ind. Eng. Chem. 49, 396-403 (1957).

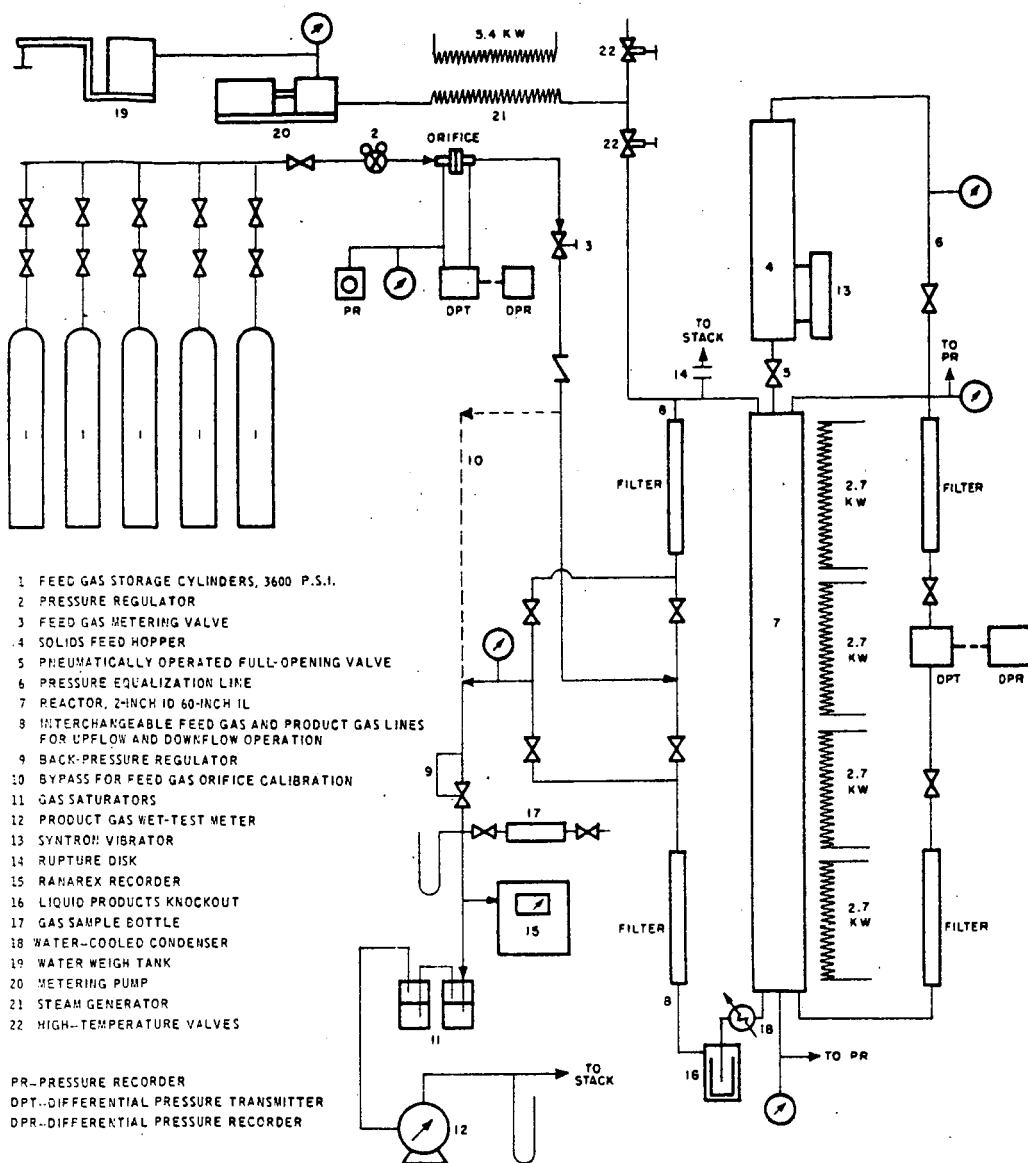


Fig. 1. Semiflow reactor system for study of rates of hydrogasification of solid fossil fuels at temperatures to 1700° F. and pressures to 3000 p.s.i.g.

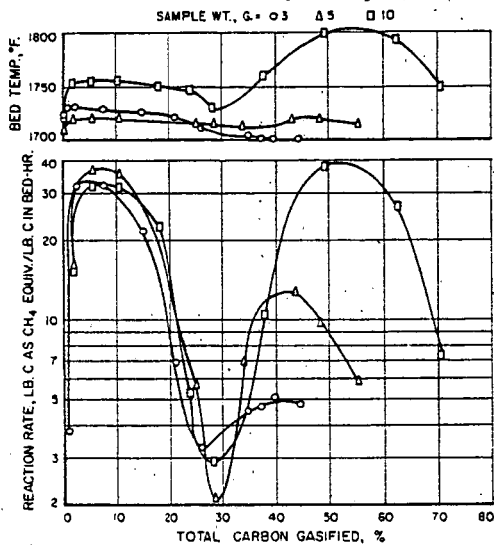


Fig. 2.-Apparent effect of sample weight on rate of char hydrogasification at 1700° F. and 1500 p.s.i.g.

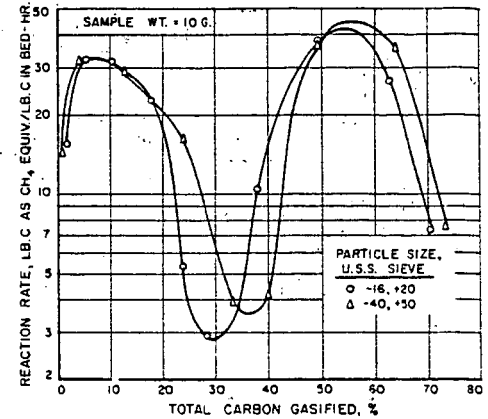
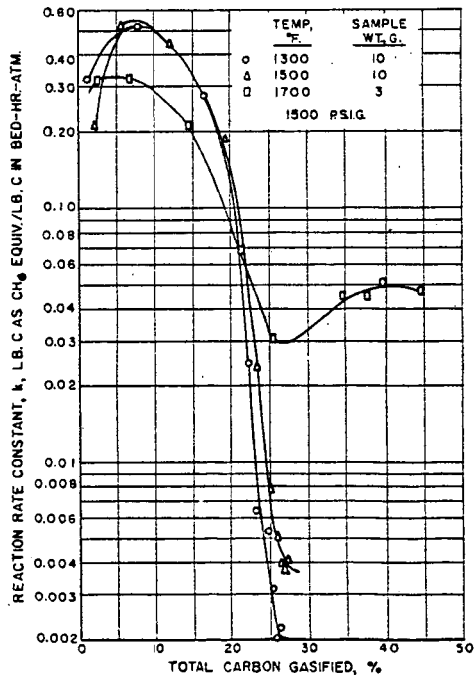


Fig. 3.-Effect of char particle size on rate of hydrogasification at 1700° F. and 1500 p.s.i.g.

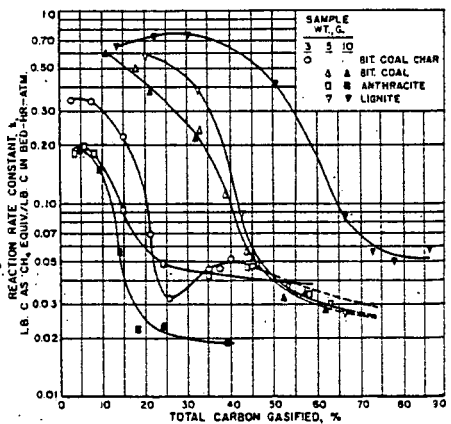


Fig. 4.-Effect of temperature and conversion on reaction rate constant for bituminous coal char

Fig. 5.-Reaction rate constants for various feeds at 1700° F. and 1500 p.s.i.g.

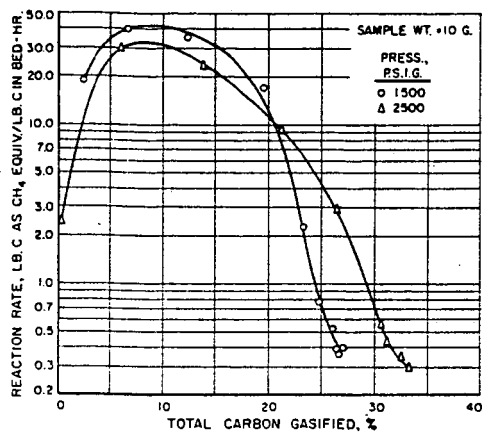


Fig. 6.-Effect of pressure on rate of char hydrogasification at 1500° F.

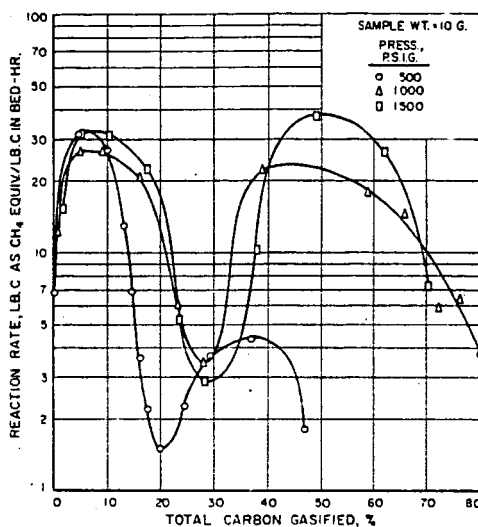


Fig. 7.-Effect of pressure on rate of char hydrogasification at 1700° F.

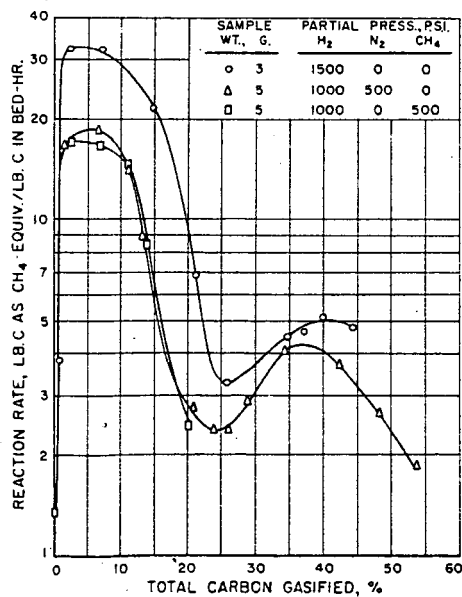


Fig. 8.-Effect of hydrogen and methane partial pressure on rate of char hydrogasification at 1700° F. and a total pressure of 1500 p.s.i.g.

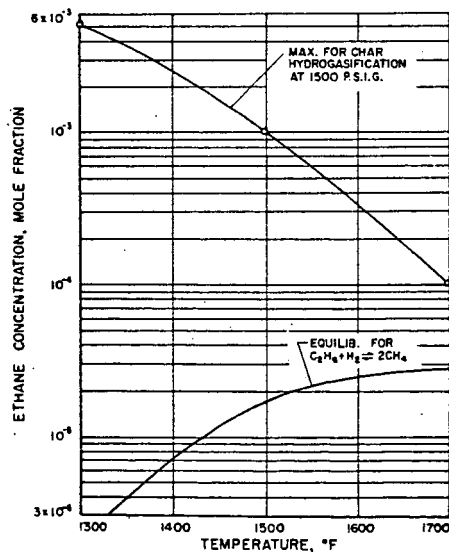


Fig. 9.-Approach of ethane concentrations to equilibrium values as a function of temperature

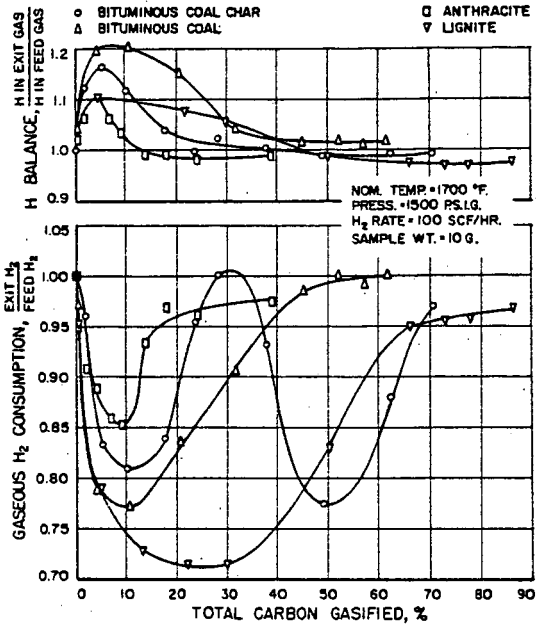


Fig. 10.-Gaseous hydrogen balances as a function of conversion of various feeds.

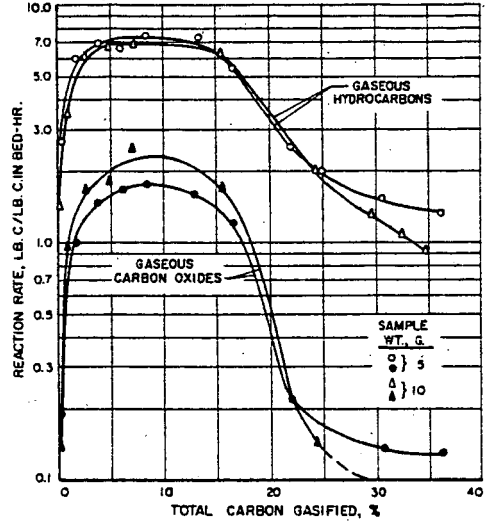


Fig. 11.-Effect of conversion on rate of gasification of coal char at 1700 °F. and 1500 p.s.i.g. with an equimolal steam-hydrogen mixture

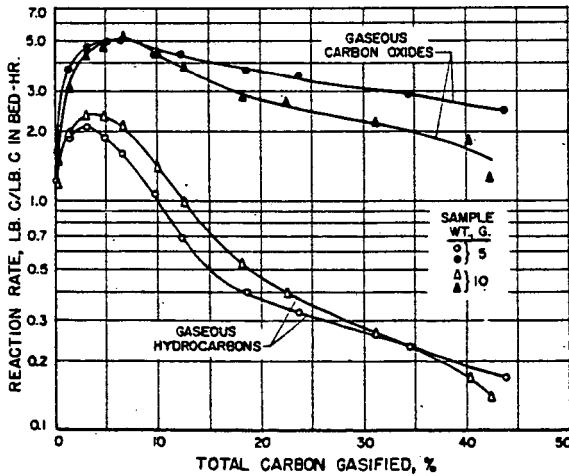


Fig. 12.-Effect of conversion on rate of gasification of coal char at 1700 °F. and 1500 p.s.i.g. with an equimolal steam-helium mixture.

THE REACTIVITIES OF SUSPENSIONS OF COALS
IN STEAM AT 900 - 950° C. (1,700° F.)

John J. S. Sebastian and Robert L. Day

Morgantown Coal Research Center, Bureau of Mines,
U. S. Department of the Interior, Morgantown, W. Va.

Investigators generally agree that the reaction of steam with various types of carbon and cokes, which has been widely investigated at the Morgantown Coal Research Center of the Bureau of Mines (5) and elsewhere, (3) (7) (8) (9) (10) (14) (15) (16) (18) is related to the reaction of steam with coal. Despite this relationship, knowledge of the kinetics of the steam-carbon reaction does not disclose nor reveal the kinetic behavior of coals of various rank and type in coal gasifiers. The conclusions drawn from studies of the reactivities of various types of carbon furnish little or no information on process rates, which can be used in the design of improved types of commercial coal gasification equipment.

Several investigators (2) (11) (12) (13) studied the kinetics of the reactions of coals, generally with air, oxygen or carbon dioxide, but restricted their research to relatively low temperatures, specific types of coals, fixed beds of coarse particles, etc. Others tried to fit theoretical rate equations to data from large-scale gasifiers, modifying their constants accordingly. Attempts to extrapolate these results to other types of coals suspended or entrained in steam at considerably higher temperatures and pressures (4) have never proved satisfactory and, in many cases, have failed. It is doubtful that a generally applicable rate equation can be established for substances as complex structurally and as widely different in composition as coals of various rank, type or grade. Generalization for all types of coals, cokes or chars, or the use of questionable assumptions to extend the applicability of a rate equation to all gasification conditions does not seem justified.

A "falling particle" technique has been developed by Dotson and Holden (5) of the Bureau of Mines at Morgantown, W. Va., for the determination of the reaction rates of carbons with steam. The method originally devised for finely divided carbons was recently modified by the authors and developed for the rapid determination of the reactivities of coals. The essential feature of the method is that it closely simulates the conditions existing when powdered coals entrained in steam are gasified in large-scale gasifiers.

The purpose of the work here described was to determine the "relative reactivities" of various types of coals when their particles react with steam at 1,700° F. Specifically, the object was to separate the overlapping effects of thermal decomposition and actual steam-carbon reaction when steam interacts with coals at high temperatures.

"Reactivity" of solid fuels is generally defined (7) as the velocity or time-rate of the reaction between a solid fuel and an oxidizing gas, usually O_2 , CO_2 , or H_2O , under a given set of experimental conditions, including temperature, pressure (4), particle size, size consist, and bulk density. "Relative reactivity" is defined here as the relative rapidity of reaction between a fuel and an oxidizing gas (steam in our case) in a given apparatus under the same set of experimental conditions. It is an experimentally obtained index figure, useful in comparison with other fuels. Pertaining to an average (measured) residence time, the term "relative reactivity"

signifies no more than what the name implies: reactivities of various fuels related to each other. It should not be confused with "kinetic reaction rate."

The term "kinetic reaction rate" is a more fundamental characteristic of a given fuel reacting with a given gas; it is independent of the gasifier design, and is usually more significant from a process engineering standpoint. However, its determination is more time consuming. The kinetic reaction rate usually expresses, in form of a rate equation, the functional relation between reaction rate and reactant concentration at any given temperature and pressure. For maximum usefulness from a design standpoint, full knowledge of the kinetic rate includes the effects of all variables on the reaction rate, particularly temperature and pressure (4) (17), and the physical state of the reactants, such as particle size, size consist, and bulk density. The effects of mass transfer rate and flow pattern, insofar as they affect the overall reaction rate, should also be known.

Although work is being planned on the determination of the kinetic rates of the reaction of steam with coals at higher temperatures and pressures, this paper is restricted to the study of the more rapidly determined relative reactivities of coals (-60 + 65 mesh) interacting with steam at 1,700° F. and atmospheric pressure. The reactivities are expressed in terms of (1) "fuel conversion," given as weight-loss in grams per gram of dry, mineral matter - free coal; or (2) "carbon conversion," shown as grams of carbon gasified per gram of carbon in the coal. In either case, the conversion of the coal to gas is due both to thermal decomposition and reaction with steam.

Apparatus and Experimental Technique

The reactor developed and used to determine the relative reactivities of coals by the falling particle technique is shown schematically in Figure 1. The 3-inch inside diameter 9-foot long alloy steel reactor tube is electrically heated by 9 (pairs) prefabricated semicircular embedded-coil-type heating elements 11.5 inches high and 5 inches outside diameter, each controlled by a variable transformer. Elements at the top and bottom serve to balance the heat losses; the other 7 elements control the temperature in the 85-inch long isothermal zone. Longitudinal temperature profiles or traverses are determined from time to time, and the heat input is adjusted to maintain isothermal conditions.

Doubly distilled water passing through a rotameter is vaporized in a small electrically heated tube, and the steam thus formed is preheated to 800 - 1,000° F. before injection into the reactor. The steam flow-rate is adjusted for the desired steam-to-coal ratio, generally 3 pounds of steam per pound of dry mineral matter - free fuel, and the vibratory feeder is started. The uniformly sized (-60 + 65 mesh per inch) coal particles in the feed bowl move upward along a spiral track until each particle is swept by nitrogen, flowing at a rate of about 1.2 std. cu. ft. per hour, through a hole into the feed-tube and thence into the reactor. The coal feed-rate, generally 50 g. per hour in the reactivity tests described, is controlled by adjusting the voltage input to the vibrating mechanism.

The coal particles, blanketed by nitrogen, fall through a 7-inch long 5/16-inch inside diameter feed-tube, the latter surrounded by a 5/16-inch wide annulus (not shown in Figure 1) through which the steam is passed downward at about 1,000° F. The coal particles thus preheated in the feed-tube are entrained in the steam and enter the top of the reactor-tube through a 1-inch inside diameter circular opening at its center. The entering particles together with steam and nitrogen spread somewhat, but direct contact with the wall is prevented as they are carried downward in laminar flow (conventional Reynolds number about 20) blanketed with gases. Accelerated by gravity, they continue to fall through the steam, nitrogen, and generated gases, virtually at free-falling velocity. Calculated for a reactor temperature of 1,700° F. (900 - 950° C.) and for a low-volatile bituminous coal fed at 50 grams per hour, with

a steam-to-coal ratio of 3:1, the linear velocity of the steam-nitrogen mixture in the upper part of the reactor was 0.19 ft. per sec. As the measured average terminal velocity of the coal particles was 1.33 ft. per sec., the difference is their free-falling velocity: 1.14 ft. per sec.

Since the coal particles travel 6 times faster than the entraining steam-nitrogen mixture, it is clear that the fuel particles fall in the reactor tube almost freely through the gases. The flow, therefore, is not so much of the entrainment type, but is rather an unsteady or partial suspension, and the term "falling particle technique" properly describes it. (An isotope tracer method used to determine the residence time of the fuel particles, and thus their terminal velocity, will be described in another paper to be published by the authors.) Laminar flow inside the reactor prevents direct contact between the particles and the heated reactor tube. Nevertheless, because of the small heat capacity of the fuel particles, and the effective transfer of heat --- partly by radiation from the reactor walls and partly by convection and conduction through the steam medium --- the falling particles are rapidly heated to the isothermal reactor temperature of 1,700° F.

The concentration of fuel particles in the upper part of the reactor, under the conditions stated, is estimated to be about 50 mg per dm^3 of reactor volume containing a gas mixture of 85 percent steam and 15 percent nitrogen. On an average, approximately 8 1/2 particles of -60 + 65 mesh coal are in partial entrainment (suspension) at any given time in each cm^3 of steam-nitrogen mixture flowing at a rate of 265 cc. per sec. (33.9 cu. ft. per hour) in the upper part of the reactor at 1,700° F. The average distance between the suspended particles, if they are assumed to be spherical and have an average diameter of about 0.21 mm., is approximately 6 mm. The latter value thus estimated is analogous to the term "mean free path," although used here in a different sense.

As shown in Figure 1, the residue and product gas recovery system is at the bottom of the reactor tube. The solid residual is collected in a receiver bottle, and is cooled, weighed and analyzed. Most of the excess steam and some fine soot collects in the condensate receiver; the rest of the soot is removed from the gas by means of a wash bottle. Traces of tar vapors in the product gas are caught on filter papers in a Buchner funnel, and the gas is metered, sampled, and vented.

A photograph of the apparatus is shown in Figure 2. Next to the control board in the foreground, the insulated reactor tube is seen with the product recovery train below it. The fuel-feeding and steam-generating systems are located on the upper platform partly visible at the top of the picture.

As the reactivity of powdered or granular fuel is affected by the size of the particles, it was necessary to investigate possible degradation of particles as they fall through the reactor-tube. Do the solid fuel particles abrade each other and, if so, is this size reduction balanced, in case of bituminous coals, by swelling of the particles when they pass through the plastic stage, usually between 700° F. and 1,000° F.? To answer these questions, the apparent (or bulk) specific volumes of two different coals and a char were determined, before and after a single passage through the reactor under the usual conditions at 1,700° F. Specific volumes were determined by filling a 10-cc. graduated cylinder with the particles, uniformly tapping, and then weighing the contents. The results are shown in Figures 3 and 4 with the apparent (bulk) specific volume in each case given below the photomicrograph of the sample. The specific volume data shown on these pictures are helpful in this evaluation since any increase in the apparent (bulk) specific volume or, conversely, decrease in bulk density may be due to (1) formation of fines (degradation), and/or (2) swelling of each particle with corresponding increase in porosity.

In addition to the microscopic examinations, the extent of degradation in fall was determined by drop-testing samples (-60 + 65 mesh per inch size) through the reactor-tube, in still air, at room temperature. A Wyoming high-volatile bituminous-C

coal (Serial No. 16) and a char, made by low-temperature carbonization from a Colorado bituminous-A coal, (Serial No. 7), were so tested for size degradation. In each case the procedure was identical: 100 grams of the sample was dropped 123 inches at a rate of 72 grams per hour (1.2 g. per min.), and the product was screened through a 65-mesh per inch standard screen, uniformly shaking and tapping it in each case. The results were negative. In both cases the size degradation was small, although the char was somewhat more resistant to breakage than the coal. The breakage index, which is the percent retained on the 65-mesh screen before the drop-test minus that retained after the drop-test, was 1.7 percent for the coal and 0.2 percent for the char. The time of fall during the drop-tests, determined visually, was 4.4 seconds for the coal and 3.5 seconds for the char.

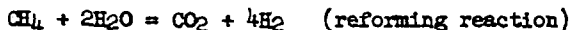
These results confirm what is evident from Figures 3 and 4: any size degradation from attrition of the particles by themselves and by the reactor wall is negligible and is well within the expected experimental error. Even this slight size reduction is more than balanced in the case of bituminous coals by the swelling of the particles as they pass through the plastic stage. There is plenty of evidence of swelling and formation of hollow spheres, as shown by the photomicrographs in Figures 3 and 4, as well as by the considerable increase in bulk specific volumes.

Experimental Fundamentals

Tests to determine the relative reactivities of coals were carried out under as nearly identical conditions as possible, thus maintaining at all times the major operating variables as constant as practicable. The most essential variables affecting the reactivities of powdered coals are: (1) type and size of test-reactor; (2) type, chemical composition and microstructure (porosity) of the coal; (3) particle size of the coal, its size consist and density; (4) coal throughput; (5) steam input rate (or steam-to-coal weight-ratio); (6) residence (or contact) time; (7) temperature; and (8) pressure. In developing a rapid practical method for testing coals for reactivity, the objective was to establish the correct magnitude for these variables in order to obtain measurable, but not excessive, fuel and carbon conversions.

An important variable in need of study was the required steam-to-coal ratio. The results of this study are illustrated in Figures 5 and 6. Figure 5 shows the effect of steam concentration (in terms of steam-to-carbon weight-ratios) on the components of the gases evolved. The yields of gases are seen to increase with increasing steam-to-carbon ratios, but most of the increase in the total gas yield was due to the rising trend in hydrogen evolution. This interesting fact points to a possible interaction of steam with hydrocarbon groups and other radicals attached to the coal molecule, and it appears that the interaction increases with the steam concentration. Although the diagram in Figure 5 refers to a low-volatile bituminous coal, yield curves showing identical trends were obtained with high-volatile bituminous coals.

The interaction of steam appears to facilitate thermal decomposition at a lower temperature, causing the detachment of alkyl groups and other radicals from carbon atoms in the coal matrix. This may result in the formation of "defect sites," probably with an electron lost or removed from the carbon atom from which a radical (possibly in ionic state) was detached. The existence of such defect sites owing to electron absences (or "positive holes") has been recognized by Gray (6) and his co-workers. The methane, ethane, other paraffin hydrocarbons, carbon monoxide, etc., thus entering the gas phase may react with additional steam to form CO_2 and H_2 . For example:



and



This is a plausible explanation of the hydrogen evolution (Figure 5) accompanying the interaction of steam with the coal molecule. There is plenty of evidence that steam thus interacts with coal both in carbonization and gasification, i.e., whenever thermal decomposition of coal takes place in the presence of steam (14). The defect carbon sites, often called "reaction sites" or "active sites," thus formed are vulnerable to attack by steam:



The importance of steam-to-carbon ratio thus established, experiments were made to determine its effect on the reactivity, measured as fuel or carbon conversion. Figure 6 shows that for both high and low volatile coals the reactivity rises asymptotically up to a ratio of about 3:1. Above this ratio, additional steam does not significantly increase the carbon conversion, i.e., a maximum has been reached. A ratio of 3:1 was thus chosen, as too much excess steam would increase the flow-rate, thereby decreasing the contact time below the limit of effective conversion needed for most of the reactivity tests.

Similarly, accurately measurable conversion was the criterion used in determining or choosing the optimum values of other essential variables. Thus, all of the tests were made with coals closely sized to pass a 60-mesh per inch U. S. standard sieve but retained on a 65-mesh sieve. The coal-feed rate was fixed at about 50 grams per hour and kept as constant as possible throughout each test. The temperature was kept uniform throughout the 83-inch long isothermal zone between 1,650 and 1,750° F., the maximum variation being $\pm 25^\circ$ F. The average residence time of the coal particles in the isothermal zone ranged from 5.2 seconds for subbituminous and low or high-volatile bituminous coals to 6.6 seconds for anthracites. (The determination of these values by an isotope-tracer method will be discussed by the authors in a future paper.)

The optimum values for the variables, thus determined, were kept as constant as possible so that the results of the reactivity tests depended only on the type, composition, and microstructure of the coal tested.

Materials Tested

Descriptions of the types of fuels tested for their reactivities are given in Table 1. The coals are presented in the order of increasing rank, ranging from lignites to anthracites. Also included in Table 1 are several types of chars derived by low-temperature carbonization from the specific types of coals shown in the table. Although the reactivities of these chars were determined in the same apparatus by the same technique described above for coals, the objective of the work with chars was sufficiently different to merit separate discussion in a future paper.

Proximate and ultimate analyses of the fuels tested are shown in Table 2 on a dry, "mineral matter - free" basis. Included in this table are in each case the percent mineral matter, calculated in conformity with ASTM standards (1) and the C/H ratio. Use of the "mineral matter - free basis" resulted in a much better alignment of data along the curves shown in various diagrams representing the functional relation between reactivity and various coal constituents or ratios.

Results and Discussion

Usually two, but in some cases up to five, reactivity tests were made on each of the 12 types of coals listed in Tables 1 and 2. The test results for each batch of coal were averaged and plotted on the following diagrams.

All of the reactivity test data (including data on several chars produced by low-temperature carbonization at the Bureau of Mines Denver Coal Research Center from

some of the coals investigated) are shown in Figure 7. This diagram illustrates the relative reactivities, in terms of fuel conversion, of coals of various rank (geological age) and their corresponding chars (connected with broken lines and arrows), as a function of steam concentration. Expressed on dry, mineral matter - free basis, coals of the same rank fall approximately along straight lines, each line indicating a given reactivity level. Most of the lines tend to be horizontal or slightly upward sloping and are usually parallel. The deviations in slopes, however, may not be significant owing to experimental errors in analyses or sampling. Actually, they should slope slightly upward, as in Figure 6, although for the shorter range of steam-to-coal weight-ratios, 2.2 to 3.5 shown in Figure 7, the upward trend is not as noticeable.

In general, it may be concluded that the reactivities of coals are inversely proportional to their rank or geological age. From this it follows that the reactivity is a function of the chemical composition and microstructure (porosity, density, etc.) of the coal as these, in turn, depended on the type of vegetation and geologic factors that existed when the coal beds were formed in various prehistoric ages. Since coals of various rank characteristically differ in volatile matter --- the ASTM (1) classifies them into ranks largely on the basis of volatile matter (on mineral matter - free basis) and calorific value --- it is evident that the reactivity must be related to the volatile matter as determined by the standard ASTM test. However, volatile matter and gas yield measured in reactivity tests are related terms, although by no means are they identical. The volatile matter test is intended to duplicate, to some extent, coke oven conditions in small-scale carbonization in a crucible at 950° C. (1,740° F.); the reactivity test is a combination of carbonization and gasification in steam medium at about 1,700° F. The gas yield, therefore, does not include the water formed as a result of carbonization, but it does include the product gases resulting from the steam-carbon reaction (CO, CO₂, and H₂) to the extent that this reaction takes place at 1,700° F. When fuel conversion is plotted versus volatile matter (Figure 8) and against gas yield (Figure 9), similar S-curves result, but the latter curve is much steeper. The significance of this difference is subject to further interpretation with additional experimental evidence on hand.

Thus, as has been claimed by several investigators (13), the reactivities of coals of various rank and type are functions of the volatile matter as determined by the standard ASTM test. Yet, the functional relation is not linear, as claimed in the past with considerable deviations admitted, but a mild-sweep S-curve, as shown in Figure 8.

While volatile matter has served for some time as an approximate, although auxiliary, index of rank, the results of this investigation show that the total carbon content and C/H ratio are more sensitive indicators of the ranks of coals. In plotting the reactivity against the carbon in coals, it was found that both the fuel and carbon conversions are cubic parabolic functions of the total carbon content. When plotted on mineral matter - free basis, not a straight line but a well-defined S-curve is obtained (see Figure 10). The reactivity decreases with increasing carbon content, very rapidly in case of younger coals, much more slowly with h.v. bituminous coals, and rapidly again in case of l.v. bituminous coals and anthracites.

On the other hand, the reactivities of coals, expressed in terms of either fuel or carbon conversion, are nearly perfect hyperbolic functions of the carbon-to-hydrogen weight-ratio (C/H), as shown in Figure 11. This appears to be significant both from the standpoint of fuel classification and process engineering, i.e., selection of coals for effective gasification. The C/H ratio appears to be an excellent indicator of rank, and may also be an indicator of the quality of synthesis gas, or that of high-B.t.u. gas or liquid fuel that can be produced by gasification and subsequent synthesis. In spite of this, it is not suggested that either the volatile matter, or total carbon content, or C/H ratio could be used as the sole index of rank.

An entirely different method of plotting the reactivity data is presented in Figures 12 and 13. The purpose of these diagrams was to determine the extent of the

reactivity, in terms of fuel conversion, caused by (1) thermal decomposition (devolatilization) and (2) the actual steam-carbon reaction. The effects of these two factors overlap in the reactivity tests described. We can say with considerable certainty that each particle of coal thermally decomposes with the evolution of volatile matter as its temperature rises to 1,700° F. The steam thereupon reacts with carbon atoms deprived of hydrocarbon, hydroxyl, carboxyl, and other side chains, i.e., it reacts with the so-called "fixed carbon." As the volatile matter evolved in thermal decomposition consists of much volatile carbon (in the form of CH₄, CO₂, CO, etc.), the fixed carbon remaining is always numerically less than the total carbon in the coal. Thus, if we deduct the percent of volatile matter (i.e., grams of coal converted to gas per 100 gram sample), as determined by the ASTM test at 1,740° F. (950° C.), from the fuel conversion (in terms of grams of coal converted to gas per 100 gram sample) at about 1,700° F., the difference will be the percent fixed carbon that reacted with steam to form CO, CO₂, and H₂. The two temperatures, 1,740° F. and 1,700° F. are sufficiently close to permit the approximation.

An interesting observation can be made and conclusion drawn by examining closer the diagram in Figure 12 on the reactivity of fixed carbon in relation to the total carbon content of coals of various rank. It shows that the actual steam-carbon reaction generally decreases with increasing order of rank from lignites to anthracites. However, a similar plot of conversion by the steam-carbon reaction alone versus the fixed carbon content (Figure 13) shows more clearly than the previous diagram that the rapidly descending curve tends to become asymptotic beyond 65 percent fixed carbon on dry mineral matter - free basis. In other words, steam at 1,700° F. reacts with carbon in younger coals with surprising ease, but less and less easily with carbon in older coals of increasing rank, while the carbon in coals from h.v. bituminous rank to anthracites is nearly equally reactive.

The conclusion drawn is significant, yet understandable in light of the explanation given above under Experimental Fundamentals. Lignites and other young coals have many more alkyl side chains and several other radicals attached to the benzenoid coal matrix than older bituminous coals, and still less in anthracites. When these radicals crack off the carbon atoms as a result of the interaction of steam, the "defect" sites remaining are vulnerable to attack by H₂O molecules, which explains the decreasingly lower reactivities of coals from lignites to anthracites.

Acknowledgments

The authors wish to acknowledge the helpful suggestions of the following Bureau of Mines personnel: Harry Perry, Dr. H. H. Lowry, and Dr. L. L. Hirst.

Table 1

DESCRIPTION OF TYPES OF FUELS TESTED FOR THEIR REACTIVITIES

Serial No. ^{1/}	Rank of coal *Type of char	Name of bed	Mine	Locality
		Description of carbonization conditions		
1	Young Lignite			Sandow, Texas
2*	Char made from Texas lignite (Serial No. 1)	Carbonized at 930° F. with an air-to-coal ratio of 3.73 std.cu.ft/lb. maf coal.		
10	Older lignite	Healy	Reynolds	Lake de Smet Area, Buffalo, Johnson County, Wyoming
12*	Char made from Lake de Smet lignite (Serial No. 10)	Carbonized at 930° F. with an air-to-coal ratio of 4.01 std.cu.ft/lb. maf coal.		
3	Subbituminous-B coal	Adaville No. 1	Elkol Kemmerer Coal Co.	Hams Fork Region, Frontier, Wyo.
16	High-volatile coal bituminous-C	No. 7 Seam	D. O. Clark	Superior, Wyoming
11	High-volatile coal bituminous-C	Rock Springs No. 3	Sweetwater No. 2	Green River Area, Wyoming
4	High-volatile coal bituminous-A	Pittsburgh	Pittfair	Shinnston, W. Va.
5	High-volatile coal bituminous-A	Sewickley	Bunker	Monongalia County, West Virginia
6	High-volatile coal bituminous-A	East Allen	East Allen	Garfield County, Colorado
7*	Char made from Colo. bituminous-A coal (Serial No. 6)	Carbonized at 1,200° F. with an air-to-coal ratio of 13.9 std.cu.ft/lb. maf coal.		
13*	Char made from Colo. bituminous-A coal (Serial No. 6)	Carbonized at 1,200° F. with an air-to-coal ratio of 6.9 std.cu.ft/lb. maf coal.		
15	Medium-volatile bituminous coal	Sewell	Wyoming	Wyoming, West Virginia
8	Low-volatile coal semibituminous	Pocahontas No. 4	Island Creek Coal Co.	McDowell County, West Virginia
9	Anthracite		Penn. & Reading Coal and Iron Co.	Locust Summit, Pennsylvania
14	Anthracite		Underkoffers	Iykens, Dauphin County, Penna.

^{1/} The serial numbers shown identify the type of fuel tested in subsequent tabulations and diagrams. All coals are shown in the order of increasing rank. An asterisk next to the serial number signifies char. See the corresponding heading above for coals and chars, respectively.

Table 2

ANALYSES OF FUELS TESTED

Serial No. 1/	Type of fuel	Mineral matter in fuel, percent	Components, percent mineral matter-free basis				C/H Ratio			
			V.M.	F.C.	C	H				
1	Young Texas lignite	15.7	48.8	51.2	72.9	5.5	18.6	1.4	1.6	13.3
2*	Char made at 930° F.; air-to-coal ratio: 3.72/	20.8	32.5	67.5	77.0	5.8	16.2	1.7	1.3	20.3
10	Older Wyoming lignite	20.0	46.4	53.6	71.7	4.8	22.1	1.0	.4	14.9
12*	Char made at 930° F.; air-to-coal ratio: 4.02/	26.8	29.9	70.1	78.1	3.4	16.2	1.2	1.1	23.0
3A	Wyo. subbituminous-B coal, Adaville No. 1 bed	3.4	42.2	57.8	74.2	5.0	18.8	1.3	.7	14.8
B		3.1	42.5	57.5	73.2	5.2	19.9	1.2	.5	14.1
16	Wyo. high vol. bituminous-C coal, No. 7 bed	3.8	40.4	59.6	78.3	5.3	14.2	1.3	.9	14.7
11	Wyo. high vol. bituminous-C coal, Rock Springs, No. 3 bed	12.1	32.2	67.8	82.8	5.5	9.1	1.8	.8	15.1
4	W. Va. high v. bituminous-A coal, Pittsburgh bed	11.3	38.2	61.8	81.7	5.9	7.2	1.6	3.6	13.9
5	W. Va. high v. bituminous-A coal, Sewickley bed	15.6	39.9	60.1	82.3	5.9	8.0	1.6	2.2	14.0
6	Colo. high v. bituminous-A coal, East Allen bed	24.0	37.3	62.7	83.7	6.2	7.9	1.7	.5	13.5
7*	Char made at 1,200° F.; air-to-coal ratio: 13.92/	49.2	5.1	94.9	82.5	2.7	12.3	1.2	.6	30.6
13*	Char made at 1,200° F.; air-to-coal ratio: 6.92/	31.3	5.7	94.3	92.2	2.0	3.2	1.7	.9	46.1
15	W. Va. medium vol. bituminous coal, Sewell bed	2.8	20.7	79.3	89.5	4.7	3.5	1.6	.7	18.9
8A	W. Va. low vol. semibituminous coal, Pocahontas	5.2	14.0	86.0	91.0	4.4	2.8	1.3	.5	20.7
B	No. 4 bed	5.5	13.8	86.2	91.2	4.4	2.6	1.3	.5	20.7
9A	Pennsylvania anthracite from Locust Summit, Pa.	14.2	5.8	94.2	91.9	2.8	3.7	1.0	.6	32.8
B		15.5	4.8	95.2	91.8	3.2	3.3	1.1	.6	28.7
14	Pennsylvania anthracite from Lykens, Pa.	13.3	5.7	94.3	92.2	3.4	2.3	1.2	.9	27.1

1/ Designations A and B represent the analyses of different batches of the same coal. An asterisk next to the serial number signifies char.

2/ Air-to-coal ratios are based on std. cu. ft. air injected per lb. of coal carbonized.

Literature Cited

- (1) ASTM Standard Methods D 388-38.
- (2) Batchelder, H. R., Busche, R. M., Armstrong, W. P., Ind. Eng. Chem. 45, 1856 (1953).
- (3) Binford, J. S., Jr., Eyring, H., J. Phys. Chem. 60, 486 (1956).
- (4) Blackwood, J. D., McGrory, F., Australian J. Chem. 11, 16 (1958).
- (5) Dotson, J. A., Holden, J. H., Koehler, W. A., Ind. Eng. Chem. 49, 148 (1957).
- (6) Gray, T. J., Detwiler, D. P., et al., "The Defect Solid State," Interscience Publishers, New York, 1957.
- (7) Guerin, H., "Le Probleme de la Reactivite des Combustibles Solid," Dunod, Paris, 1945.
- (8) May, W. G., Mueller, R. H., Sweetser, S. B., Ind. Eng. Chem. 50, 1289 (1958).
- (9) Peters, W., Laak, G. W., Brennstoff-Chem. 42, 84, 323 (1961).
- (10) Pilcher, J. M., Walker, P. L., Jr., Wright, C. C., Ind. Eng. Chem. 47, 1742 (1955).
- (11) Schroeder, H., Brennstoff-Chem., 35, 14 (1954).
- (12) Sebastian, J. J. S., Meyers, M. A., Ind. Eng. Chem. 29, 1118 (1937).
- (13) Sebastian, J. J. S., The Reactivities of Bituminous Coals, presented before the Gas and Fuel Chemistry Division, A. C. S., Atlantic City, N. J., Sept. 1941 (unpublished).
- (14) Sebastian, J. J. S., U. S. Pat. 2,955,988 (Oct. 11, 1960).
- (15) Van Krevelen, D. W., and Schuyer, J., "Coal Science," p. 321-335, Elsevier, New York, 1961.
- (16) Walker, P. L., Jr., Rusinko, F., Jr., Austin, L. G., Gas Reactions of Carbon, Ch. in "Advances in Catalysis," Vol. 11, 384 pp., Academic Press, New York, 1959.
- (17) Warner, B. R., J. Am. Chem. Soc. 65, 1447 (1943); 66, 1306 (1944).
- (18) Zielke, C. W., Gorin, E., Ind. Eng. Chem., 49, 396 (1957).

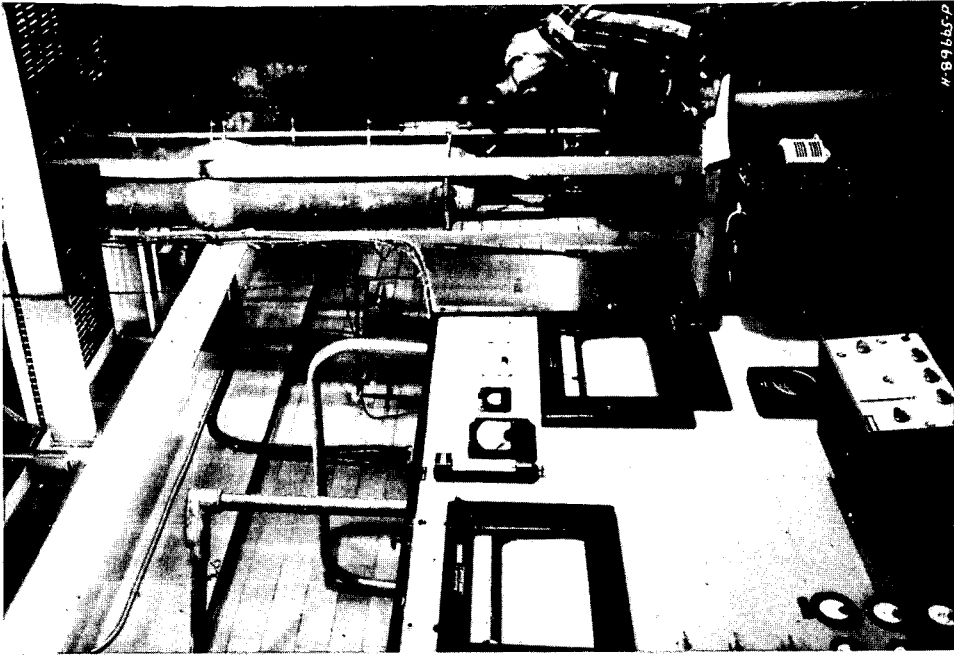


Figure 2. Photograph of Apparatus used for Study of the Kinetics of Reactions of Coals and Chars with Steam.

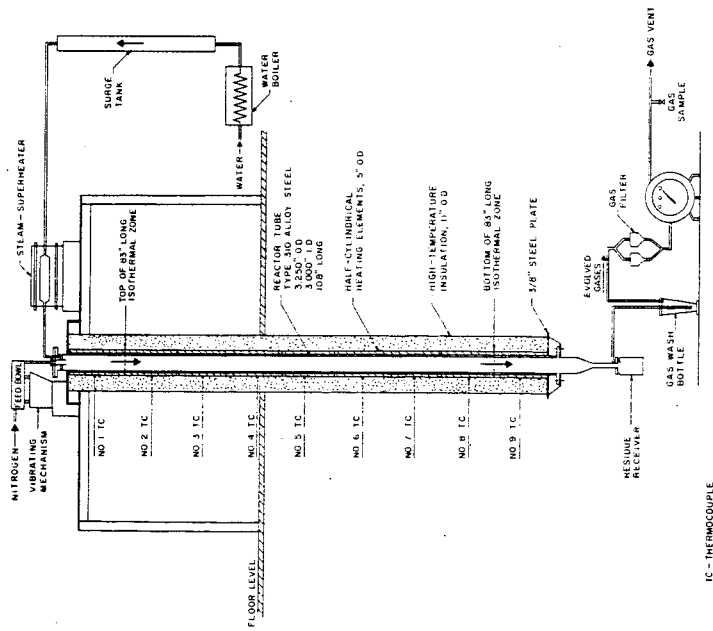
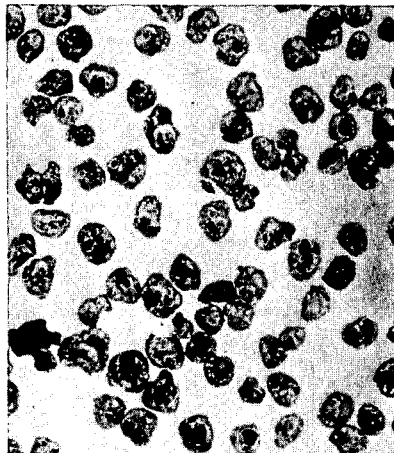
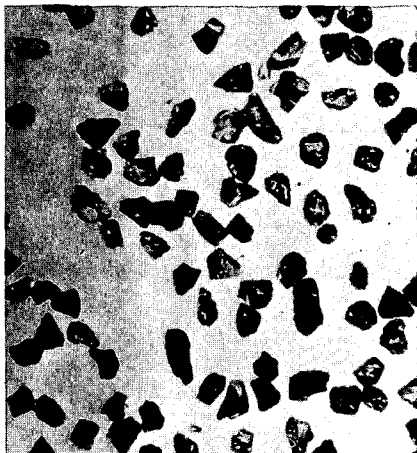


Figure 1. Isothermal Reactor for the Study of the Kinetics of Steam-Coal Reaction at High Temperatures



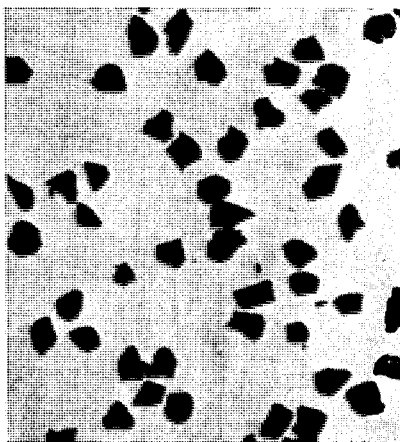
No. 11 - Wyoming H.V. Bituminous-C coal.
Size: -60 + 65 mesh/in; sp vol:
1.39 cm³/g

No. 11-R - Single pass residue obtained
from testing No. 11 coal.
Sp vol: 4.13 cm³/g



SCALE: MILLIMETER
1.0 mm = 1,000 microns

Figure 3. Photomicrographs of a Bituminous-C Coal and its Residue from Reactivity Test made at 1,700° F in Steam Medium (approximate enlargement 17X).



No. 6 - Colorado H.V. Bituminous-A coal.
Size: -60 + 65 mesh/in; sp vol:
1.32 cm³/g

No. 6-R - Single pass residue obtained
from testing No. 6 coal.
Sp vol: 2.99 cm³/g



SCALE: MILLIMETER
1.0 mm = 1,000 microns

Figure 4. Photomicrographs of a Bituminous-A Coal and its Residue from Reactivity Test made at 1,700° F in Steam Medium (approximate enlargement 17X).

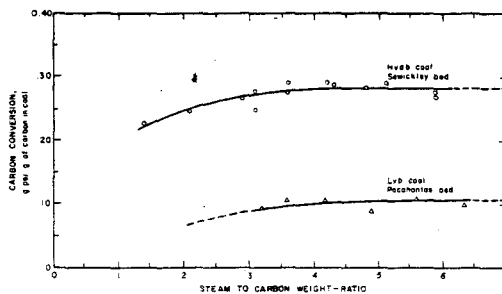
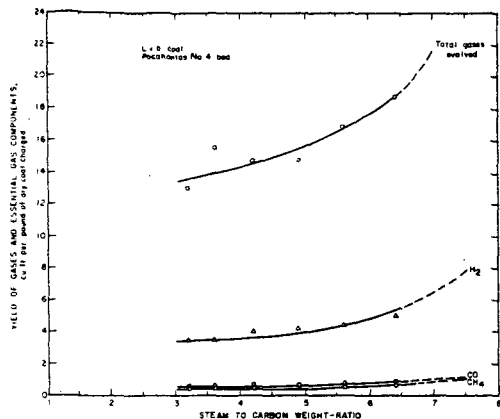


Figure 5. Effect of Steam Concentration on Gas Yield, 1700° F

Figure 6. Effect of Steam Concentration on Carbon Conversion, 1700° F

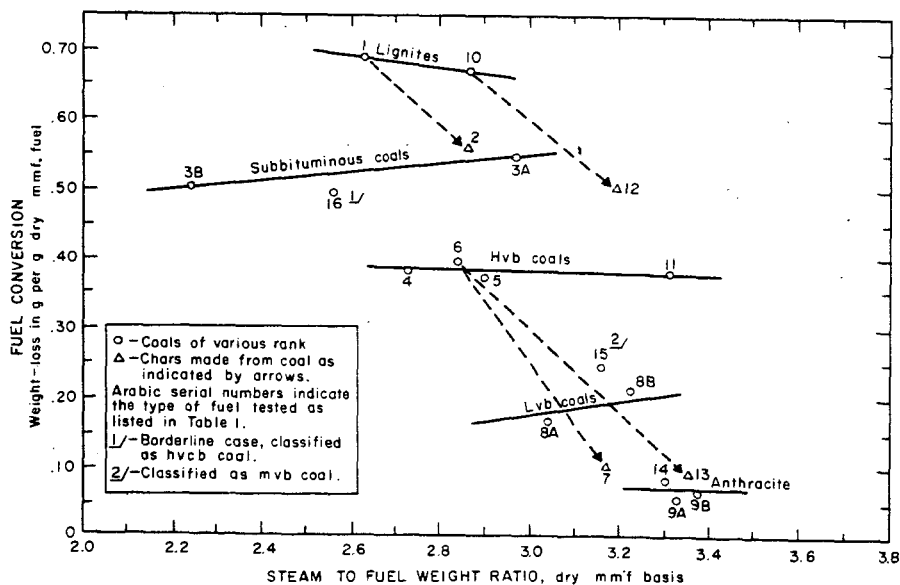


Figure 7. Comparative Reactivities of Coals and Chars

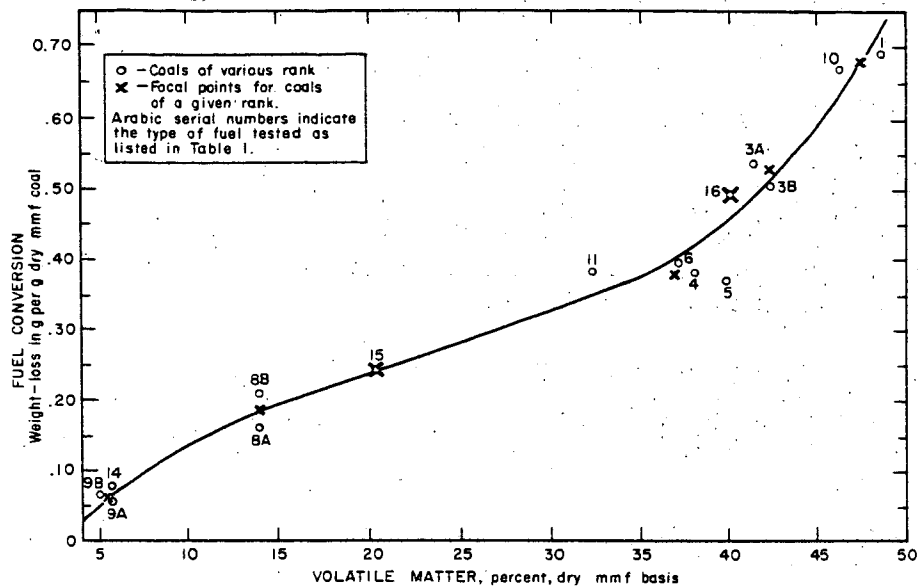


Figure 8. Fuel Conversion as a Function of Volatile Matter
— Steam Reacting with Coals at 1700° F

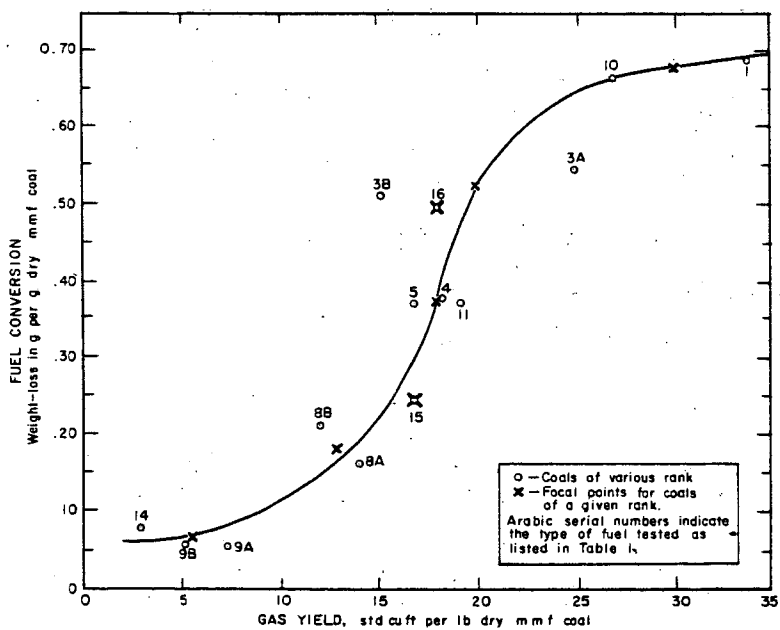


Figure 9. Relation Between Fuel Conversion and Gas Yield
— Steam Reacting with Coals at 1700° F

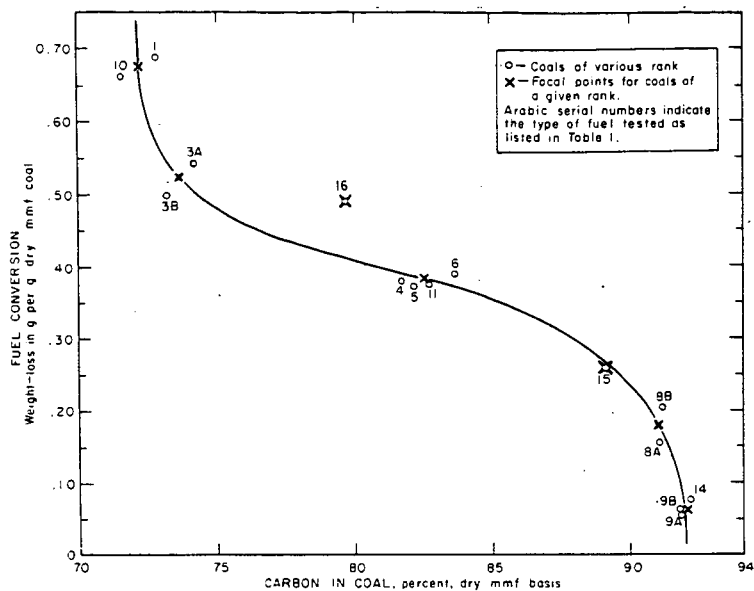


Figure 10. Fuel Conversion as a Function of Carbon Content
 — Steam Reacting with Coals at 1700° F

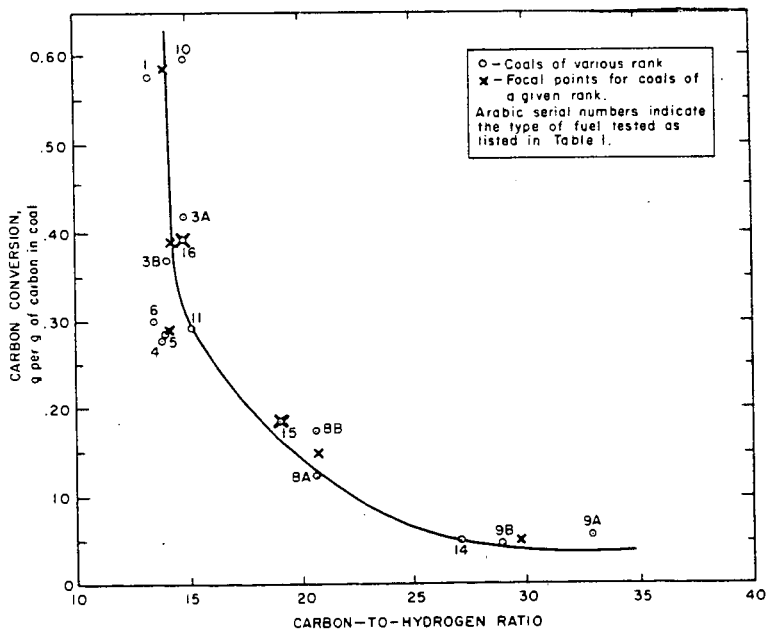


Figure 11. Carbon Conversion as a Function of Carbon-to-Hydrogen Ratio
 — Steam Reacting with Coals at 1700° F

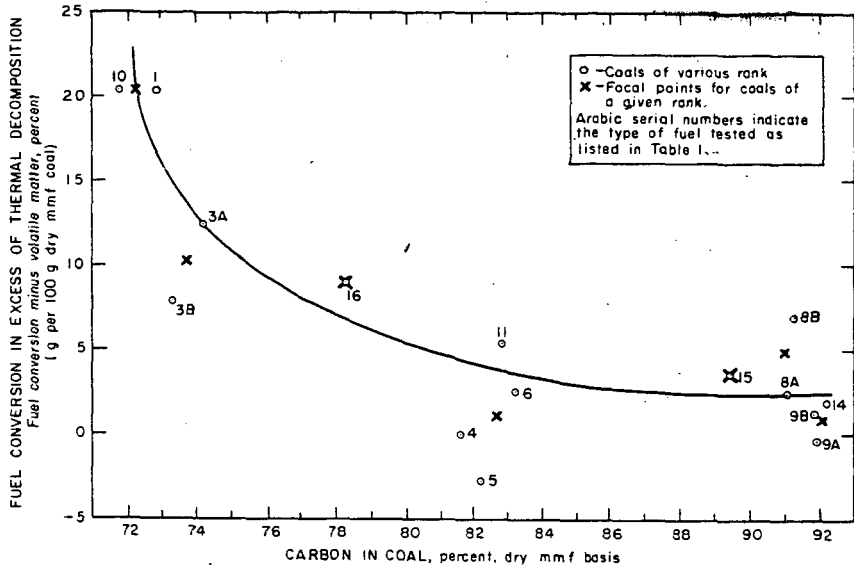


Figure 12. Relation Between Total Carbon in Coal and the Reactivity of Fixed Carbon — Steam Reacting with Coals at 1700° F

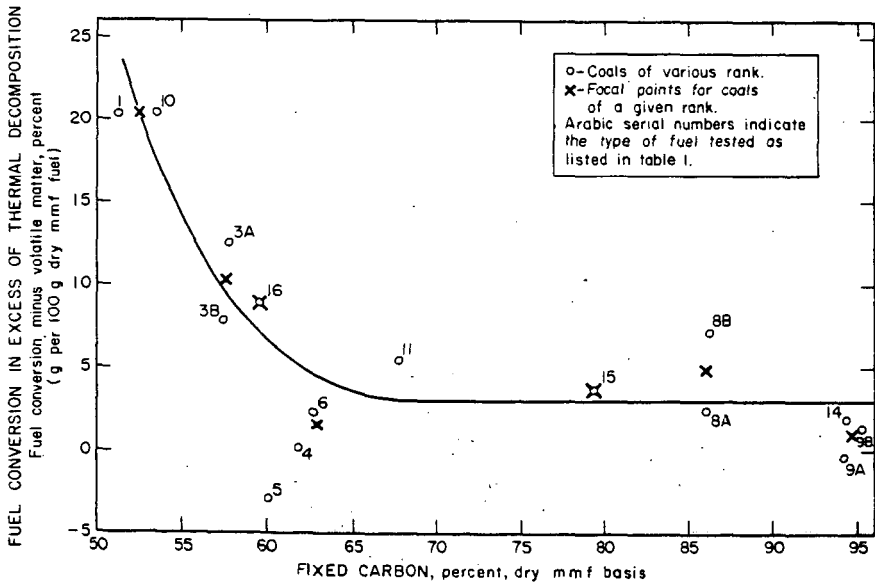


Figure 13. Relation Between Fixed Carbon in the Coal and the Reactivity of Fixed Carbon — Steam Reacting with Coals at 1700° F

Kinetics of Coal Combustion: The Influence of Oxygen Concentration
on the Burning-Out Times of Single Particles

Geoffrey Beeston and Robert H. Essenhigh

Department of Fuel Technology and Chemical Engineering
University of Sheffield, England

1. INTRODUCTION

Single particles of coal burn in two stages. The first is a volatile combustion stage; and the second, with which this paper is primarily concerned, is burn-out of the solid carbon residue left after generation and combustion of the volatiles. Kinetically, this second, burn-out stage is a heterogeneous process in which oxygen reacts directly, at-and-with the solid surface. It has, therefore, been studied extensively, but as it were by proxy using relatively pure carbon in place of the coal; and the validity of extrapolating such results directly to coal residues has generally been then taken very much for granted. Direct work on coal has, of course, been done in the past but the results (1-3) have generally been too few, and the conditions too imprecise, for kinetic studies. Further experiments have, therefore, been carried out on single particles of coal under more precisely specified conditions, to check proposed kinetic equations. The first results obtained, described elsewhere (4,5), were concerned with the variation of burning time as a function of particle diameter and coal rank, with other parameters such as oxygen concentration, temperature, and ambient velocity, kept constant. The success of those first experiments then encouraged extension of the work to investigate the influence of other parameters, and the next one chosen for investigation, was the oxygen concentration; this is of particular interest as it also has direct bearing on the assumed but disputed (6) order of reaction at the solid surface. The object of this present paper is, therefore, to report the results of these further experiments on the influence of oxygen concentration on the burn-out times of the coal particle residues, together with a comparison between the experimental and predicted behaviour.

2. THEORY

As the general theory has been covered extensively in previous reviews and papers (4, 5, 7-9) only the salient points will be quoted in summary here.

The theory is based on the original analysis by Nusselt (10) in which he assumed that the rate controlling process in the reaction was the rate of diffusion of oxygen from the mainstream to the solid particle surface, through a boundary diffusion layer. Reaction at the solid surface was assumed to be instantaneous, or effectively so, and it was also assumed to be first order with respect to the oxygen partial pressure adjacent to the solid surface. With these limiting conditions, Nusselt's prediction was that the total burning time (t_b) of a solid carbon sphere would be proportional to the square of the initial particle diameter (d_0):

thus

$$t_b = K_D d_o^2 \quad (1)$$

where K_D is a predictable burning constant that is a function of temperature and oxygen partial pressure.

This equation was tested in the previous experiments; in the first instance (4) just as it stands using only a few coals, but subsequently (5) the number and rank range of coals was increased to determine the influence of coal rank. To do this, burning times (of both volatiles and residues) of particles in the size range 4000 to 300 microns were measured as a function of diameter. The particles were burned in air, between two small heating coils of resistance wire, under relatively quiescent ambient conditions, at an effectively constant temperature of about 1000°C. In all, 10 coals were ultimately tested, ranging in volatile percentage from 5 to 40, and all were found to obey the eqn. (1). The value of the burning constant K_D had, of course, to be adjusted to allow for the effects of volatile loss and swelling, but the experimental values of the burning constant, K , were found (5) to be in good agreement with the following predicted relationship between K and K_D

$$K = [(C_f/100)/f] \cdot K_D \quad (2)$$

where C_f is the fixed carbon percentage; and f is a swelling factor whose values were found by measurement to be: unity for coals of V.M. less than 5%; and 1.5 for coals of V.M. greater than 10%. The basis of this prediction was the assumption that the coals first lost volatiles at constant diameter, and then swelled by the linear factor f . This then provided a correction factor to the solid density σ that appears in the theoretical relation for K_D

$$K_D = \sigma/3\rho_o D_o (T/T_o)^{0.75} \cdot \ln(1 - p_o) \quad (3a)$$

$$= k/\ln(1 - p_o) \quad (3b)$$

$$\approx k/p_o \quad (\text{for small } p_o) \quad (3c)$$

where ρ_o is the s.t.p. density of air; D_o is the s.t.p. diffusion coefficient of oxygen through nitrogen; T is the absolute temperature; and p_o is the ambient fractional oxygen concentration (of value 0.21 for air).

This set of equations therefore provided us with relations between burning time, or burning constant, and the two additional variables: oxygen concentration and temperature, to be checked by comparison with measurement in further experiments. Our choice of variable for the experiments reported here was the first: that of oxygen concentration, for the reasons outlined in the Introduction. In doing this, we only used a single coal since, as the quantitative influence of rank is given by eqn. (2), we assumed that validation on a single coal chosen at random should be satisfactory. The experiments were then carried out by measuring burning time as a function of oxygen partial pressure, using five different sizes of particle taken from the single coal, as described in the section following.

3. EXPERIMENTAL

To burn the particles in variable but controllable oxygen atmospheres, a small combustion unit was used inside a large perspex (plexiglass) box so that the ambient atmosphere could be controlled at will. The combustion unit was, in principle, that used in the previous experiments (4, 5), in which the coal particles were cemented to silica fibres and held by these, cantilever-fashion, mid-way between two horizontal heating elements of electrical resistance wire.

The coal used was Winter (ex-Grimethorpe); a medium bituminous coal, No. 7 of the set prepared and used previously (5), of analysis: Ultimate - 84.0%C, 5.5%H, 8.3%O, 1.8%N, 0.4%S (d.m.f. by Fereday and Flint (11) equation); Proximate - 36.0% V.M., 2.6% H₂O, 1.7% ash, 0.77% CO₂.

The perspex box used to house the combustion unit had dimensions: 1.5 by 1.5 ft. in plan section, by 3 ft. high, (6.75 cu. ft.). The oxygen atmosphere inside could be adjusted as required over the range 3% to 70% O₂. To make up the required atmosphere, oxygen or nitrogen was metered in as required, and the analysis then checked by Orsat. The reason for making the box so large was that the oxygen depletion during combustion of a particle would not then be significant, and the atmosphere could, therefore, be taken as being effectively infinite, with the 'main stream' or ambient oxygen concentration constant during the reaction thus meeting the specified boundary conditions required by the theoretical analysis. In fact, the box was large enough for a number of particles to be burned without having to open and recharge the box for each particle, and without significant change in the box's atmosphere. To take advantage of this, a rail carrying 18 carriages was mounted in the box, and to each carriage could be attached one silica thread with its coal particle cemented on ready for burning. After burning, the oxygen concentration was checked by Orsat analysis.

The particles on the carriages were moved into position between the coils, as and when required, by means of a control rod extending outside the box. The heating coils were larger than those used previously. In place of the 2-cm diameter flat spirals, wound from 18-gauge Nichrome resistance wire, the new heaters were square elements, of face area about 5 x 5 cm., made of Nichrome strip. This strip was about 1/2 cm. wide, and was wound with 1/2 cm. spacing on a 1/2 cm. thick former; the gaps between the set of strips on one side of the former were, of course, substantially covered by the return strips on the other side so that the whole face area was radiant. The two heating units were then mounted horizontally with their faces about 1.5 cm. apart. The heating was electrical, as before, controlled by a variable transformer unit; with this, element temperatures of up to 1060°C, as measured by an optical pyrometer, could be reached.

Burning times were measured with a stop watch in place of the photocell and pen recorder units used previously. The photocell was abandoned because of light shielding and other difficulties experienced with the larger heating elements. This meant that very short volatile burning times could not be measured - those larger ones that were, were measured with a second stop watch. However, the volatile measurements that were made were found to exhibit such considerable variability in the different oxygen atmospheres that their value was greatly reduced. Most measurements were therefore restricted to the residue burning times alone, using the stop watch which was found to be perfectly satisfactory for these.

With this apparatus, the residue burning times were measured at different levels of oxygen concentration as the principal variable, for each of the following particle sizes: 1870; 1300; 928; 649; and 388 microns. The particles were derived from the single coal, and burned in effectively infinite atmosphere, at an approximately constant temperature of 1000°C.

4. RESULTS

4.1 Qualitative Behaviour - The general behaviour of the particles was as observed before (4, 5): the particles burned in two stages, with the volatiles (when they burned at all) igniting first and burning with the characteristic luminous, flickering flame; and this was then followed in the burn-out stage by the much steadier glow of residue combustion. The particles did not ignite immediately; they required time to heat up to ignition, and this ignition time increased with decrease of oxygen concentration. This may indicate that preliminary, but significant oxidation may be occurring, with significant heat generation, before the volatiles ignited in flaming combustion. This requires closer investigation.

As in the previous experiments, the volatiles of the smaller particles often failed to ignite because of their small quantity and this failure increased, as was to be expected, as the oxygen was reduced. Where the volatiles did ignite in reduced oxygen, the usual fractional lag in time between finish of the volatile flame and start of the residue combustion was occasionally increased to a long delay ranging from two to thirty seconds. At the low oxygen concentrations, below 6%, the burning times also started to become very scattered, and at 3%, the particles failed to ignite at all.

At the other end of the scale, at high oxygen concentrations, the particles showed increasing tendency to decrepitate or explode. This happened whether the coils were already up to temperature before the particle was inserted (as was the case in general in these experiments), or whether the particle was already in position (as in the previous experiments) before switching on the heating current. If decrepitation is due to too rapid generation of volatiles before the coal becomes sufficiently plastic, this suggests that the volatiles generation must be influenced, contrary to previous expectation, by the ambient oxygen concentration. This would seem to imply that the oxygen causes some significant and rapid change in the constitution of the potential volatile material before generation, though how it should do this is by no means clear; this also requires further detailed study. In contrast, the general residue behaviour is far better understood, and more predictable, as described in the sections following.

4.2 Influence of Oxygen Concentration - By combining eqns. (1) and (3b) we have for burn-out of the residues:

$$t_b = [(C_f/100)/f] \cdot kd_o^2 / \ln(1 - p_o) \quad (4)$$

To test this equation, the experimental data obtained have, therefore, been presented in two graphs, Figs. 1 and 2. Fig. 1 is a plot of: $\log_{10} t_b$ against $\log_{10} [\ln(1 - p_o)]$, to show that the slopes of the lines obtained are, within

reason, close to 45° , or -1 . Fig. 2 is the alternative plot of t_b against the reciprocal of $\ln(1 - p_o)$, to show that the plots obtained are again acceptably linear and passing through the origin. Within the limits of accuracy of the measurements, these plots are, therefore, considered to substantiate eqn. (4).

- 4.3 Influence of Particle Size - From eqn. (4) it is clear that the slopes of the lines in Fig. 2 (written as m) are related to particle size by

$$m = [(C_f/100)/f]k.d_o^2 \quad (5)$$

This equation has in turn been tested by plotting $(m)^{1/2}$ against d_o , as shown in Fig. 3. Here again the plot is reasonably linear, and also passes through the origin. Again within the limits of accuracy of this plot, it is considered to substantiate eqn. (5).

- 4.4 Comparison with Prediction - Now, the slope of Fig. 3 (written as M) is an experimental quantity whose value is predicted from the appropriate terms in eqns. (3a) and (5), thus:

$$M^2 = [(C_f/100)/f] \sigma/3\rho_o D_o (T/T_o)^{0.75} \quad (6)$$

For the Winter coal, C_f is 60.7; f is 1.5; and σ is 1.25. For air, ρ_o is 1.3×10^{-3} g/cc; D_o for oxygen diffusing through nitrogen at temperature T_o (273°K) is 0.181 sq.cm/sec. The particle temperature is taken as 1000°C (1273°K), as in the previous experiments. With these values, the calculated value of M^2 is 225; we therefore have for $M_{(calc.)}$ a value of 15, which is precisely the experimental value obtained from the slope of Fig. 3. This exact agreement is clearly fortuitous; but within an error of 5%, which is the estimate of the overall error in both experimental and calculated values, it is clear that agreement is still satisfactory. Since this agreement was obtained by using the rank-influence equation (2), this also supports the assumption made that validation of the tested equations using a single coal, but chosen at random, would probably be satisfactory.

- 4.5 Burning Constant - This is the constant K_D or K of eqn. (1). It is calculated almost universally from measurements made in air, so tabulated values (as in Reviews 7, 8) are given for $p_o = 0.21$. From eqns. (1), (2), (3), and (6), it is clear that

$$K = M^2/\ln(1 - p_o) \quad (7)$$

Hence with a value for: M^2 of 225; and for $\ln(1 - p_o)$ of 0.235 when p_o is 0.21; this gives a value for $K_{(calc.)}$ of 957 sec/sq.cm. This is lower than (though close to) the value obtained in the previous experiments (5) for this same coal (previous value: - 1095 sec/sq.cm) but this may be accounted for in part by the difference between the logarithmic term $[\ln(1 - p_o)]$ and the first term of its expansion $[p_o]$ since the former has been used in this paper, but the latter was used in the previous paper (5); the theoretical alternatives are compared in the two eqns. (3b) and (3c). Use of the first term expansion as in eqn. (3c) is very common, and is generally accepted as being valid for

air or vitiated air. Just how widely the two terms differ at enriched concentrations, is shown by Fig. 4 in which the logarithmic term is plotted against p_o . In vitiated air the two are clearly reasonably comparable, but even in air itself the difference amounts to nearly 12% (0.235 compared with 0.21). Use of the \ln term in place of p_o in the previous experiments would therefore, reduce the value of 1095 to 978. The further difference between this and the new value of 957 is well within 5% but can in any case be attributed to uncertainty in the precise temperature in the two cases. Agreement, however, is regarded as acceptable.

The significance of the logarithmic term also showed up in the graphs of Figs. 1, 2, and 3. To check their sensitivity to the first expansion term in place of the full expression, similar plots were prepared (not reproduced) with p_o in place of $\ln(1 - p_o)$. The plots were found to vary significantly as follows: in equivalent Fig. 1, the plots showed slight but detectable curvature in spite of the fairly considerable scatter; in equivalent Fig. 2, convincingly straight lines could be run through the points, but the plots then showed marked intercepts on the oxygen-function axis, and the displacements from the origin were found to be statistically significant; finally, in equivalent Fig. 3, a straight line could again be run through the points, but again only with a statistically significant intercept. This agreement with the logarithmic term thus provides by far the best substantiation of the original Nusselt analysis in terms of the diffusion-film theory of reaction-rate control. What is yet undetermined, however, are the limits of applicability of the Nusselt equation and analysis; this is considered briefly in the next section.

5. DISCUSSION

- 5.1 Reaction Order - As stated in the Introduction, one of the principal reasons for carrying out the work described was to provide a more direct check on the assumed order of reaction at the solid surface. Now, because of the adjacent diffusion layer, that under these quiescent conditions is rate-controlling, it is only possible to check the surface order of reaction indirectly. To do this we assume some appropriate value for the surface order of reaction and then deduce what net, overall, or 'global' order of reaction should then follow. First of all, in choosing an order for the surface reaction, we have (7) two extreme limiting values: (1) zero, when the temperature is low enough for the surface chemisorption sites to be fully saturated at all times; and (2) unity, when the temperature is high enough for the sequence of chemisorption, followed by desorption, to be effectively instantaneous. At intermediate temperatures the reaction approximates to a fractional order. If internal or pore reaction also takes place, the lower limiting order is then raised from zero to 1/2.

Superimposed on this pattern is the oxygen supply by boundary layer diffusion. Now, in the first place, if the temperature is high enough for first order reaction to prevail then we get the burning time equation that combines both the diffusional and adsorption resistance (9),

$$t_b = K_c d_o + K_D d_o^2 \quad (8)$$

where K_c is the high-temperature chemical burning constant; and K_D is the

diffusional burning constant. This clearly has limits, respectively, of a linear equation, or a square law equation, according to whether diffusion is unimportant or dominant.

At the other extreme of low temperatures, when the reaction order is zero, the burning time equation is linear only (9)

$$t_b = K'_c d_o \quad (9)$$

where K'_c is the low-temperature chemical burning constant.

At intermediate temperatures the burning time is proportional to some intermediate power of the diameter, d_o^n , where n lies between 1 and 2. It is, therefore, obvious that determination of the power index n in any burning time experiments will give a clear guide to the relative importance of the three factors considered: (i) rate of diffusion; (ii) rate of chemisorption; and (iii) rate of oxide-film decomposition. In particular, a value of 2 for n is quite unambiguous in implying that the rate of boundary layer diffusion dominates the reaction control: and the significant corollary of this is that the surface rate-of-adsorption reaction must be first order.

In concluding that the reaction in our experiments was in the high temperature region, and diffusion controlled, we have altogether three confirmatory points provided by the experimental results. (1) The first is the 'square-law' agreement illustrated by the square-root plot of Fig. 3; if the additional chemical term in eqn. 8 — $K_c d_o$ — was also important, the line would be curved with a tendency to an intercept on the t axis. Other checks such as plotting (t_b/d_o) against d_o confirmed that K_c was negligible under the conditions of experiment. (2) We also have the agreement between t_b and the oxygen function $\ln(1 - p_o)$. Since K_c is inversely proportional to p_o (9), then if this was important the plot of t_b against $1/p_o$ would not have been so poor in comparison with the plot of Fig. 2 against $1/\ln(1 - p_o)$, as discussed in sec. 4.5. (3) There is finally the excellent agreement between the experimental and calculated values of the burning constant (written as K instead of K_D after correction for coal rank and swelling by eqn. 2) as described in sec. 4.5.

Since the reaction is evidently diffusion controlled, it follows that the surface reaction must be first order.

- 5.2 Boundary Layer Thickness - A secondary point of interest that also emerges from this is a reflexion on the question of boundary layer thickness. In calculating heat and mass transfer to spheres it is almost universal to use Nusselt's concept of the effective or 'fictitious' boundary layer thickness. If the oxygen concentration at the solid surface of the particle of radius, a , is zero, its value at any other radius, r , from the center of the particle is given approximately by

$$p/p_o = 1 - a/r \quad (10)$$

Since p rises to the main-stream value p_o only when r becomes infinite, the

real, physical boundary layer must clearly be of infinite thickness if it is defined as the distance required for p to reach the main-stream value. If, however, (following Nusselt (10)) the real behaviour indicated by eqn. (10) is replaced by an equivalent behaviour such that p is assumed to rise linearly to p_0 and then to remain constant with r , the main stream value is then reached at the Nusselt fictitious film thickness at $r = 2a$, or one radius out from the surface of the particle. It should be realised, however, that at $r = 2a$, $p = p_0/2$ (from eqn. 10); in other words, the actual, physical rise in p is only half the fictitious value. This can be represented in another way by relating the fictitious film thickness to a definable real, or physical film thickness. This can be defined with physical realism as the distance within which p rises to, say, 99% of the main stream value (this is a standard solution to continuum problems in which some relevant parameter reaches its limiting value only at infinity). We then have that, writing the boundary layer thickness as δ ,

$$\delta_{(\text{physical})} = 100a = 100\delta_{(\text{fictitious})}$$

The significance of this becomes immediately apparent when considering the behaviour of dust flames since the interparticle distance at a stoichiometric concentration is generally of the order only of 30 particle diameters. This means that in real, physical terms, as opposed to fictitious film-thickness terms, most of the oxygen is already well inside the boundary layer of one particle or another in the flame. It is clear, therefore, that direct extrapolation of the results in this paper to particles in dust flames should be made with caution.

Now, in addition to the points made above, a further complication that emerges is the additional inadequacy of the fictitious film concept, even for purposes of calculation, over the range of oxygen concentrations used in our experiments. Because our range was high, and the oxygen function $\ln(1 - p_0)$ could not be approximated by p_0 (as shown in Fig. 4), it means that eqn. (10) — which is also based on the same approximation of p_0 for $\ln(1 - p_0)$ — is also inadequate to describe the behaviour of the oxygen concentration over our full experimental range. An effective film thickness can still be defined, but the expression for it is so complex as to be valueless as it is then easier to solve the initial differential equation and not to bother about the 'short cut' of using an effective or fictitious film thickness.

- 5.3 Range of Applicability - The final point to be considered as a consequence of these results is their range of applicability: the temperature range of application is of particular importance.

Now, what we have established so far is that the solid surface reaction is first order at a temperature as low as 1000°C. This, however, was unexpected, being about 200° lower than the expected value of the 'higher critical temperature'. This was estimated, by assessment (7) of the available literature, at 1200°C. Below that, through the transition range down to 800°C, the reaction order was expected to drop progressively from unity to zero. The explanation for this apparent contradiction would appear to be a consequence of the influence of the

ambient gas velocity on the boundary layer thickness. The effect of ambient velocity is to promote such increased speed of mixing of the ambient gases that the thickness of the boundary layer, however defined, is progressively reduced. Initially, this must steepen the oxygen concentration gradient, with the result that both oxygen transfer, and therefore reaction rate, are increased. This increase can proceed just so far, up to the point that the rate of chemisorption exceeds the rate of reaction, and at that point the coverage of the solid surface by the chemisorbed film must increase; the surface reaction order then becomes fractional, and can drop progressively to zero as the ambient velocity also increases. This means that the transition range of temperature between the two extreme reaction conditions is velocity dependent. This dependence is shown very clearly by the single sphere experiments of Tu, Davis, and Hottel (12), but the analytical function relating the two is still unknown.

It would therefore seem that previously published experiments that were assessed as showing a first order reaction only down to 1200°C, cannot yet be directly correlated with the results of our experiments because the previous ones were carried out in flowing systems, whilst ours were in effectively quiescent systems. The increased film thickness that must have existed in our experiments can account qualitatively for the first order reaction down as low as 1000°C, but this inter-relation between temperature and velocity is now, in our opinion, the most outstanding problem of the combustion system requiring to be resolved by future work.

6. CONCLUSIONS

For coal particles inside the size range 350 microns to 2 m.m., burning in vitiated and enriched O₂ atmospheres (3% to 70%), at about 1000°C, under quiescent ambient conditions, the combustion behaviour was found to be as follows:

(1) Qualitative behaviour was, in general, similar to that observed previously with coal particles burning in air; for particles large enough, combustion proceeded in two sequential stages: (i) volatile evolution and combustion; followed by (ii) residue combustion.

(2) Particles below 1 m.m. tended to produce too small a quantity of volatiles for their combustion, because of low limit requirements. The frequency of this combustion failure tended to increase as the oxygen concentration was reduced. At 3% oxygen, even the residues failed to ignite. At high oxygen concentrations the particles ignited and burned satisfactorily, but they showed increasing tendency to decrepitate or explode.

(3) Quantitatively, only the residue combustion was examined in detail. Burning times of the residues (t_b) were found experimentally to obey the relation predicted from the Nusselt diffusion theory of reaction control:

$$t_b = m/\ln(1 - p_o)$$

where p_o is the ambient oxygen concentration; and m is a predictable constant.

(4) The results also showed good agreement with the following predicted relation between the constant m and the initial particle diameter d_0 :

$$m = M^2 d_0^2$$

where M is another predictable constant.

(5) The experimental value of the second constant M was also found to be in good agreement with the predicted value, as calculated from the relation

$$M^2 = [(C_F/100)/f] \sigma/3 \rho_0 D_0 (T/T_0)^{0.75}$$

where C_F is the fixed carbon of the coal; f is the swelling factor (of value 1.5 for bituminous coals); σ is the solid particle density; ρ_0 is the s.t.p. density of air; D_0 is the s.t.p. coefficient of oxygen diffusing through nitrogen; T is the absolute temperature and T_0 is the reference temperature of 273°K. The predicted and experimental values of M^2 were in fact identical, at 225; although this exact agreement was fortuitous it is still entirely satisfactory within the expected limits of error.

(6) The burning constant K in the Nusselt square-law equation

$$t_b = K d_0^2$$

was also calculated, being given by

$$K = M^2 / \ln(1 - p_0)$$

The value was 957 c.g.s. units, and this is in adequate agreement with values obtained previously for this same coal under similar (though not identical) experimental conditions.

(7) This general agreement with prediction therefore substantiates the primary assumption of the theoretical analysis: that the order of reaction at the solid particle surface with respect to oxygen concentration is unity. It also follows from the results that the rate of diffusion is the slow step that dominates the reaction rate, and that the importance of the chemisorption process is negligible under the conditions of experiment. There is background evidence from other previous experiments, however, indicating that this is true only for the fully quiescent system; and that, in a velocity field at these temperatures, the chemisorption process is likely to become significant, and increasingly so with increasing velocity. This is now the outstanding point requiring investigation in any subsequent work.

ACKNOWLEDGMENTS

The work described in this paper formed a part of a general program of research on Pulverized Fuel Firing, sponsored by the Electricity Supply Research Council of Great Britain. The work was carried out in the Department of Fuel Technology and Chemical Engineering, University of Sheffield, England. The authors are indebted to the ESRC for financial support of this work and for permission to publish this paper.

REFERENCES

1. Griffin, H. K., Adams, J. R. and Smith, D. F. Ind. Eng. Chem. 21(1929) 808.
2. Godbert, A. L. Fuel 9(1930) 57.
Godbert, A. L. and Wheeler, R. V. "Safety in Mines Research Board", Paper No. 73 H.M.S.O., London, 1932.
3. Orning, A. A. Trans. A.S.M.E. 64(1942) 497.
Omori, T. J. and Orning, A. A. - *ibid*- 72(1950) 591.
4. Essenhigh, R. H. and Thring, M. W. Proc. Conf. "Science in the Use of Coal", Sheffield, 1958; Paper 29 p. D21: Institute of Fuel, London, 1958.
5. Essenhigh, R. H. Paper No: 62-WA-35; to be presented at A.S.M.E. Winter Annual Meeting; Nov. 1962.
6. Frank-Kamenetskii, D. A. "Diffusion and Heat Exchange in Chemical Kinetics" Princeton University Press (Trans. 1955) Ch. II, pp. 64, 65.
7. Essenhigh, R. H. and Perry, M. G. Introductory Survey "Combustion and Gasification", Proc. Conf. "Science in the Use of Coal" Sheffield, 1958 p. D1: Institute of Fuel, London, 1958.
8. Essenhigh, R. H. and Fells, I. General Discussion on "The Physical Chemistry of Aerosols" Bristol, 1960; Paper No. 24, p. 208: Faraday Society, London, 1961.
9. Essenhigh, R. H. J. Inst. Fuel (Lond.) 34(1961) 239.
10. Nusselt, W. V.D.I. 68(1924) 124.
11. Fereday, F. and Flint, D. Fuel 29(1950) 283.
12. Tu, C. M., Davis, H. and Hottel, H. C. Ind. Eng. Chem. 26(1934) 749.

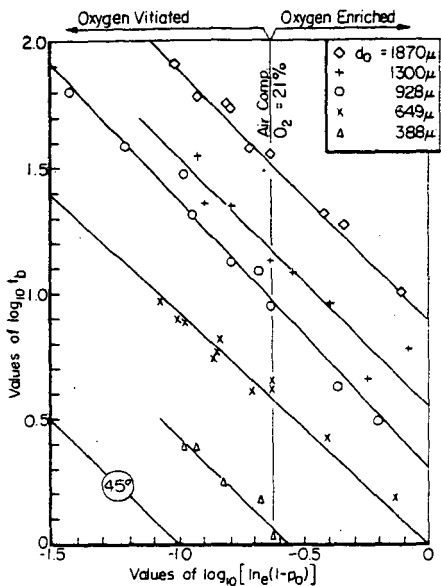


FIG. 1 - Double logarithmic plot of burning time, t_b , against the oxygen partial pressure function, $\ln_e(1-p_o)$.

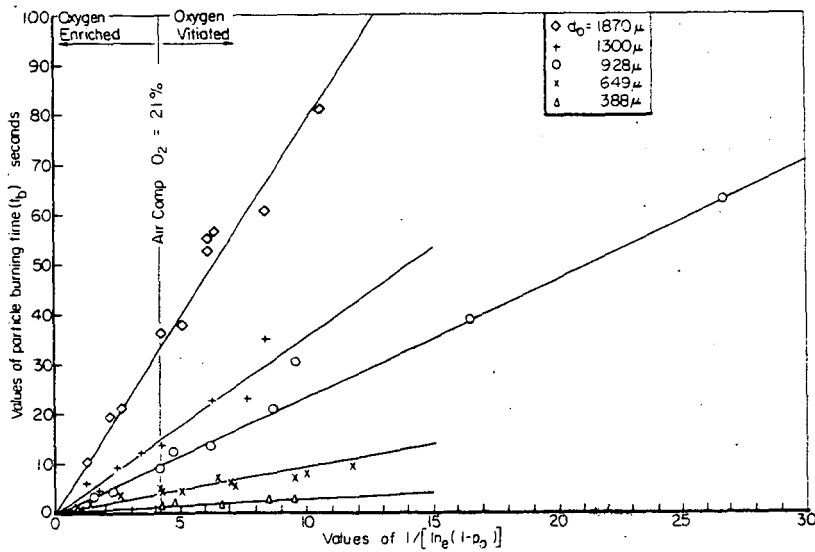


FIG. 2 - Linear plot of burning time, t_b , against the reciprocal of the oxygen partial pressure function: $\ln_e(1-p_o)$.

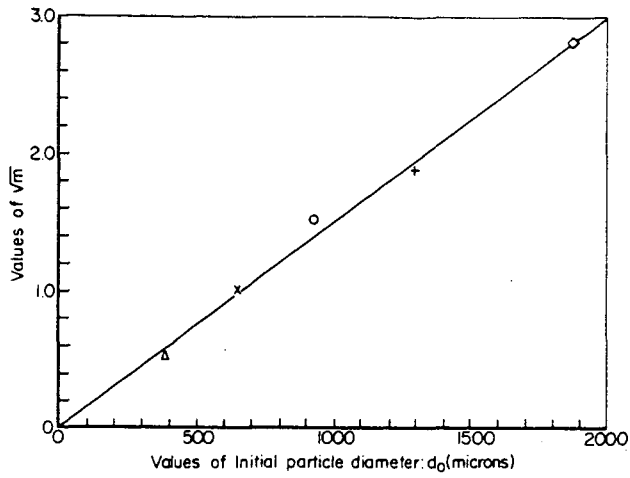


FIG. 3- Variation of square root of fig. 2 slopes (m) as a function of initial diameter of particle (d_0).

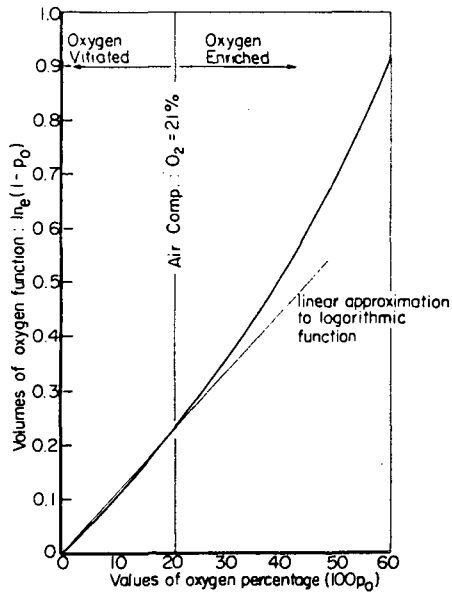


FIG. 4-Variation of oxygen function $\ln_e(1-p_0)$ with oxygen partial pressure p_0 .

The Theory of Gasification and its Application
to Graphite and Metallurgical Coke

by W. Peters and G.-W. Lask

Bergbau-Forschung GmbH, Essen-Kray

The theory of heterogeneous reactions^{1,2)} is applicable to the combustion and gasification of solid fuels. In connection herewith the passage of materials, i.e. the diffusion of the reacting gas through the boundary film and its penetration into the pores of the fuel, plays an important part, in dependency upon the temperature. A great number of measured values agree fairly well with the theoretical postulates.

For the determination of the reactivity, which varies in dependency upon the coking conditions, one preferred measuring method is prevailing today³⁾. The relation between the measured results and the coking conditions on the one side⁴⁾ and the suitability of the coke for metallurgical purposes on the other side⁵⁾ has been the object of a recent publication.

1. Theoretical bases of the Kinetics of the heterogeneous reactions in the gasification of coke

1.1. The rapidity constant of the chemical reaction

The gasification of fixed carbon with carbon dioxide (Boudouard's reaction) is a reaction of the first order⁶⁾. Thus, the speed of the reaction



is governed by the equation:

$$\frac{dx}{dt} = k \cdot O \cdot m \cdot c \quad (2)$$

where

- x = quantity of converted carbon (g)
- t = reaction time (sec)
- m = quantity of coke (g)
- O = sum of the external and internal surfaces (cm^2/g)
- c = concentration of CO_2 (g/cm^3)
- k = reaction speed constant ($\text{cm}^3/\text{cm}^2 \text{ sec}$)

In the range of the technically interesting temperatures the back reaction, i.e. the decomposition of the carbon monoxide



does not play any part.

Equation (2) indicates the effective conversion in such cases where k is so small that the stream of gas can reach the reactive surface quickly enough. At sufficiently low temperatures this will always be the case; For Boudouard's reaction on industrial coke the upper temperature limit is situated at about 1100 °C.

When the reaction gas flows through a bed of coke (Fig. 1), formation of CO leads to a continuous decrease in the CO_2 concentration. Moreover, the speed of flow will increase, which is due to the increase of the number of molecules engaged in Boudouard's reaction. In these conditions, the quantity of CO_2 converted in the unit of time along a layer of infinitely small thickness is determined by the equation

$$\frac{dn}{dt} = k \cdot 0 \frac{m}{l} c(x) dx = -d[v(x) c(x)] \quad (4)$$

where n = C atoms transferred
 m = quantity of coke (g)
 l = height of the layer (cm)
 $c(x)$ = CO_2 concentration at point x (g/cm^3)
 $v(x)$ = voluminal velocity at point x (cm^3/sec)

Let us assume that the stream of CO_2 having a speed v_0 and a concentration c_0 penetrates into a coke layer of equal cross sectional area at any point; then the speed v_0 at any point of this layer is

$$v(x) = \frac{2v_0 \cdot c_0}{c_0 + c(x)} \quad (5)$$

Substitution of equation (5) into equation (4) and integration over x from zero to 1 leads to

$$2v_0 \cdot c_0 \int_0^1 \frac{1}{c(x)} \cdot d\left[\frac{c(x)}{c_0 + c(x)}\right] = - \int_0^1 k \cdot 0 \cdot \frac{m}{l} dx \quad (6)$$

After integration between the limits indicated equation (6) adopts the following form:

$$2 \ln \frac{2c_1/c_0}{1 + c_1/c_0} + \frac{1 - c_1/c_0}{1 + c_1/c_0} = - \frac{k \cdot 0 \cdot m}{v_0} \quad (7)$$

where c_1 = the concentration of CO_2 in the outgoing gas (g/cm^3)

Often the differentiation plays a great part in the experimental determination of the reaction speed. m , c_0 and v_0 can be fixed in such a way that the required apparatuses do not become too expensive. c_1 can be determined by gas analysis; its value should range between 40 and 80 %. With lower CO_2 concentrations we come into a range where the concentration of CO inhibits Boudouard's reaction (10-13). Higher CO_2 concentration, by contrast, require a very high accuracy of analysis, as in

their range even great changes of the reaction speed entail only slight modifications of the CO_2 concentration.

With the experimental conditions as described and the values of CO_2 concentration found in the outgoing gas, the product $k \cdot O$ can be calculated quite simply. As, however, it is difficult to determine the surface of reaction O , k and O are combined to form the reaction speed constant k_m which is based upon the weight unit instead of the unit of surface:

$$k_m = k \cdot O \quad (8)$$

This value k_m is called "reactivity" in the following chapters; its dimension is $\text{cm}^3/\text{g sec}$.

If the method used for the determination of the reactivity involves direct weighing of the loss of weight of the coal, whilst the CO_2 concentration in the outgoing gas, c_1 , differs only slightly from its concentration c_0 when entering the reaction chamber, it is easier to use equation (2)⁰ in the form:

$$\frac{dx}{dt} = k' \cdot m \cdot c' \quad (9)$$

where k' = reaction speed constant ($1/\text{sec}$)
 c' = concentration of CO_2 (g/cm^3) under the existing conditions
 concentration of CO_2 (g/cm^3) under standard conditions

In this case the loss of weight during gasification is indicated by k' , and the following numerical relation exists between k_m and k' :

$$k' = 5,02 \cdot 10^{-4} k_m \quad (10)$$

1.2. Reactivity as a function of temperature

The dependence of the reactivity upon temperature is expressed in Arrhenius's formula:

$$k_m = H \cdot e^{-\frac{E}{RT}} \quad (11)$$

where H = the frequency factor ($\text{cm}^3/\text{g sec}$)
 E = activation energy (kcal/Mol.)
 R = gas constant (kcal/mol degree)
 T = the absolute temperature (degrees Kelvin)

By plotting $\log k_m$ or $\log k'$ against $\frac{1}{T}$, we obtain a straight line with the gradient $\frac{E}{R}$. From this gradient, the activation energy E can be de-

terminated. Figure 2 shows schematically the run of this straight line within range I.

1.3. The influence of diffusion upon the reaction speed constant and the energy of activation.

The validity of all the foregoing considerations is unrestricted only as long as the problems of molecular passage of materials during the gasification process do not yet come into play. With rising temperatures, however, the chemical reactivity will increase to such a degree that the diffusion of the gasifying agent in the carbon and towards the carbon, as the slowest step of a whole chain of physical and chemical reactions, becomes the dominant factor (1,2).

1.4. Pore diffusion

With rising temperature the reaction speed increases in conformity with equation

$$k = k_0 \cdot e^{-\frac{E}{RT}} \quad (12)$$

and the diffusion speed according to equation:

$$D = D_0 \cdot T^{1,8} \quad (13)$$

where D = diffusion speed (cm²/sec)
 D_0 = diffusion speed constant (cm²/sec)

As k rises much more sharply than D , the concentration of the gasifying agent in the pores of the fuel begins to decrease, beyond a certain temperature limit, as compared with its concentration in the ambient gas. This means that the conversion can utilize the internal surface only to a lesser degree, as expressed in equation

$$\frac{dx}{dt} = \left(\frac{dx}{dt} \right)_{\max} \cdot \eta \quad (14)$$

Beyond a zone of transition the utilization coefficient η is proportional^{to} the reciprocal value of the catalyser coefficient ρ (1,2).

$$\rho = L \cdot \sqrt{\frac{2k}{rD}} = \frac{1}{\eta} \quad (15)$$

where L = length of pores (cm)
 r = diameter of pores (cm)

For coke it is admissible to replace the length of pores by half the diameter of the lump $d/2$. Substitution of equations (14) and (15) into equation (2) leads to

$$\frac{1}{m} \frac{dx}{dt} = 0. c_0 \frac{1}{d} \sqrt{2 r D k} \quad (16)$$

As, according to equations (12) and (13), the reaction speed k rises much more rapidly than the diffusion speed D with the temperature,

$$\frac{dx}{dt} \propto e^{-\frac{E/2}{RT}} \quad (17)$$

This is to say that in the case of pore diffusion the activation energy is reduced to half its value. In figure 2 this is schematically represented by the straight line within range II.

1.5. Boundary film diffusion

If the reaction speed continues to increase with rising temperature, the conversion is restricted to the external surface of the fuel. Around the piece of coke forms a boundary film through which the gasifying agent will diffuse towards the place of the reaction. Under these conditions the reaction speed mainly depends on this diffusion process which is governed by Fick's first law:

$$\frac{dx}{dt} = - D F \frac{dc}{d\delta} \quad (18)$$

where F = external surface of the coke (cm^2)
 δ = distance from the coke surface (cm)

In the boundary layer the concentration shows a linear decrease:

$$\frac{dc}{d\delta} = - \frac{c_0}{\delta} ; \quad c = \frac{c_0}{\delta} \delta \quad (19)$$

Substitution into equation (18) leads to

$$\frac{dx}{dt} = D \cdot F \cdot \frac{c_0}{\delta} \quad (20)$$

The determination of δ is an aerodynamic problem which can be solved as follows: The transfer of heat on surfaces is governed by the general law:

$$\frac{dq}{dt} = \alpha \cdot F \cdot \Delta T \quad (21)$$

where q = quantity of heat (cal)
 α = coefficient of heat transfer ($\text{cal}/\text{cm}^2 \text{ sec}^\circ\text{C}$)

On the other side the flow of heat in a layer can be expressed as follows:

$$\frac{dq}{dt} = \lambda \cdot F \cdot \frac{dT}{d\delta} \quad (22)$$

where λ = thermal conductivity (cal/cm sec °C)

According to equation (19), the temperature gradient $\frac{dT}{d\delta}$ is constant

as well as $\frac{dc}{d\delta}$; thus,

$$\frac{dq}{dt} = \lambda \cdot F \cdot \frac{\Delta T}{\delta} \quad (23)$$

Division of equation (23) by equation (21) leads to the next equation from which the thickness of the boundary layer δ can be determined.

$$1 = \frac{\lambda}{\alpha} \delta ; \quad \delta = \frac{\lambda}{\alpha} \quad (24)$$

From many measurements the ratio $\frac{\alpha}{\lambda}$ is known for pieces of coke in a

free stream of gas, as well as for coke grains in layers and fluidized beds; as a rule the following basis is assumed:

$$\bar{Nu} = b \cdot Re^a \quad (25)$$

where \bar{Nu} = Nusselt's number

$$\left(\frac{\alpha \cdot d}{\lambda} \right)$$

Re = Reynolds number

$$\left(\frac{w \cdot d}{\nu} \right)$$

d = coke diameter

a and b = constants which are independent of the conditions of flow (cm/sec)

ν = kinematic viscosity

By substituting into equation (24) the value of $\frac{\alpha}{\lambda}$ obtained from equation (25), we get the thickness of the boundary layer δ whose value is substituted into equation (20):

$$\frac{dx}{dt} = D \cdot F \cdot \frac{b \cdot c_0}{d} \cdot Re^a \quad (26)$$

With sufficient accuracy the kinematic viscosity ν can be assumed to be equal to the diffusion speed D , whose dependency upon the temperature is expressed by equation (13). Using a shape factor f , the external sur-

face of the mass of coke (m) can be calculated from the equation

$$F = \frac{6 f m}{\rho d} \quad (27)$$

where F = shape factor
 ρ = apparent density of the piece of coke (g/cm^3)

To derive c_o from the standard concentration c_{No} , the temperature T and the pressure p have to be taken into account as usually:

$$c_o = c_{No} \frac{273 p}{T 760} \quad (28)$$

Taking into account equations (13), (27) and (28) we obtain from equation (26) the final formula:

$$\frac{1}{m} \frac{dx}{dt} = 2.16 f b D_o^{1-a} \frac{c_{No}^p}{\rho} d^{a-2} T^{0.8 - 1.8a} \quad (29)$$

In practice, the power a is about 0.5, so that the final formula in most cases reads as follows:

$$\frac{1}{m} \frac{dx}{dt} = 2.16 f b \sqrt{D_o} \frac{c_{No}^p}{\rho} \frac{1}{d \sqrt{d}} \frac{1}{T^{0.1}} \quad (30)$$

In the range of boundary film diffusion the dependency upon the temperature T is almost negligible, as appears from the horizontal stretch of the curve in range III (see fig. 2). The proportionality to $1/d^{1.5}$ reflects the great importance of the piece size in gasification processes at very high temperatures.

1.6. Dependency on the conditions of gasification

Practically, each range of reaction is characterized by a straight line in the Arrhenius diagram, the three straight sections being linked together by shorter or wider arches. If the conditions are changed, the straight lines are shifted, as will be shown in detail in the light of the three final equations, applicable to the three ranges, viz. (2), (19), and (30).

In the range of chemical reaction the particle size d is not influential upon the intensity of gasification. In the other ranges crushing of the coke leads to a higher intensity of gasification; in fact, in range II the way of diffusion up to the internal surface is reduced, whereas in range III the reactive external surface is enlarged. In the Arrhenius diagram (Fig. 3) the straight lines show a parallel upward displacement with decreasing particle size in the range II and III, whereas the transition zone between range I and II is shifted to the left, i.e. towards higher temperatures.

In ranges I and II the increase in the internal surface O entails a proportional intensification of gasification. In range II, where CO_2 is completely converted on the external surface, the internal surface does not play any part. In the Arrhenius diagram (Fig. 4) the straight lines show a parallel upward displacement with increasing surface O in ranges I and II, and the transition from range II to III is shifted to the right.

The speed is influential upon the decrease in CO_2 concentration during the passage through the layer of coke. Only for this reason, not directly the intensity of gasification is influenced by the speed of flow in ranges I and II. In range III, however, the speed of flow does influence the thickness of the adhering boundary layer. Here, a decrease in the boundary layer thickness results in a steeper gradient of concentration, in stronger boundary film diffusion and in a greater intensity of gasification (Fig. 5).

2. Measurements

2.1. Apparatuses

2.1.1. Gas-analytical method

For determining the reactivity of fine-grained coke we have used an apparatus (Fig. 6) which differs only slightly from that designed by Koppers and Jenkner (15-17). Recent experiments of Dahme and Junker (18) as well as of Hedden have confirmed the usefulness of this arrangement and have made it possible for conclusions to be drawn from the results with regard to the kinetics of reaction (19). The measuring method (20) may be briefly described as follows:

Analytically pure CO_2 flows at a speed of $2.5 \text{ cm}^3/\text{sec}$. through a reaction tube 20 mm in diameter. This tube is blown from quartz, the coke sample is resting upon a frit. In our tests the weight of the coke in the tube was 2.5. or 5 g. The gas flows downstream through the layer of coke and leaves the reaction zone through the frit. Through a pipe the outgoing gas flows into the analyser, viz. an azotometer, which has been adapted to the special purpose. In many cases an infra-red analyser was used. The oven is designed in such a way that the reaction temperature is reached after 10 minutes and the first measurement can be carried out after 15 minutes. The temperature is measured 10 mm above the frit with a platinum-rhodium couple.

2.1.2. Measurements on lumps of coke

For the determination of the intensity of gasification of lumpy coke up to temperatures of 1500°C an apparatus has been developed (see Fig. 7) which is not based on the principle of gas analysis but on the gravimetric determination of the loss of weight. The samples used in this method, are coke cylinders 40 mm high and 20 mm in diameter. A ceramic tube is suspended from a balance which records the time and the loss of weight. Through the tube a platinum-rhodium couple is introduced into the coke sample. This arrangement makes it possible to continuously observe the temperature of reaction in the coke sample during

weighing. Because of the endothermic reaction, this temperature differs from the temperature of the gas; at high temperatures the difference may reach values of some 50 °C. The throughput of gas is 400 l/h for each measurement. This means that the concentration of CO in the outgoing gas is only small and negligible in the calculation.

2.2. Measuring results

Our reactivity measurements were preceded by investigations intended to determine the influence of different factors upon the measuring accuracy.

2.2.1. Material used and sampling method

The electrode graphite used in our tests was ash-free, and thanks to its high graphitizing temperature it could be looked upon as a good primary material for the measurements intended. Microscopical determination of the pore volume and the pore structure, however, revealed significant differences from which an influence upon the reactivity was to be expected. In fact, the values found varied within the following limits:

Porosity:	19.3 to 29.3 %
Average pore size:	14 to 19 μ
Number of pores per mm:	12 to 16

The electrode graphite samples were received from the producer in form of cylinders 20 mm in diameter. For the tests they were cut to size, 40 mm long. The granular samples were obtained by grinding several cylinders.

Particularly careful sampling was required for the metallurgical coke which had been made in a semi-industrial coke oven at a heating flue temperature of 1300 °C; in fact, wide fluctuations in the properties of the individual pieces of coke have to be expected even if they come from the same charge. The coke was dry-quenched in an air-tight chamber; its ash content was 8.08 %. The sampling method was as follows: A representative sample was taken from about 150 kg of coke; this sample was crushed and screened into two fractions 3 - 2 mm and 1 - 0.5 mm. From the remaining coke long lumps were selected, extending from the wall of the coke oven up to its center, and well-preserved at both ends. Part of these lumps were cut into pieces so that the outer, the middle and the inner ends were separately available and could be ground and screened into the same fractions as the mean sample. From the remaining lumps cylindrical samples were prepared, by means of a 20 mm hollow drill, and these cylinders were grouped, according to their position in the big lumps. The number of utilizable cylinders was rather limited on account of the cracks and fissures in the coke.

2.2.2. Weight loss during high-temperature treatment in nitrogen.

It is well known that coke will lose weight in inert atmosphere at temperatures higher than the carbonizing temperature. It was necessary for us to determine the amount of this loss in order to estimate the weight of the error introduced into the gravimetric measurements. In

Fig. 8 the loss of weight is plotted against the time for different temperatures. Between 900 °C and 1500 °C the curves are similar. After a steep rise during the first 30 minutes they become flatter. The loss of weight reaches considerable values, e.g. 10 % at 1500 °C after 20 hours. The qualitative explanation of this phenomenon is very simple. Apart from after-carbonization at temperatures beyond the carbonization temperature, adsorbed gases are liberated, although to a lesser degree, volatile inorganic ash components are distilled, and oxides in the ash are reduced by the surrounding carbon, especially at high temperatures. A quantitative determination of these different concomitant phenomena, however, seems hardly possible.

2.2.3. Temperature difference between gas and coke

In the course of our preliminary tests we found out that the temperature of the coke which had been attained in nitrogen fell off when carbon dioxide was fed to the apparatus. This fact is due to the endothermic character of the gasification reaction which consumes more heat than the quantity supplied to the coke by radiation from the wall of the oven and, to a lesser degree, by convection. With decreasing temperature of the coke, the heat transfer is improved, and at a certain temperature difference radiation will be sufficient to make up for the heat consumed by the gasification reaction. Fig. 9 gives the results of measurements which show the difference of temperatures reigning in the ambient gas on the one side and in the core of the coke pieces on the other at different reaction temperatures.

Up to 1100 °C no perceptible difference is to be observed, as the heat required for the reaction at the given temperature is supplied by radiation. With rising temperature, however, the reaction speed increases rapidly and the heat consumption of the reaction will increase to such a degree that a considerable temperature difference does appear. Beyond 1400 °C the curve is flattening out which indicates that the reaction has reached range III where the gasification intensity becomes a function of the boundary film diffusion and is, according to equation (30), practically independent of the temperature.

2.2.4. Burn-off as a function of time

The burn-off in CO₂ as a function of time was determined on cylindrical samples, using only the gravimetric method. It was found that at the same temperature and after the same time the loss of weight of the graphite cylinders differed very much. This is to be explained by the large differences of the pore volume, as mentioned above. In range III where the internal structure of the graphite cylinders is no longer influential upon the gasification reaction, these differences disappear.

As expected, the differences of burn-off were still larger in the tests on coke cylinders. But here, as before, we could observe the trend that at high temperatures the burn-off after the same lapse of time was constant, no matter whether the samples had been taken from the middle of the chamber or from the wall of the oven. At lower temperatures it is always the samples taken from the middle of the chamber that show the highest loss of weight.

A comparison of the burn-off curves of graphite and coke leads to the result that for graphite the loss of weight per unit of time remains almost constant even after gasification of 50 % of the material. In case of coke, a slow-down of the loss of weight per unit of time with progressing combustion is clearly evident, at least up to 1200 °C. It is most of all the coke samples taken from the middle of the chamber that show this trend.

2.2.5. Reactivity of lumps between 900 and 1500 °C.

From the burn-off curves the reaction speed can be calculated using equation (9). In Fig. 10, the values calculated in this way have been marked on an Arrhenius diagram similar to that shown in the first part of this paper.

The lower curve represents the measurements made on graphite, the upper one on coke. The diagram shows the reaction speed at different stages of burn-off, ranging between 10 and 50 %. The lower section of the graphite curve, up to 1200 °C, is a straight line. From the gradient we can calculate the activation energy for the purely chemical reaction in range I; its value is 65 kcal/Mol. After a short arch the curve adopts again the form of a straight line starting at 1400 °C with a flat gradient. The activation energy in the range of pore diffusion, as calculated from the gradient of this second straight part, amounts to 34 kcal/Mol. This value agrees fairly well with the theoretical postulates according to equation (17), from which it is to be expected that the activation energy in this range should be 50 % of what it amounts to in range I. As for the conditions in the range of boundary film diffusion, the measurements made do not permit any conclusions to be drawn.

The upper curve of Fig. 10 shows the results of measurements made on coke. In the lower part the individual values found by this method are so widely dispersed that nothing can be said about the activation energy, but we come back to this question later on. It is interesting to note that this wide dispersion of the individual values disappears more and more. This proves that the chemical reactivity of the coke samples, taken from the different parts of the oven, differs very much. In fact, the lumps taken from the middle of the oven show a higher reactivity than those taken from the wall. This is to be explained by the fact that the final carbonization temperature reigned much longer near the wall of the oven which entails a higher degree of gas emission and a decrease in reactivity.

With rising temperature the wide dispersion of the values measured disappears; beyond 1350 °C all points are close together and differences caused by the position of the samples in the coke oven are no longer noticeable. The conclusion to be drawn from this observation is that with rising temperature the importance of the chemical properties decreases more and more, whereas structure and external surface become the dominating factors. This statement is confirmed by a comparison of the graphite and the coke curves which approach with rising temperature. In the pore diffusion range whose starting point for electrode graphite is about 100 °C higher than in the case of metallurgical coke, the ratio of the gasification intensities goes down to 1.6 at 1300 °C. At this temperature the internal structure of the coke becomes the decisive factor. Above 1300 °C the ratio of the gasification intensities of both materials is about 1.5 on the average, which corresponds to the difference.

of their apparent densities. It seems that the measurements were carried out not yet entirely within the limits of range III, i.e. the zone of pure boundary film diffusion.

2.2.6. Reactivity in dependency upon the position of the coke in the oven

In Fig. 11 we have reproduced the reactivity values of the fine-grained mean samples from the three zones of the oven as determined by the coincide gas-analytical method. It is understandable that the values obtained from these mean samples do not show the dispersion which was observed with the cylindrical samples. Here all the values measured coincide with the Arrhenius lines; this is true of the 3 to 2 mm as well as of the 1 to 0.5 mm size fraction. In both cases the reactivity increases from the wall of the oven towards the centre. In the preceding chapter it was already said that this is due to the final temperature of the coke, and to the length of time during which the final temperature has been effective. From the wall of the oven up to its centre line the reactivity increases by more than 100 %. The results obtained from the sample representing the whole of the charge do not agree with the mean value of the samples representing the three different zones of the coke oven. This leads to the conclusion that there is no linear relation between reactivity and the position of the coke in the oven. As the Arrhenius lines are parallel, the activation energy is the same for all measurements, irrespective of the position of the coke in the oven, namely 67 kcal/Mol.

2.2.7. Relation between reactivity and coke size

The theoretical considerations have made it clear that in the range of purely chemical reaction, i.e. range I, diffusion need not be taken into account. This is to say (Fig. 12) that the coke size does not matter, because below a certain temperature the gasifying agent (CO_2) will reach the whole reactive surface of the coke pieces, even of different diameter, without any perceptible decrease in concentration as compared with the ambient gas.

The experimental values confirm the conclusions reached on theoretical grounds. In Fig. 10 we have marked on the graphite curve the results obtained from both cylindrical samples and the granular samples 3 - 2mm. In the range of temperatures examined (1000 - 1100 °C) the values agree perfectly. For metallurgical coke Fig. 12 shows that the reactivity measured on lumps and on granular samples is the same up to 1050 °C. Above this temperature the cylindrical samples show the influence of the pore diffusion which, in the case of granular material would only appear after a further rise of temperature. These results, however, are only valid for coke originating from the chamber wall. Similar measurements on lumps from the centre of the oven led to a wider dispersion of the results so that it is not possible to draw exact conclusions from them.

In Fig. 11 we have also given the results of measurements made on granular coke of different size. Here the finer size fraction 1 - 0.5mm, does not show the same reactivity as the 3 - 2 mm fraction. This observation is no argument against the theory; it finds its explanation in the treatment after sampling. The finer fraction will always be composed

of unhomogeneous material. Crushing and grinding leads to a concentration of high-ash and weaker particles, and differences are unavoidable. Further investigations have shown that to all appearance the ash content is an important factor.

2.2.8. The influence of ash on reactivity.

In a large series of tests which are still going on, we are studying the influence of the ash content and the ash components on the reactivity of the coke. Very clean coal (ash content under 0.5 %) was coked with selected additions. It was found that Boudouard's reaction is accelerated by iron oxides and CaCO_3 , whereas SiO_2 will slightly inhibit the reaction. Very efficient is Na_2CO_3 . The following table shows the first results of reactivity tests made on very clean coke, with or without additions, at a temperature of 1050°C ; the coking temperature was 1150°C in all cases.

Material	Addition	k_m at 1050°C ($\text{cm}^3/\text{g sec}$)
Very pure coke	-	0.485
"	SiO_2	0.304
"	Fe_3O_4	0.825
"	CaCO_3	2.78
"	Na_2CO_3	7.55

For the time being we are not able to say whether the large differences between these values are due to catalytic or other influences.

Literature

- 1) Handbuch der Katalyse I, G.-M. Schwab, Wien, Springer-Verlag (1943)
- 2) Catalysis Vol. 2, Paul H. Emmett, Reinhold Publ. Co., New York (1955)
- 3) Placed to the Meeting of Experts on the Reactivity of Coke and semi-coke of the ECONOMIC COMMISSION FOR EUROPE COAL COMMITTEE (1962)
- 4) H. Echterhoff, K. G. Beck und W. Peters, Blast Furnace, Coke Oven, and Raw Materials Proceedings, Philadelphia, Vol. 20 (1961) S. 403-414.
- 5) W. Peters und H. Echterhoff, Blast Furnace, Coke Oven, and Raw Materials Proceedings, Philadelphia, Vol. 20 (1961) S. 158-170.
- 6) K. Hedden, Dissertation Göttingen (1954)
- 7) E. Wicke, K. Hedden, Z. Elektrochem. 57, 636/41 (1953)
- 8) E. Wicke, Fifth Symposium on Combustion, Univ. of Pittsburgh, 1954, Reinhold Publ. Co., New York, 1955, 245/52
- 9) K. Hedden, Brennstoff-Chem. 41, 193/224 (1960)
- 10) C. N. Hinshelwood, J. Gadsby, K. W. Sykes, Proc. Roy. Soc. (London) A 187, 129/51 (1946)
- 11) J. Gadsby u.a., Proc. Roy. Soc. (London) A 193, 357/76 (1948)
- 12) F. J. Lang, K. W. Sykes, Proc. Roy. Soc. (London) A 193, 377/99 (1948)
- 13) K. Hedden, E. Wicke, Proc. Third Conference on Carbon, Buffalo (1957)
- 14) W. Peters, G.-W. Lask, Brennstoff-Chem. 42, 84/90 (1961)
- 15) H. Koppers, A. Jenkner, Arch. Eisenhüttenw. 5, 543/547 (1931/32)
- 16) H. Koppers, A. Jenkner, Koppers-Mitt. 1, 15/16 (1922)
- 17) H. Koppers, VDI-Zeitschrift 66, 651 (1922)
- 18) A. Dahme, H. J. Junker, Brennstoff-Chem. 36, 193/224 (1955)
- 19) W. Peters, Glückauf 96, 997/1006 (1960)
- 20) W. Peters, G.-W. Lask, Brennstoff-Chem. 42, 323/328 (1961)

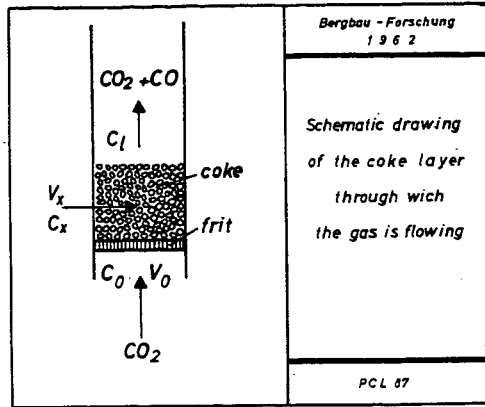


Figure 1

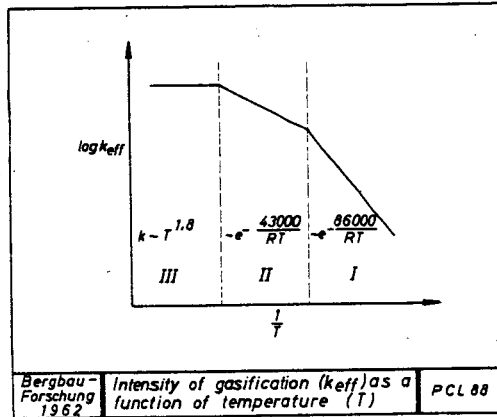


Figure 2

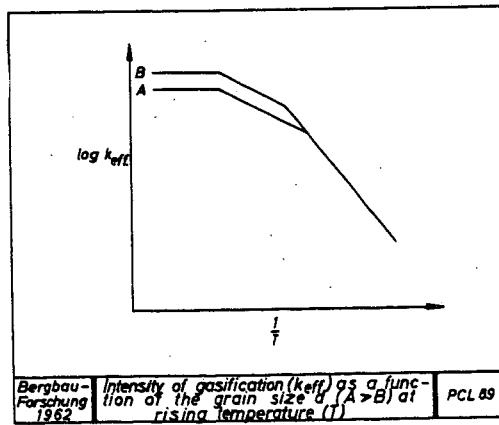


Figure 3

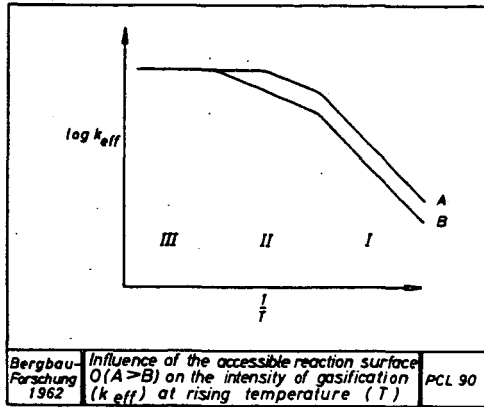


Figure 4

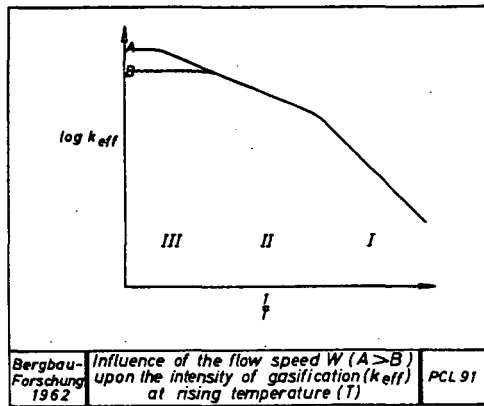


Figure 5

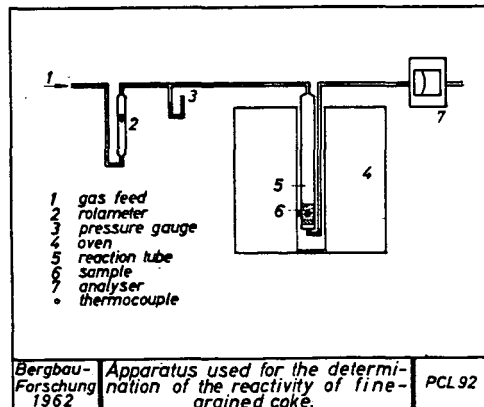


Figure 6

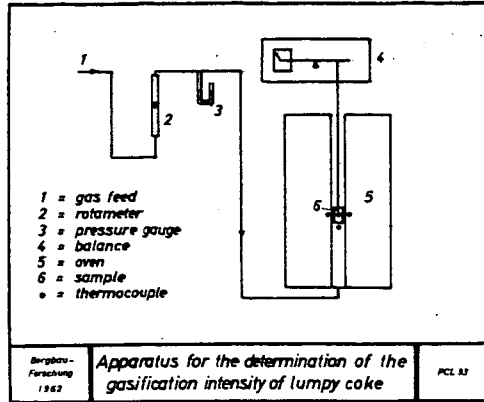


Figure 7

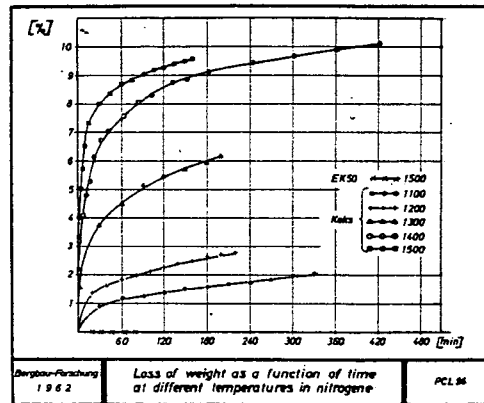


Figure 8

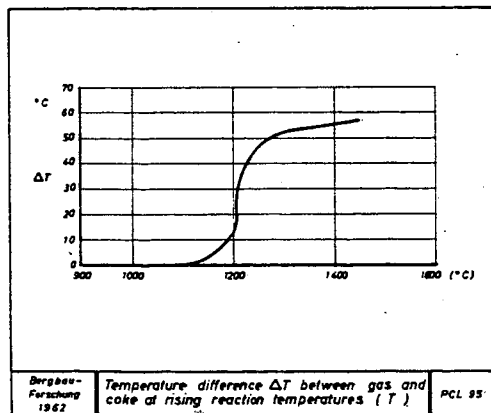


Figure 9

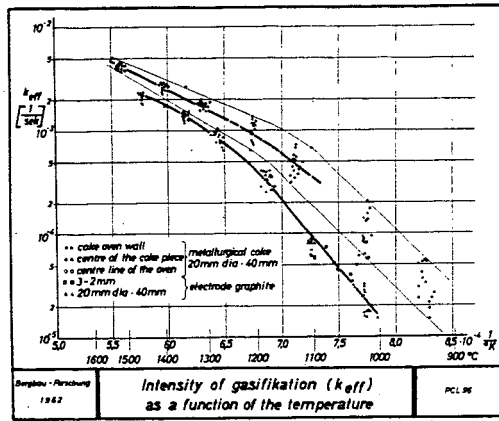


Figure 10

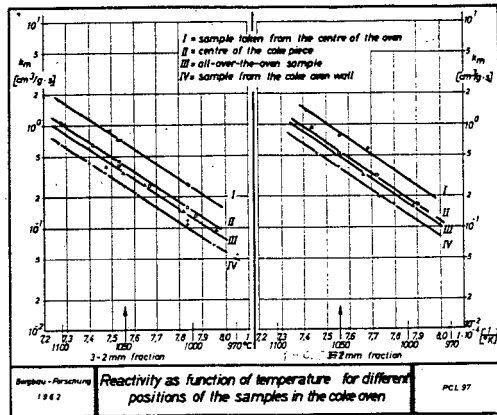


Figure 11

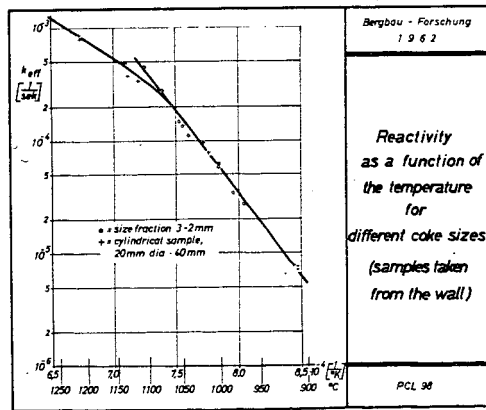


Figure 12

RELATION OF COKE STRUCTURE TO REACTIVITY

by

N. Schapiro and R. J. Gray
United States Steel Corporation
Applied Research Laboratory
Monroeville, Pa.

Introduction

The question of what criteria should be used to determine the relative quality of coke for blast-furnace use has never been satisfactorily nor completely answered. The size, strength,¹⁾* porosity, and reactivity of coke are certainly important properties that should be considered as criteria of coke quality. It is not within the scope of this paper to discuss the relative importance of the various properties that affect the performance of coke in the blast furnace; all these properties are, however, related to the structure of coke.

Previous investigations²⁻⁸⁾ have evaluated quantitatively the structural properties of coke in terms of its characteristics and behavior in specific uses. Also, qualitative observations,^{7,8)} have been made of differences in the optical properties of the wall material of cokes. These optical properties are related to the stages in crystallinity of the carbon from amorphous to graphitic forms. In carbon the crystal structure causes directional variations in the transmission or reflection of polarized light (anisotropism). Investigations conducted at the Applied Research Laboratory have shown that coke structure as well as the order of crystallinity of the carbon in the coke can be determined by reflectance measurements. When the polished surface of a piece of epoxy-impregnated coke is scanned with a reflectance-measuring microscope, areas representing the coke walls are high in reflectance compared with the filled pore areas of low reflectance. Also, the intensity of the reflectance from a wall is dependent on the rank of coal from which the particular coke was produced and on the temperature at which it was produced. Formerly, a manual method of traversing coke was used to obtain qualitative measurements of pore and wall areas. This time-consuming method required the continuous presence of the operator, and a constant speed could not be maintained. These difficulties were eliminated by the construction of the automatic traversing device, which permits the scanning of a specimen at a constant rate and thus makes possible quantitative measurements.

As part of a general program to investigate the various properties of coke that could be delineated by the use of this traversing device, studies were conducted to determine whether a significant correlation could be obtained with the instrument between coke structure as indicated by pore volume and the reactivity of coke. Reactivity was chosen as the parameter because various workers in the field⁹⁻¹²⁾ have reported it to be a function of surface area and/or porosity, both of which properties are concerned with structure.

Since coke-sample preparation is a rapid routine procedure and the reflectance-scanning microscope is automated, it may be possible to obtain much valuable information on the properties of cokes in a single operation.

Experimental

The laboratory cokes used in this study were prepared by carbonizing a variety of different-rank coals used in various coal blends in U. S. Steel operations. These coal samples were crushed to minus 8 mesh and placed in 1-1/4- by 1-1/2-inch stainless-steel cylinders, which were then put into a preheated (1850-F) electric furnace in an inert atmosphere. After the carbonized coals attained the temperature of the cylinder at 1850 F, they were soaked for an additional two hours and then cooled in nitrogen gas.

* See references

The cokes so produced were cut into halves, which were then impregnated with epoxy resin containing an opaque pigment. The low-reflecting resin filled the coke pores, providing contrast with the high-reflecting coke walls. The coke surface impregnated with the resin was then polished for microscopic examination.

The commercial cokes used in the study were obtained from U. S. Steel Corporation coke plants as complete fingers (one-half oven pieces) from one oven push. Fingers were selected because they represented the extremes in the time and temperature conditions under which the cokes were produced. From these fingers, portions representing the wall, the center, and the inner end were removed, impregnated, and polished in the manner described for the laboratory-produced cokes.

The individual coke specimens prepared for the microscope study were placed on the stage of the microscope and levelled optically to assure uniform focus throughout. The stage of the microscope is driven automatically and the number and length of traverses is automatically controlled. The x motion or principal direction of travel was set to move the specimen at the rate of 5 microns per second (18 mm per hour), and the y motion was set at 4.5 degrees. The instrument arrangement used in the automatic recording of coke microstructure is shown in Figure 1. A photomultiplier tube is attached to the monocular tube of the microscope and is used to sense reflectance differences. The microscope field of view exposed to the photomultiplier is a circular area with a diameter of 12 microns. The photomultiplier photometer is used in conjunction with a recorder that charts the reflectance differences. The chart moves at the speed of 0.85 mm per second (3,048 mm per hour). Thus each millimeter on the specimen surface is represented by 169.3 mm on the recorder chart. In this study the wall and pore areas and the relative height of the reflectance peaks are measured by counting the actual areas from the recorder graphs. This method is adequate to demonstrate the technique in this stage of development. However, for future work an integrator will be installed that will make this calculation automatically.

The measurement of the extent of reaction (weight loss) of the solid coke with CO_2 at a controlled temperature is defined as reactivity.* The conditions used for each determination were (1) temperature, 2,000 F; (2) atmosphere, 100 percent CO_2 at 2.5 liters per minute; (3) particle size, minus 4 plus 6 mesh; and (4) sample weight, 1.5 grams (± 0.0050 gram). A thermogravimetric unit was used to determine the reactivity of the coke samples. Each crushed coke sample was placed on a basket with an 80-mesh platinum screen bottom and suspended in the uniform-temperature zone of the platinum-rhodium-wound furnace. The platinum basket was suspended from the left pan of an Ainsworth balance. The balance sensed the changes at the conditions in the furnace, and a Bristol recorder connected to the balance recorded the weight change as a function of time. The weight loss was calculated on the dry, ash-free basis (daf) and corrected for the incremental loss of volatile matter. Because the initial portion of the weight loss-time curve, which is essentially linear, was considered to be the most significant, the weight loss in 30 minutes was used as a parameter of reactivity.

Results and Discussion

Photomicrographs of surface sections of the laboratory cokes prepared from four different ranks of coal used in various U. S. Steel coal blends for metallurgical-coke production are shown in Figure 2 to illustrate structural differences in the cokes; it can be observed that the coke produced from Sunnyside coal contains very thin walls and large pore area, whereas the cokes from higher-rank coals such as Pittsburgh and Pratt contain thicker walls and less pore area. However, cokes produced from Pocahontas No. 3 coals approach Sunnyside in pore volume. Photomicrographs of the various forms of carbons in these same coke

* The reactivity data used in this presentation were supplied by K. K. Kappmeyer of the U. S. Steel Applied Research Laboratory.

samples at higher magnification are shown in Figure 3 to indicate the relation of carbon forms in coke to the rank of the coal used in its preparation. The cokes from high-rank coals such as Pocahontas No. 3 under polarized reflected light show extreme anisotropic effects with the appearance of a sinuous structure and high reflectance. The cokes from lower-rank coal such as Sunnyside show carbon forms that are isotropic and have low reflectance.

In the laboratory cokes, the degree of anisotropism was used as a measure of the types of carbon present. Optically anisotropic substances transmit or reflect light in unequal velocities in different directions. Cokes displaying different degrees of anisotropism appear smooth, granular, or sinuous in polarized light. Therefore, the degree of anisotropism and the surface texture of the coke are used to identify the stage of coalification of the coal from which the coke was produced.

Since organic inerts do not become fluid during carbonization, they remain virtually isotropic in coals of all ranks. Thus the amount of organic inerts can be determined by the isotropism in cokes produced from coals of all ranks except the marginal-coking high-volatile coals. Figure 4 shows photomicrographs of inerts incorporated into the coke walls.

A graph of the reflectance and relative anisotropism of the principal carbon form from each of the seven laboratory cokes is shown in Figure 5. The samples are arranged in the order of increasing rank of the coals from which they were derived. The maximum and minimum reflectance of the subject material was measured by revolving the sample on a microscope stage through 360 degrees with the polarizer set at 45 degrees. The anisotropism of the carbon materials increases as the spread between the maximum and minimum reflectance increases as shown by the peaks and troughs. Thus, the reflectance measurements provide a quantitative determination of anisotropism. Furthermore, the graph shows that the maximum reflectance is proportional to the amount of anisotropism.

When polished surfaces of the various cokes are traversed at a constant rate with a continuously recording reflectance microscope, a pattern is obtained that shows the low-reflecting pore areas and the high-reflecting wall area. The intensity or magnitude of the reflectance is dependent upon the rank of the coal and carbonization conditions. Examples of the profiles obtained in traversing the coke surfaces of two cokes produced from high- and low-rank coals are shown in Figure 6. The approximate division between the wall and the pore area is displaced to the right of the vertical base line because of the occurrence of portions of both wall and pore area in the same field of view. These two profiles show the differences in structure and in the rank of the coals used to produce the cokes. The coke produced from Sunnyside coal has large pore areas, indicated by the large vertical spaces between the peaks. The reflectance is low, as indicated by the relatively short horizontal peaks. In contrast, the coke from Pocahontas No. 3 coal shows smaller but numerous pore areas, as indicated by the short vertical distance between the peaks. The reflectance is high, as indicated by the greater length of the horizontal peaks. The profiles thus obtained verify quantitatively the differences in structures observed in Figure 2 and the differences in the forms of carbon observed in Figure 3.

Since the objective of this phase of the program of characterizing coke was to establish whether relationship could be obtained between coke reactivity and the coke structure and carbon forms as obtained by reflectance measurements, seven samples of laboratory produced coke that had previously been tested for reactivity were analyzed for structure.

From the graphic profiles obtained, the pore volume of each of the cokes was calculated; and this value was then plotted against the rank of the coals used to produce the cokes. This plot is shown in Figure 7. The curve obtained was almost identical with the curve obtained by plotting the rank of the coals from which cokes were produced against the

reactivity of these same cokes as shown in Figure 8. Since both the reactivity of coke and the structure of coke are related in the same manner to coal rank, it was logical therefore to assume that the structure of coke, as defined by pore volume, would be related to the reactivity of the coke. The pore volume of these cokes was then plotted against the reactivity of the same cokes; the resulting curve is shown in Figure 9. This curve demonstrates that a strong relationship exists between the reactivity of coke and the structure of the coke as defined by pore volume, and that the reactivity is greatest in cokes from low-rank coals, least from medium-rank coals, and intermediate from high-rank coals.

This relationship between structure and reactivity was established on the basis of cokes produced from individual coals of different rank. To determine, therefore, whether the same relationship held for cokes produced from blends of different-rank coals (such as are normally used in making metallurgical coke), samples of U. S. Steel coke-plant cokes that are made from blends of two or more coals of different rank were analyzed. Photomicrographs of sections of the four cokes analyzed for structure are shown in Figure 10. Examination of these photographs indicates that plant coke A contains thin coke walls and large void areas and is similar to the coke from low-rank coals, which comprises 76 percent of the total coal blend at Plant A. In contrast, plant coke D shows thick cell walls and much less pore area. The carbon forms present in the commercial cokes are similar to those of the cokes made from individual coals making up the blends; they are shown in Figure 11.

Graphic profiles of these same four cokes obtained with the reflectance microscope are shown in Figure 12. Examination of these profiles indicates the difference in both structure and carbon forms of the various cokes. In general, the structure and carbon forms follow those of the cokes made from individual coals. For example, the cell structure of plant coke A is characterized primarily by thin walls and large pore area because of the large amount of low-rank coal in the blend.

When the reflectance is measured in a transect of a prepared coke surface, the carbons derived from the individual coals remain distinct so that the distribution, the size, and the structure of the individual carbon particles can be determined. In addition, the efficiency of the blending with reference to amount, size, distribution, and fusion characteristics of the individual carbon structures in the coke can be assessed.

Plotting the pore volume as obtained from the graphic profile against the reactivity of these same cokes, a relationship similar to that found for cokes from individual coals of different rank was obtained, see Figure 13. The data indicate that the cokes made from a preponderance of low-rank coals have the greatest pore volume and also the highest reactivity. Plant coke B exhibits both high reactivity and large pore volume because the coal blend consists of 40 percent low-volatile coal, which is of high rank and when used alone produces coke of relatively high reactivity. Plant coke C shows relatively low reactivity and smaller pore volume primarily because of the large amount of medium-volatile coal in the blend.

It is the opinion of the authors that an even better correlation would be obtained between pore volume and reactivity if the temperature at which the cokes were carbonized were taken into consideration. Plant coke D is carbonized at temperatures higher than those used at other U. S. Steel coke plants, whereas plant coke A is carbonized at the lowest temperatures. High final coke temperatures reduce reactivity, increase the reflectance of the coke walls, and may affect the relative proportion of the dense wall and more porous inner coke. For example, coke taken from the inner and outer portions of an oven at Plant D were analyzed for reactivity and pore volume. The inner oven coke, which is exposed to lower temperature and time at a given temperature than the cokes from the outer or wall portion of the oven, showed both higher reactivity and greater pore volume than the outer portion sample. The effects of temperature and time on coke structure thus appear significant and warrant further investigation.

Summary

This investigation has established a relationship between the reactivity property of coke and its structure as defined by pore volume. The structure and hence the reactivity of coke are dependent upon the rank of the coal from which the coke was produced. Low-rank coal produces coke having the highest pore volume and thus the greatest reactivity. As the coal rank increases, the pore volume and therefore the reactivity of the coke decreases to the minimum. High-rank coals produce coke of intermediate pore volume and reactivity. Blends of coals produce coke with pore volumes and reactivities dependent upon the rank and amount of the individual coals making up the blend.

The temperature and time also affect the pore volume and the reactivity of a particular coke. These effects will be studied and reported in the future.

References

1. C. G. Thibaut, "French Research on Coke in the Iron and Steel Industry," Institute de Recherches de la Siderurgie, 1957; pp. 1-13.
2. O. O. Malleis, "By-Product Coke Cell Structure," Industrial and Engineering Chemistry, Vol. 16, 1924; pp. 901-904.
3. H. J. Rose, "The Study of Coke Macrostructure," Fuel, Vol. 5, 1926; p. 58.
4. H. J. Rose, "Selection of Coals for the Manufacture of Coke," AIME Trans., Vol. 74, 1926; pp. 600-639.
5. H. Hoffman and F. Kuhlwein, "Rohstoffliche und verkokungstechnische Untersuchungen und Saarkohlen," Gluckauf, Vol. 71, 1934; pp. 625, 657.
6. J. Krajewski, "Microscopic Research on the Structures of Coke Produced from Various Polish Coals," Translated from Polish, Bulletin Instytutu Naukowo-Badawczego Przemyslu Weglowego, Report No. 37, 1948; pp. 1-25.
7. C. Abramski, "Zusammenhange zwischen Kohlenpetrographie and Verkokung," Troisième Congres Pour L'Avancement des Etudes de Stratigraphie et de Geologie du Carbonifere: Compte Rendu, Vol. 1, 1952; pp. 1-4.
8. C. Abramski and M. Th. Mackowsky, "Methoden und Ergebnisse der Angewandten Kokamikroskopie H. Freund, Handbuch der Mikroskopie in der Technik, Band II, Teil I, Umschau Verlag Frankfurt Am. Main, 1952; pp. 311-410.
9. Onusaitis and Yurevskaya, Zvest. Akad. Nauk USSR, Otdel, Tekh, Nauk 1949, 519.
10. Burden and Dove, Conf. on Sci. Use of Coal, Sheffield, 1958, E7-E13.
11. Zoja, Benuzsi, Cvei, Rev. Met. 57, 19 161, (1960).
12. Bastick, Comp. Rend. 240, 2524 (1955), Comp. Rend. 243, 1764 (1965), J. Chem. Phys. 58, 97 (1961).

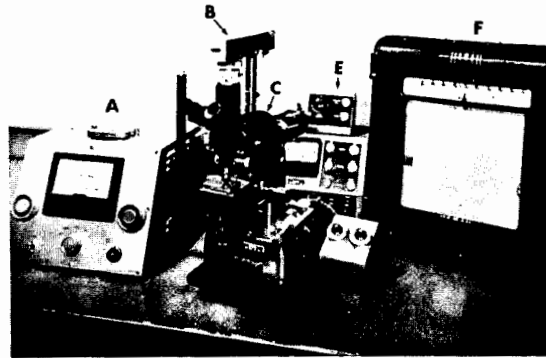


Figure 1. The equipment for automatic photometric scanning of coke specimens consists of a photometer (A), a photomultiplier sensing unit (B), an Ortholux microscope (C), an automatic stage-drive unit (D) and controls (E), and a strip-chart recorder (F).

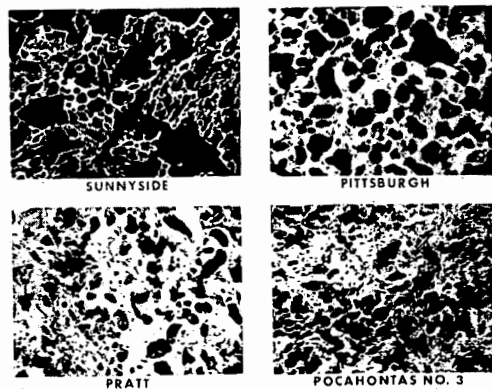


Figure 2. Coke from Sunnyside coal has very thin coke walls and much pore area, whereas coke from higher-rank coals such as Pittsburgh and Pratt has thicker walls and less pore area. Coke produced from the low-volatile Pocahontas No. 3 coal approaches that from the Sunnyside coal in that it contains much pore area. Surface sections of coke. Polarized reflected light, X50.

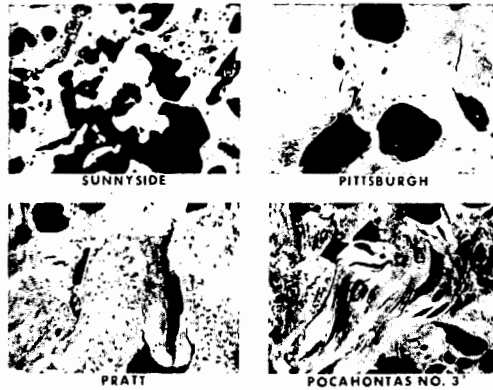


Figure 3. Sunnyside coke is low-reflecting and isotropic (smooth), whereas higher-rank coals such as Pittsburgh and Pratt produce cokes with high reflectance that show pin-point effects of anisotropism. The coke from the low-volatile Pocahontas No. 3 coal is highly reflectant and shows extreme ribbonlike anisotropism. Surface sections of coke. Polarized reflected light, X350.

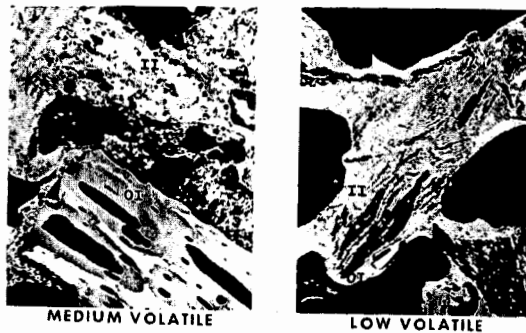


Figure 4. Organic inerts (OI) do not fuse during carbonization and remain virtually isotropic in coals of all ranks. Inorganic inerts (II) are easily recognizable in coke. Polarized reflected light, X350.

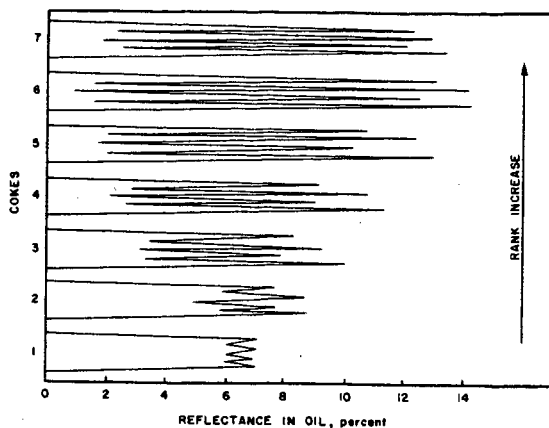


Figure 5. Reflectance in polarized light for one 360-degree revolution on a single carbon form in the following coke samples; arranged in order of increasing rank

1. Sunnyside	4. Mary Lee
2. Pittsburgh	5. Pratt
3. Pittsburgh	6. Pocahontas Nos. 3 & 4
7. Pocahontas No. 3	

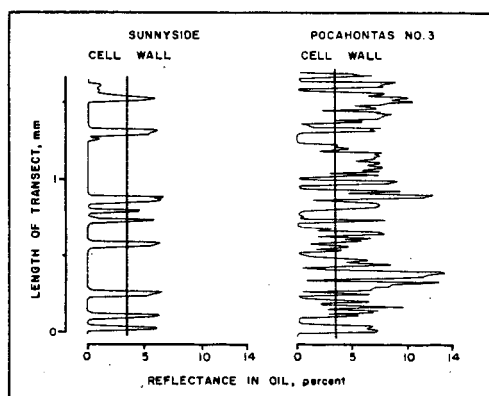


Figure 6. Graphic profile of indicated cokes showing (1) variations in reflectance of different carbon forms and (2) wall and pore areas.

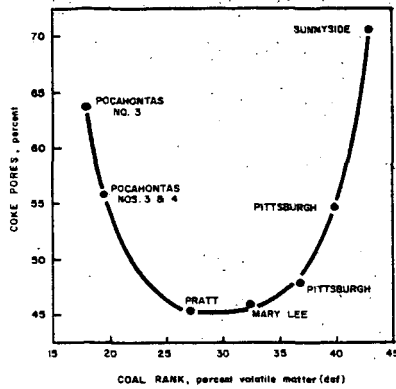


Figure 7. Relation of coke pores to the rank of the coal from which the coke was produced.

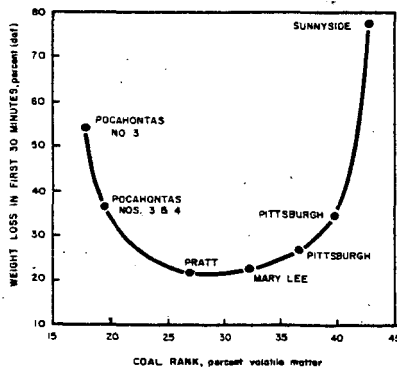


Figure 8. Relation of reactivity and coal rank for laboratory cokes.

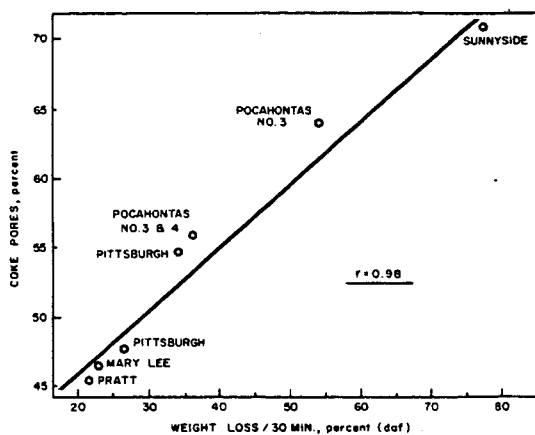


Figure 9. Relation of weight loss to coke pores at indicated conditions for laboratory cokes.

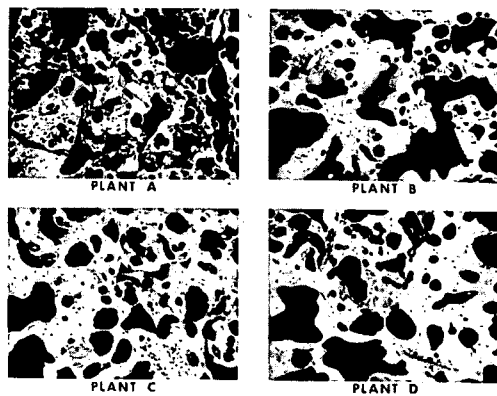


Figure 10. The coke from Plant A contains thin coke walls and much pore area, whereas the cokes from Plants B, C, and D show thickening coke walls and decreasing pore area. Polarized reflected light, X50.

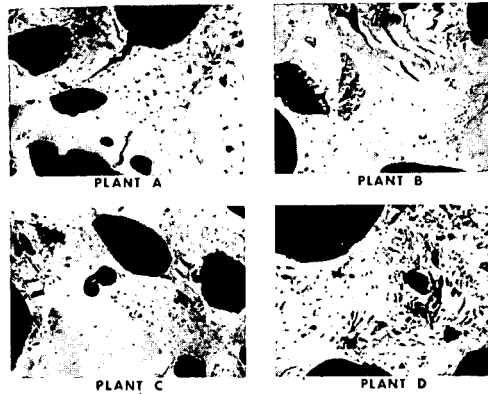


Figure 11. The plant cokes were produced from blends of either high- and low-volatile coals or high-, medium-, and low-volatile coals. The carbon forms representing the different coals are illustrated by the anisotropic effects. The coke from high-volatile coal is isotropic (smooth), the coke from medium-volatile coal shows pin-point anisotropism, and the coke from low-volatile coal shows ribbonlike anisotropism. Polarized reflected light, X350.

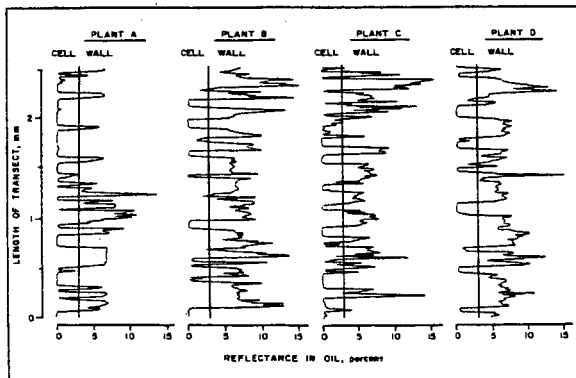


Figure 12. Graphic profiles of plant cokes showing (1) variations in reflectance due to different carbon forms and (2) wall and pore areas.

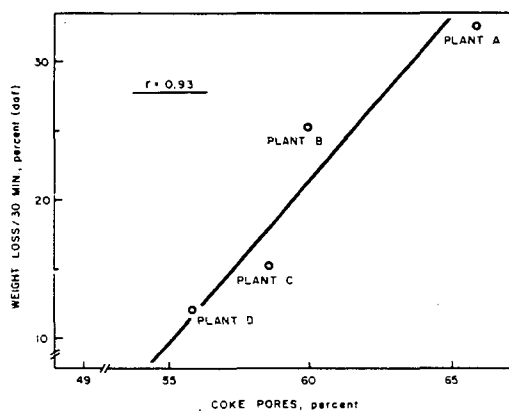


Figure 13. Relation of weight loss to coke pores at indicated conditions for plant cokes.